A UNIVERSAL CONTROLLER FOR A SINGLE-PHASE UNINTERRUPTIBLE POWER SUPPLY SYSTEM

LIMIN CHENG

A Universal Controller for a Single-Phase Uninterruptible Power Supply System

by

© Limin Cheng, B.Eng.

A thesis submitted to the School of Graduate
Studies in partial fulfillment of the
requirements for the degree of
Master of Engineering

Faculty of Engineering and Applied Science
Memorial University of Newfoundland

October 1998

St. John's Newfoundland Canada

Abstract

In this thesis, a single-phase voltage-source uninterruptible power supply (UPS) for 60Hz and 400 Hz applications is discussed. Two control strategies, namely a two-loop controller and a three-loop controller are developed. The control systems developed in this thesis have the following features: (1) stable operation at 60Hz and 400Hz, (2) no need of an external current signal, (3) high output quality, and (4) fast dynamic response. To meet these specifications, dynamic models which take into consideration the feedback variables and switching function are developed. Two suitable PI controllers for the current and voltage loops are selected according to frequency response analysis. Meanwhile, second-order feedback filters are designed to guarantee a perfect output waveform. As a result, the two-loop controller employs the output filter capacitor current and the load voltage as feedback variables while the three-loop controller uses the inverter output current as the third feedback variables.

SIMULINK models of the proposed controllers are implemented, and the steady-state and dynamic response, THD of the output voltage and voltage utilization are presented at the two standard frequencies of 60Hz and 400Hz. It is shown from the simulation results that the performance of the controllers meets the requirements. Moreover, computer simulation results of the output voltage waveform, the total harmonic distortion, voltage utilization and dynamic response show that the three-loop controller has a better performance.

Acknowledgments

I would like to express my profound gratitude and appreciation to my supervisor, Dr. J. E. Quaicoe, for his invaluable guidance, constant encouragement, and help throughout the preparation of thesis. I would also like to take this opportunity to thank Dr. B. Jeyasurya for his valuable advice.

My appreciation also goes to Dr. J.J. Sharp and Dr. M.R. Haddara, our Associate Deans and their secretary, Ms. M. Crocker, for their managerial support to my master thesis program.

I would also like to thank Memorial University of Newfoundland and Dr. J. E. Quaicoe for the fellowships and research assistantships provided to me for carrying out this study.

Finally, I am in great debt to my parents and my sister. Without their constant encouragement, understanding and support, both emotionally and financially, this work could not be completed.

Contents

List of Figures

List of Tables

Chapter 1

Introduction

UPS is the acronym for uninterruptible power supply, which is used for keeping power continuously supplied to communications systems, computers, medical systems, and data processing systems. They are the solution to many power problems including transient overvoltage and undervoltage, periodic distortions of waveforms, oscillatory transients, etc. The major function of a UPS is to provide a high quality (low total harmonic distortion value) output waveform, a fast dynamic response and the capability of carrying any load factors. UPS are widely used in industries. Parallel 60 Hz and 400 Hz output static UPS systems are used to provide power for the peripherals and the central processors in large brewery factories. Flight simulators are typically energized by 120 V 60 Hz single-phase UPS. Today, UPS is also widely used in banks, hospitals, and food-processing and airline industries. A wide variety of approaches have been reported in the literature for UPS applications [1] [2].

Two control schemes are available for UPS systems: switching control schemes and system control schemes.

1.1 Switching Control Schemes

Switches are used in various approaches such as forced-commutated thyristors, GTO (gate on and off) thyristors, power transistors and IGBT (insulated gate bipolar transistors). Two techniques are mainly used in switching control schemes:

- quasi-resonant technique; and
- pulse-width-modulated (PWM) technique

The quasi-resonant technique basically employs a conventional semiconductor power-switching device with a LC tank circuit incorporated into a circuit to shape either the voltage across the device or current flowing through it from rectangular pulses into a sinusoidal waveform. Quasi-resonant technique can be applied at zero-current-switching and zero-voltage-switching. A system will have an excellent performance when the voltage utilization is higher [3] [4] [5]. However, these techniques are very sensitive to load variations.

Pulse-width-modulated technique is achieved by comparing a high-frequency triangular carrier wave with a sinusoidal reference signal at the fundamental output frequency. According to the types of the frequencies, this technique is divided into two fields, the variable frequency PWM technique and fixed frequency PWM technique. Even though the variable frequency application has an excellent performance, the varying switching frequencies often cause unpredictable electromagnetic interference [6]. The fixed frequency PWM application is popular because it does not have the same problem as the variable frequency PWM technique and it is easy to implement by commercially available integrated circuits.

1.2 System Control Schemes

In a practical control, the control schemes are classified into two areas by the choice of using a current-source or a voltage-source.

The principle of current-source inverter operation is that the inverter is fed from a current source with a smoothing reactor connected to it in series in the dc line. The application can eliminate the harmonic components instead of increasing the value of the remaining harmonics [7] [8].

There are three types of control strategies for voltage source UPS systems:

- state-space feedback control
- sliding mode control
- current-control

The state-space control strategy provides a uniform and powerful representation in the time domain [9] [10]. The main drawback of this control system is the assumption that the state variable is measurable and available for regulation. In a practical system, it is difficult to measure all of these state variables.

The theory of sliding mode is used to constrain the state trajectories of a system to a suitable surface (known as the switching or sliding surface) in a state space. It is shown that the control scheme is flexible in design, robustness and invariance to bounded disturbances [11]. However, a disadvantage of the sliding mode controllers is the chattering dynamic that are produced. The chattering is aggravated by small time delays in the control system.

Current control strategies employ the instantaneous current control loop [12] [13]. The current-controlled voltage-source is very popular since it has extremely good dynamics, nearly sinusoidal waveform except for the harmonics which are basically linked to the switching frequency [14] [15] [16].

Abdel Rahim [16] proposed a current control scheme for UPS application which provided improved performance over other system control schemes. The proposed scheme employed proportional controllers in both current and voltage loops, and thus had significant phase error. In addition, external current command was used to achieve high quality output waveform. However, the external current command is difficult to implement. Finally, the proposed scheme could only operate at one standard frequency (f=60Hz). The performance of the current control schemes at higher frequencies have not been reported.

The purpose of this study is to develop a universal control scheme which can overcome the limitations of the existing current control schemes.

1.3 The Objective of the Thesis

The objective of the thesis is to develop an UPS control system with multiple feedback loops. The control system is called a universal control system since it is designed to adapt the output frequency to an input command. Since many applications are fulfilled at 60Hz and 400Hz, the goal is to develop a universal control scheme that satisfies the specification of high quality of output voltage, low THD, fast dynamic response, high voltage utilization, negligibly phase error, wide power factor load conditions and stable operation under wide variations in parameters at 60Hz and 400Hz.

1.4 Organization of Thesis

UPS applications require that load current and voltage follow the sinusoidal waveform with the resistive-inductive load. Many applications in power electronics also

require stable sinusoidal output at 60 Hz and 400 Hz. This thesis presents the development of a multiple feedback control system for UPS applications.

In chapter two, a SIMULINK model of the basic UPS system is developed. The basic model employs a proportional controller in the forward path. The performance of the basic system is examined at the standard frequency of 60Hz and at a higher frequency. A modified control system is developed in the chapter, where PI controllers are introduced in the forward and feedback channels. Although this modification does not solve the problem of instability at the high frequency condition, it showed improvement in the quality of the output voltage waveform.

In chapter three, state-space analysis of the UPS system is developed. Using Fourier analysis, the discontinuous model of the UPS system is converted into a continuous model. Small signal models of the PWM inverter, filter and load, and the controlled variables are employed to obtain the transfer functions of the controlled variables. The frequency response characteristics of three possible PI controllers are discussed. Based on the steady state error produced, a PI controller is selected. Later, a voltage loop PI controller and feedback compensator are selected to reach the goal of minimizing the steady-state error.

The development of the proposed control systems is introduced in chapter four. A two-loop control system with inner capacitor current loop and outer capacitor voltage loop is implemented in SIMULINK. Based on the simulation results, it is found that the control system is not able to operate reliably at both 60Hz and 400Hz. The limitations of the control scheme are discussed in the chapter. A modified two-loop control strategy is

proposed to overcome the limitations of the basic two-loop control strategy. From the output voltage and current waveforms, it is found that the two-loop control system is feasible. Realizing that the inductor current impacts the waveform quality and the performance of the system, a three-loop control system which incorporates the inductor current as a second inner current loop is proposed. Its output results also satisfy the requirements of high quality output voltage waveforms.

The performances of the above control systems are presented in chapter five. Simulation results of the output voltage, capacitor current and inductor current, THD values of the output voltage, dynamic response and phase error at the standard frequencies of 60Hz and 400Hz for the control strategies are presented. From these results, it is found that the three-loop control strategy provides an improvement in the quality of the output voltage, voltage utilization and dynamic response. The three-loop control strategy is therefore selected for further investigation. It is shown that the three-loop system has an excellent performance during power factor change, and it maintains high voltage utilization and high quality output voltage waveform at both 60Hz and 400Hz.

Finally, the significant properties of the proposed control system and the contribution of this work are emphasized and further studies are suggested in chapter six.

Chapter 2

SIMULINK Model of the Basic UPS System

2.1 Introduction

In this chapter, the basic two-loop control strategy for a single-phase voltage-source uninterruptible power supply (UPS) system is described. For this, a SIMULINK model of the control scheme is developed to study the performance of the basic UPS system. It is shown that the model is capable of providing stable and high quality load voltage at the standard frequency of 60Hz by comparing the results in Reference 38, but the system appears to be unstable towards higher frequencies. It is demonstrated through this preliminary study that using the capacitor current as the inner feedback loop variable and capacitor voltage as the outer feedback loop is a feasible control approach. It is also shown that the performance of the control scheme can be improved by modifying the linear controllers in the inner current loop.

2.2 The UPS System

Typically, UPS systems are static converters, although currently some systems are made using rotating machinery in combination with solid-state conversion. There are mainly three configurations of UPS systems: line-preferred, inverter-preferred and line-interactive. All UPS systems contain a storage battery.

A line-preferred system includes a rectifier charger, a static inverter and a static automatic transfer switch [32]. Normally, power flows directly from line to load through a transfer switch, and therefore the system does not have the feature of continuous line conditioning. In some systems, however, a regulator is installed in the downstream of the static switch to overcome this problem. In the event of incoming power outage, the critical load is transferred through a static switch to a phase-synchronized static inverter, which is operated by a floating storage battery to provide uninterrupted power.

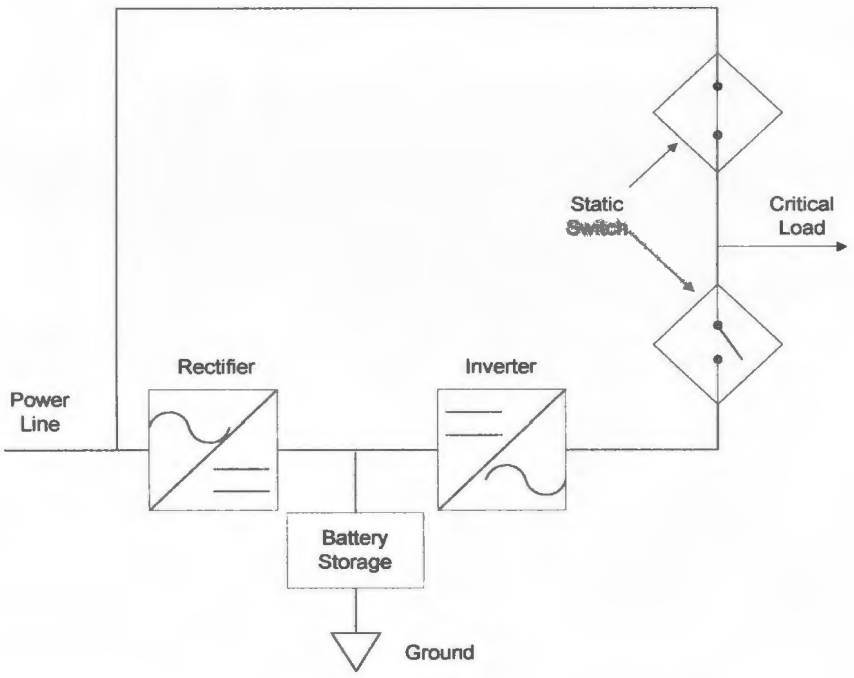

Figure 2.1 Structure of the line-preferred UPS system

An inverter-preferred system has the same standard configuration as the line-preferred system. The system is often used for critical equipment when the equipment needs to be fully isolated and equipped with power conditioning [32]. Its mode of operation should not be changed during a power failure. During the ac power failure, power would be supplied to the equipment by a battery through the inverter. There is absolutely no power interruption during the power transfer to the battery. Long-term protection is also available by adding an automatic-starting engine generator, which feeds the load through an inverter to provide conditioned power. After the restoration of the ac line, the charger supplies power to the inverter and recharges the battery automatically, restricting excess peak demands. Various rates of battery recharge may be set, depending upon the application. Since full inverter load must be provided continuously as well as battery recharging, it needs a larger rectifier charger than that of the line-preferred system.

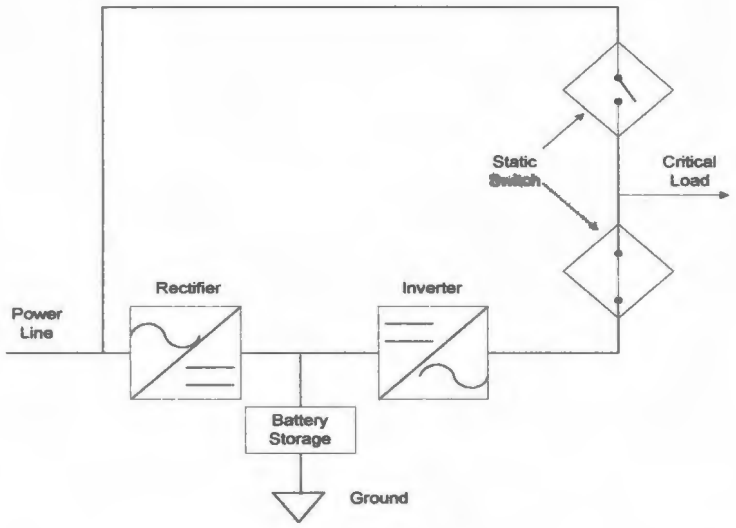

Figure 2.2 Structure of the inverter-preferred UPS system

Like the line-preferred system, a line-interactive system is used for smaller, less critical computer systems [32]. It can provide more power conditioning than a line-preferred system but is inherently less reliable than an inverter-preferred system. Normally, power flows through a single-throw static switch and an inductor to the critical load and to the converter. In this case, the converter acts as a battery charger. However, the failure of the converter at any time would result in a total loss of the output. Once the failure of ac line occurs, the static switch is opened and the function of the converter is changed to an inverter to deliver power. The system is somewhat vulnerable because the loss of output may occur if failure of the converter occurs at any time. Changing a new converter during the service is by no means a bumpless operation. These problems do not exist with the inverter-preferred system. An inductor is used to prevent overcurrents, especially in the case of a short circuit in a inverter or loads.

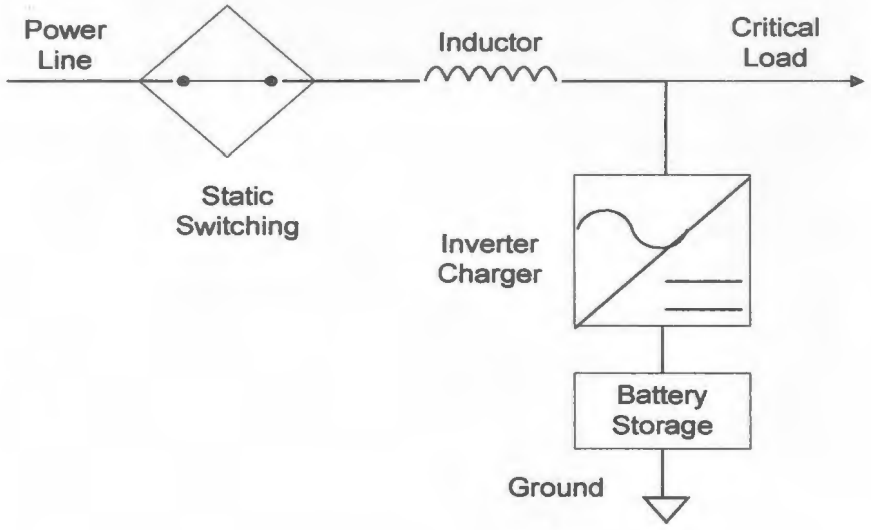

Figure 2.3 The structure of the line-interactive UPS system

In general, the inverter-preferred system provides smooth power conditioning and is the preferred configuration for UPS system. In this thesis, the inverter-preferred system is investigated.

2.3 Simulation with SIMULINK

SIMULINK [34] is the software for dynamic system simulations. It is widely used in many fields because it can do most types of simulations for industrial applications. Companies and research institutions such as Jet Propulsion Laboratory, General Motor, ABB-Industrial System and Hydro Quebec choose SIMULINK as a research tool for modeling and simulation of a wide variety of dynamic systems, including linear, nonlinear, discrete-time, continuous-time and hybrid systems. With the assistance of MATLAB software, SIMULINK runs in a powerful environment. Other software language such as M-files, C and Fortran can be incorporated into SIMULINK for analysis. This makes SIMULINK even more powerful. In this study, SIMULINK is used to investigate the performance of the various control schemes, and to develop and optimize the UPS system.

2.4 Equivalent Circuit of the UPS System

The block diagram of a half-bridge inverter-preferred UPS system is shown in Fig. 2.4. The inverter, which converts dc power to ac power, supplies the power to a resistive-inductive load L_l-R_l. This inverter is powered by an ac to dc converter with L_F and C_F filter in the dc circuit. The capacitance of the capacitor, C_F, is chosen to be large

enough to obtain adequate low voltage impedance to the alternating current component in the dc circuit. The capacitor C_F acts as a dc power source to the inverter. The input voltage to the inverter, $2V_{dc}$, is divided by the two filter capacitors C_{f1} and C_{f2}. Thus, the average voltage of the common terminal of the capacitor filters is V_{dc}. The resistive-inductive load L_l-R_l is connected to the common terminal of the two identical capacitor filters, C_{f1} and C_{f2}. Two anti-parallel diodes (known as feedback diodes) are connected in parallel with the switches (forced-commutated thyristors, GTO thyristors or power transistors) Q_1 and Q_2. The current in the opposite direction of the voltage would pass through the feedback diodes. In each half of one switching cycle, alternatively turning on and off the switching transistors, Q_1 and Q_2, results in an alternating voltage to the load. Hence, an alternating current with the same frequency as the switching is provided by C_f.

2.5 Basic Control Scheme for the UPS System

A novel multiple feedback control scheme for the UPS system was developed by N. Abdel-Rahim [37]. The structure of the control scheme is shown in Fig.2.5.

For successful operation of the single-phase voltage-source UPS system, the control scheme consists of an inner capacitor current feedback loop and an outer capacitor voltage feedback loop. Two proportional controllers are employed in both current and voltage loops when the voltage feedback signal is compared with reference waveform, the error signal e_v is produced through a proportional controller. The voltage error signal e_v is summed with the difference between the actual capacitor current and a reference capacitor current signal. The current error signal e_c is conditioned by a

proportional controller in the current loop to produce the error signal e. The error signal e is compared with a fixed-frequency triangular waveform. The resulting PWM signal is used to control the inverter switching devices in order to produce the required sinusoidal waveform [37].

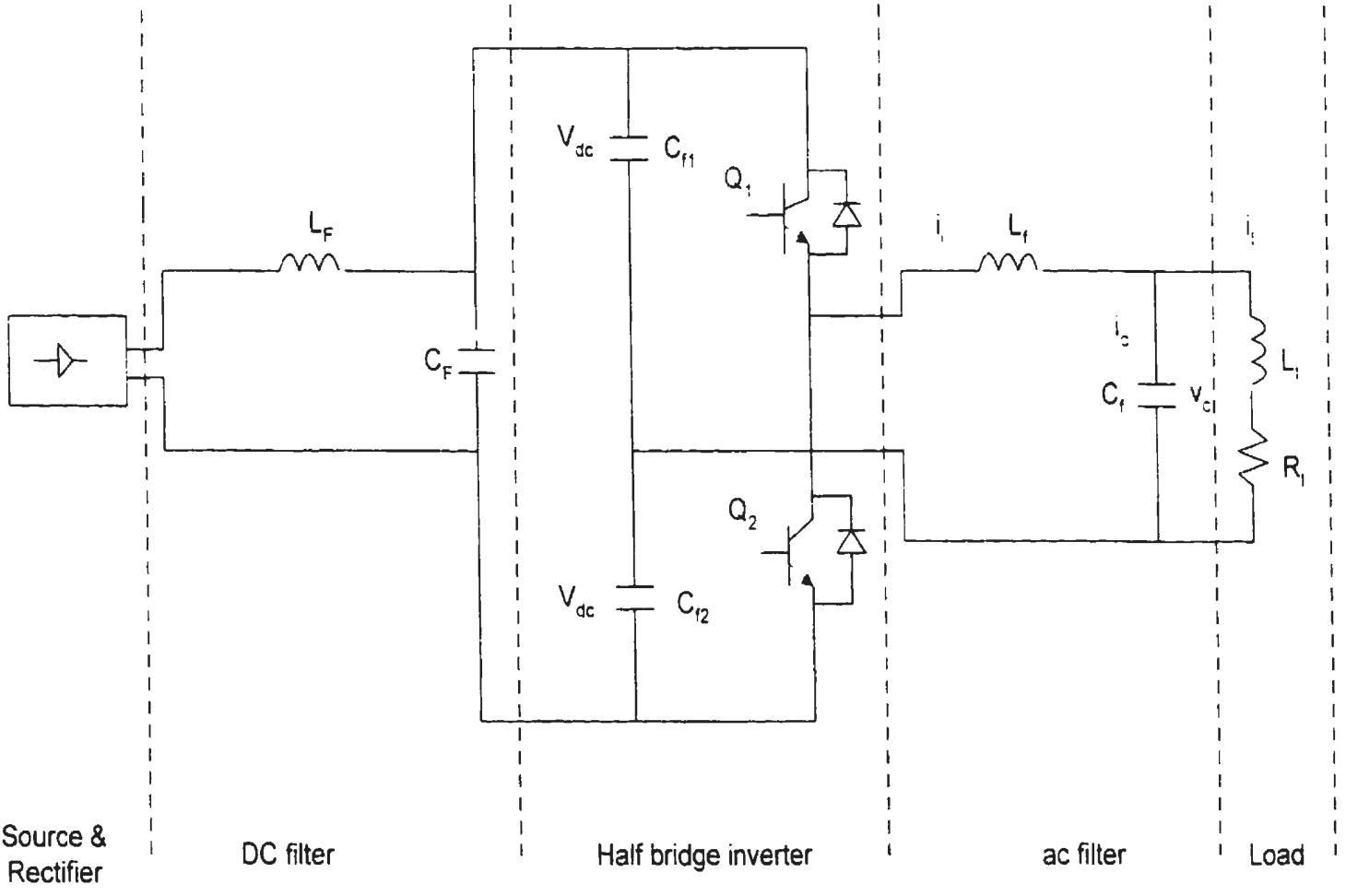

Figure 2.4: Equivalent circuit of the inverter-preferred UPS system

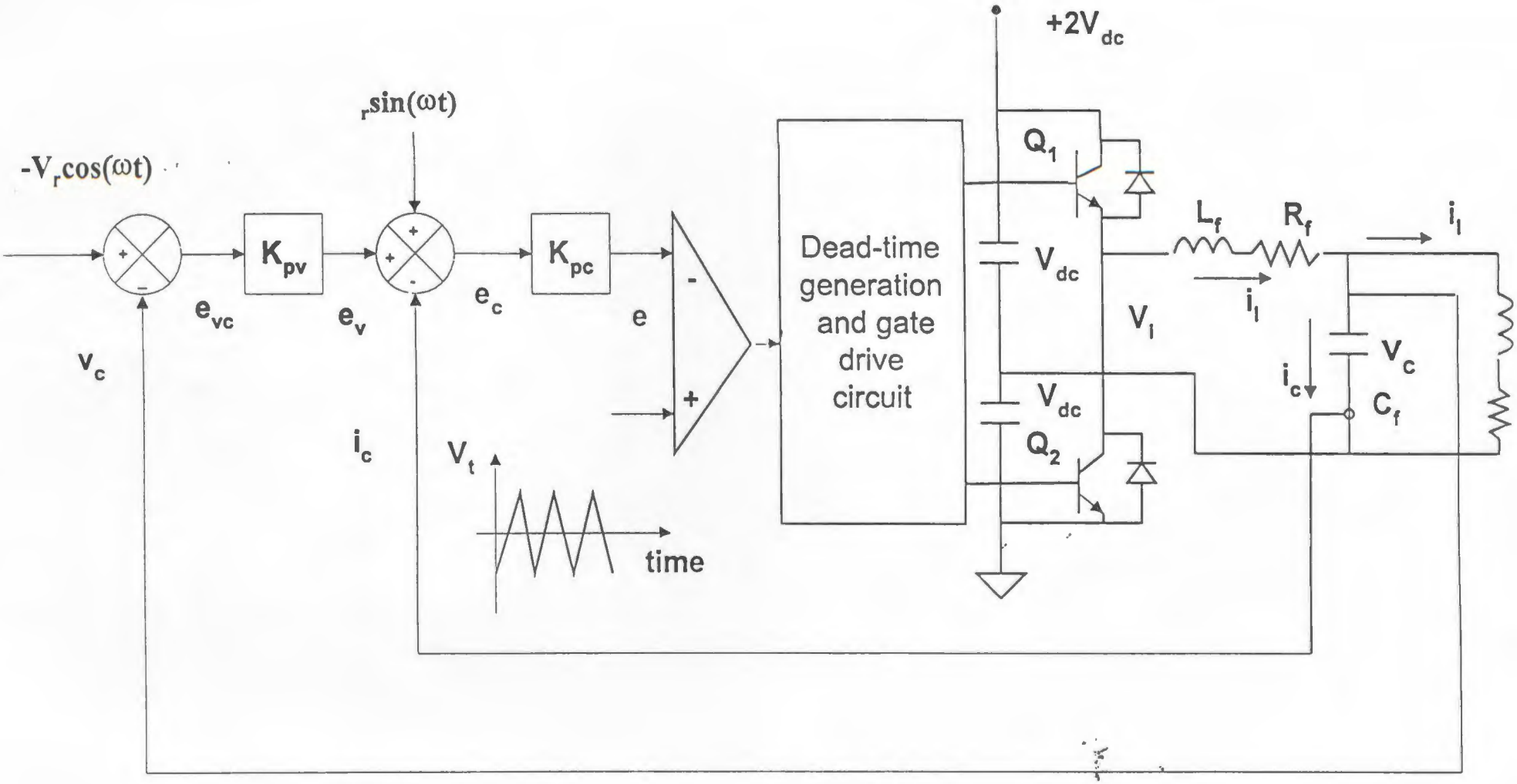

Figure 2.5: The structure of the basic multiple feedback control scheme for the UPS system [37]

The block diagram representation of the basic control scheme is shown in figure 2.6. In this figure, the input command is established by some means external to and independent of the feedback control system, and is a replica of the required output voltage. The reference input is derived from the input command as the actual input signal to the system. The controlled variable (load voltage) can be directly measured, and its feedback signal is obtained via a proportionality device. The primary variable error is obtained by subtracting the primary feedback variable from the reference input through a comparison device. A secondary feedback variable (capacitor current) and secondary variable command are subtracted from the primary variable error and conditioned by the linear controller2 to produce the control signal, which is converted to the actuating signal through a switching controller. A power converter (in this case, an inverter) is then used to transform the actuating signal to the manipulated variable. The manipulated variable is generally at a higher energy level than the actuating signal. It may also be modified in form.

2.6 Basic SIMULINK Model of the Control Scheme

In this section, the development of the models of the individual blocks in the control scheme for SIMULINK implementation is discussed.

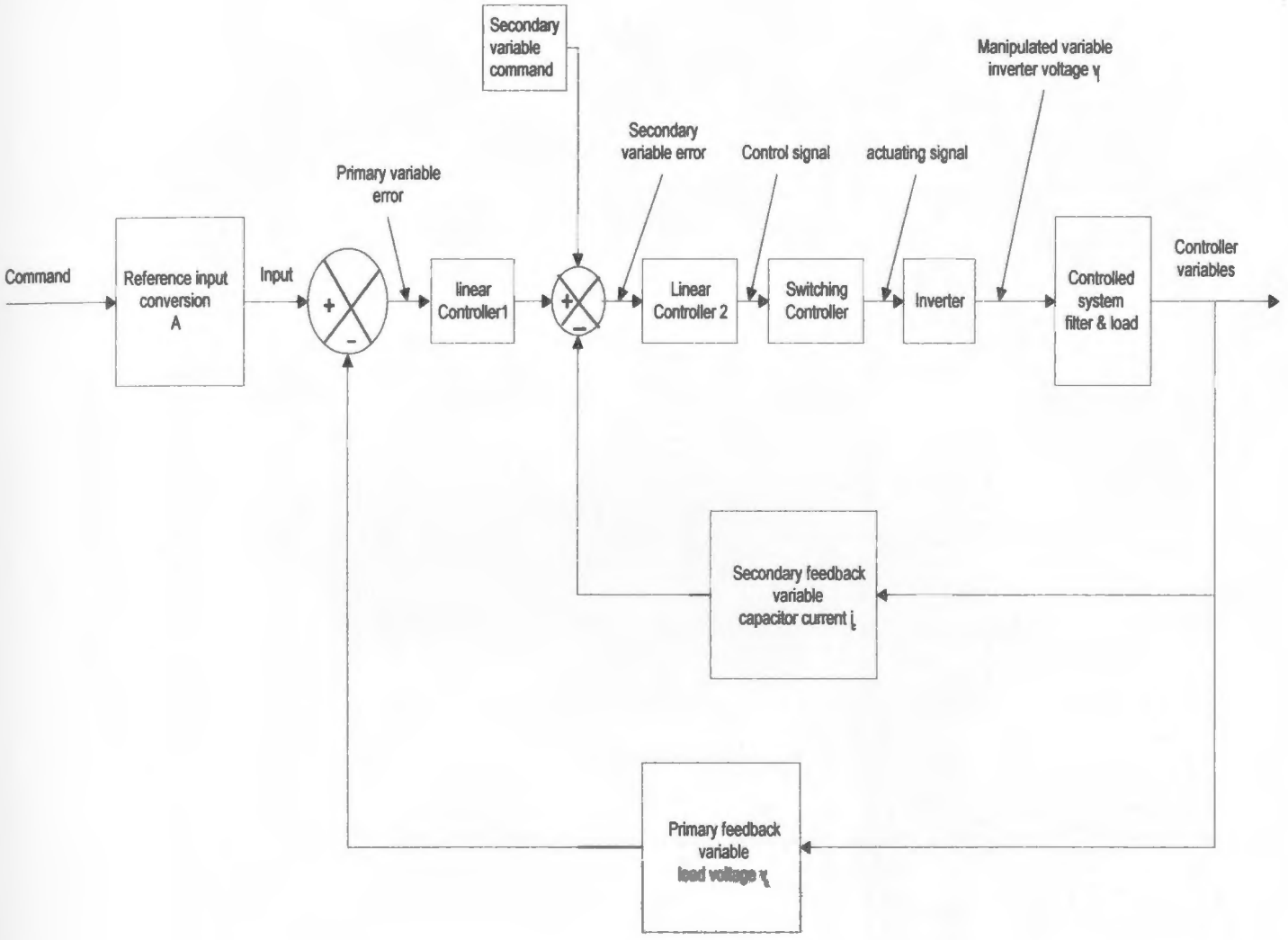

Figure 2.6: Block diagram of the basic control scheme

2.6.1 Model of the controlled system (ac filter and load)

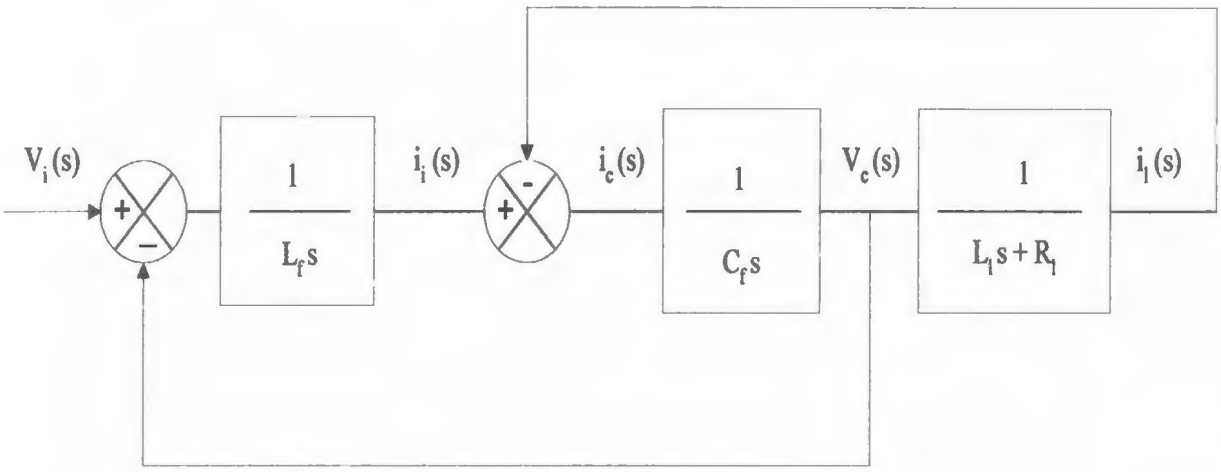

Figure 2.7: Model of the AC Filter

Figure 2.7 shows the L_f–C_f filter model with feedback signals. It is assumed that the resistor R_f is so small that it can be ignored in the analysis. Generally, the feedback variables are output signals which are functions of controlled variables. By continuously subtracting the output signals from the reference input signals, actuating signals can be obtained. In this model, the filter is connected to a resistive-inductive load. The output variables of the L_f–C_f filter in terms of the controlled current and voltage are chosen as the feedback variables.

Three feedback subsystems can be derived from the filter–load system shown in figure 2.7. In the first feedback sub-system, the capacitor voltage of the L_f–C_f which

represents the load voltage is chosen as a feedback variable. The block diagram for this sub-system is shown in figure 2.8.

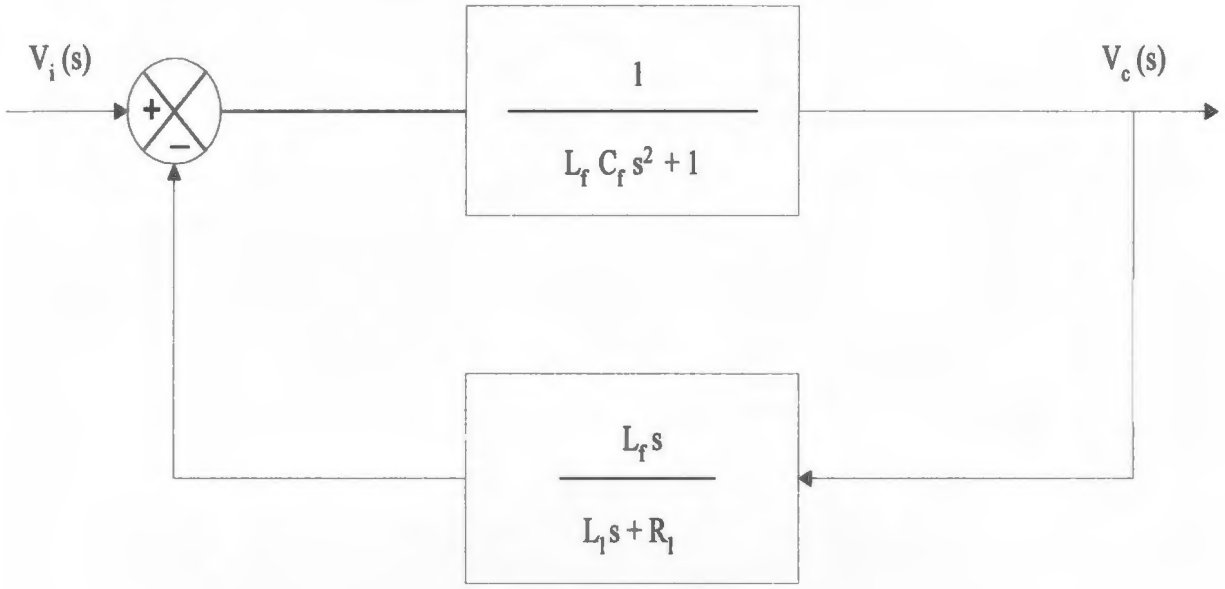

Figure 2.8: Capacitor voltage as a feedback variable

The corresponding transfer function can be derived as

$$\frac{V_c(s)}{V_i(s)} = \frac{V_l}{L_f C_f} \frac{s + \frac{R_l}{L_l}}{s^3 + \frac{R_l}{L_l} s^2 + \frac{1}{C_f}\left(\frac{1}{L_f} + \frac{1}{L_l}\right) s + \frac{R_l}{L_l L_f C_f}} \qquad (2.1)$$

When the capacitor current is chosen as a feedback variable, the feedback system can be represented by the block diagram shown in figure 2.8. The corresponding transfer function can be derived as

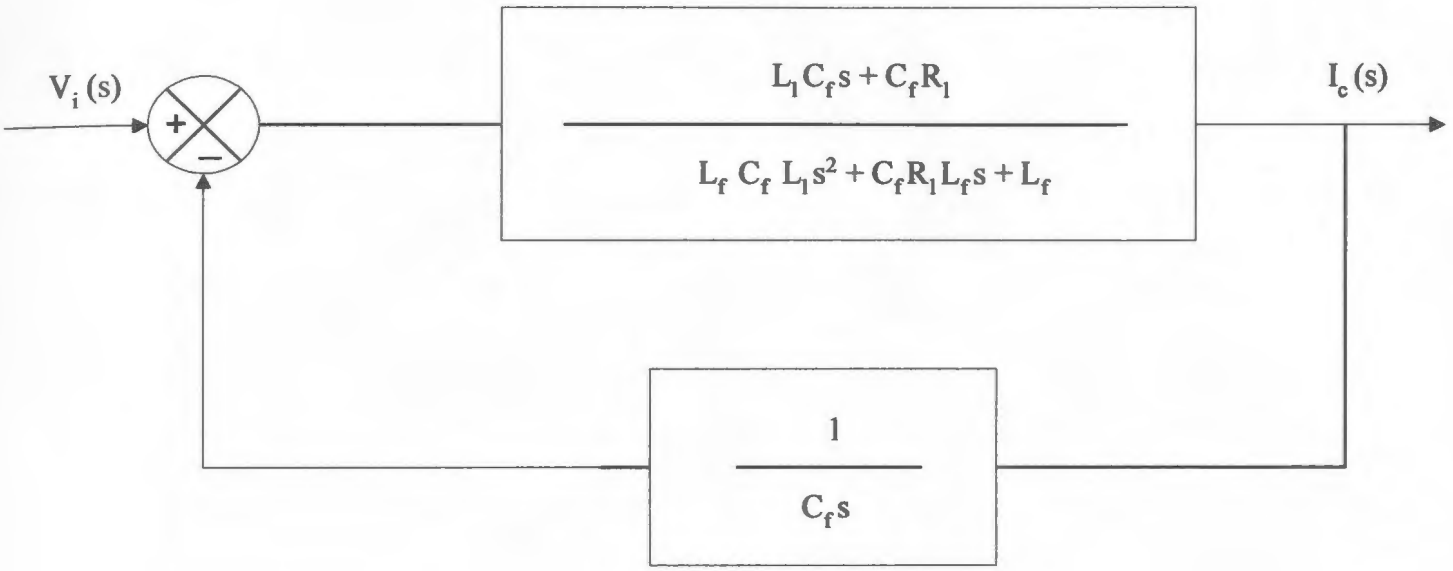

Figure 2.9: Capacitor current as a feedback variable

The third subsystem uses the filter inductor current as the feedback variable. The block diagram for this sub-system is shown in Figure 2.9, and the corresponding transfer function is obtained as

$$\frac{I_c(s)}{V_i(s)} = \frac{V_i}{L_f} \frac{s\left(s + \frac{R_l}{L_l}\right)}{s^3 + \frac{R_l}{L_l}s^2 + \frac{1}{C_f}\left(\frac{1}{L_f} + \frac{1}{L_l}\right)s + \frac{R_l}{L_l L_f C_f}} \qquad (2.2)$$

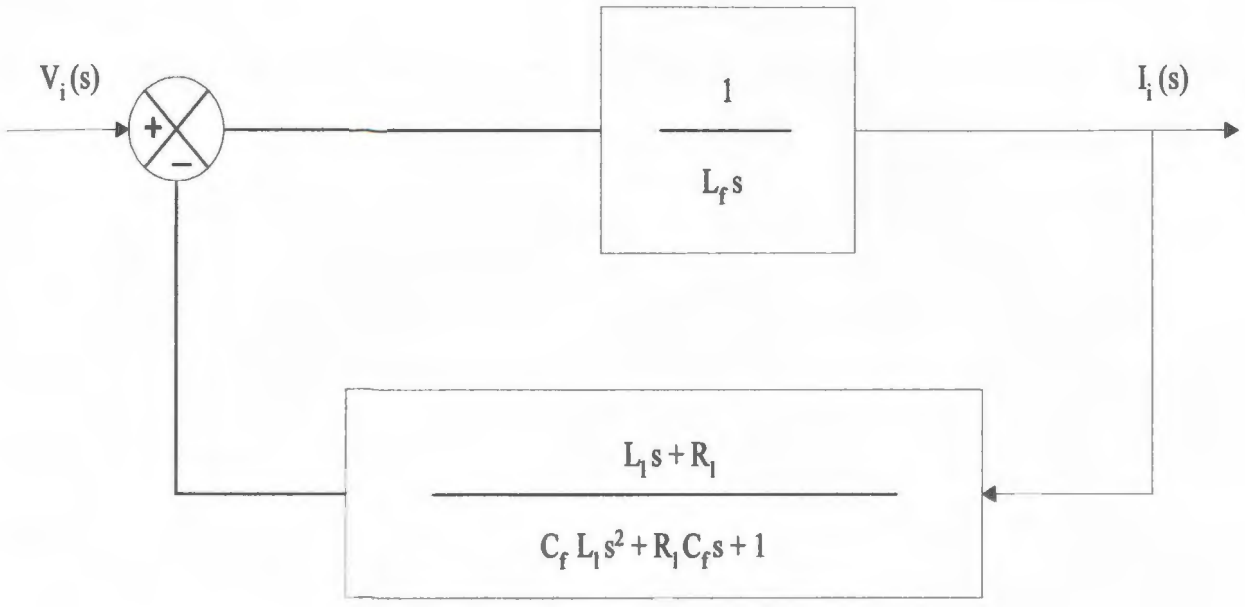

Figure 2.10: Inductor current as a feedback variable

$$\frac{I_i(s)}{V_i(s)} = \frac{V_i}{L_f} \frac{s^2 + \frac{R_l}{L_l} s + \frac{1}{C_f L_f}}{s^3 + \frac{R_l}{L_l} s^2 + \frac{1}{C_f}\left(\frac{1}{L_l} + \frac{1}{L_f}\right) s + \frac{R_l}{L_f C_f L_l}} \tag{2.3}$$

2.6.2 Model of the switching controller and inverter

The technique of modulating the duration of ON/OFF pulses applied to the switching transistor (forced-commutated thyristors, GTO thyristors, power transistors) is called pulse-width modulation (PWM). The purpose of pulse-width modulation is to change the duty cycle, d. According to the formula, $d = t_{on} f_s = t_{on} / (t_{on} + t_{off})$, the duty cycle, d, can be changed by modulating either t_{on} or t_{off} or both. Commonly, there are two

schemes of PWM: 1) the variable frequency scheme and 2) the fixed frequency scheme. In the variable-frequency scheme, PWM is achieved by keeping t_{on} fixed and changing t_{off}. However, there is a problem with the variable-frequency PWM, which results in unpredictable electromagnetic interference (EMI) due to varying switching frequencies. In the fixed-frequency scheme, on the other hand, PWM is achieved by changing both t_{on} and t_{off} duration but maintaining a constant switching period. This PWM scheme is the most popular one because of its ease of implementation by using commercially available integrated-circuit controllers and also because of its easily managed EMI filtering.

Depending on the control signals required to achieve the pulse-width modulation, two modes of PWM, the voltage-mode and the current-mode, can be selected. The voltage-mode PWM derives its control signal from the output voltage of a switching inverter. The current-mode PWM derives its control signal from the output current voltage of the switching inverter, but it is somewhat difficult to implement. No integrated-circuit current-mode controller is commercially available yet. In the control scheme used for the UPS system, the duty cycle of the switching inverter is determined by the current error signal in the secondary feedback variable. The error signal is constantly compared with a triangular carrier at a fixed frequency to produce the PWM signal for driving the inverter switches.

Figure 2.11 illustrates a typical PWM waveform. In the figure, the reference wave is sinusoidal. The carrier wave is a triangular waveform with a constant frequency. The frequency of the reference wave may change, depending on the frequency of the output voltage [14].

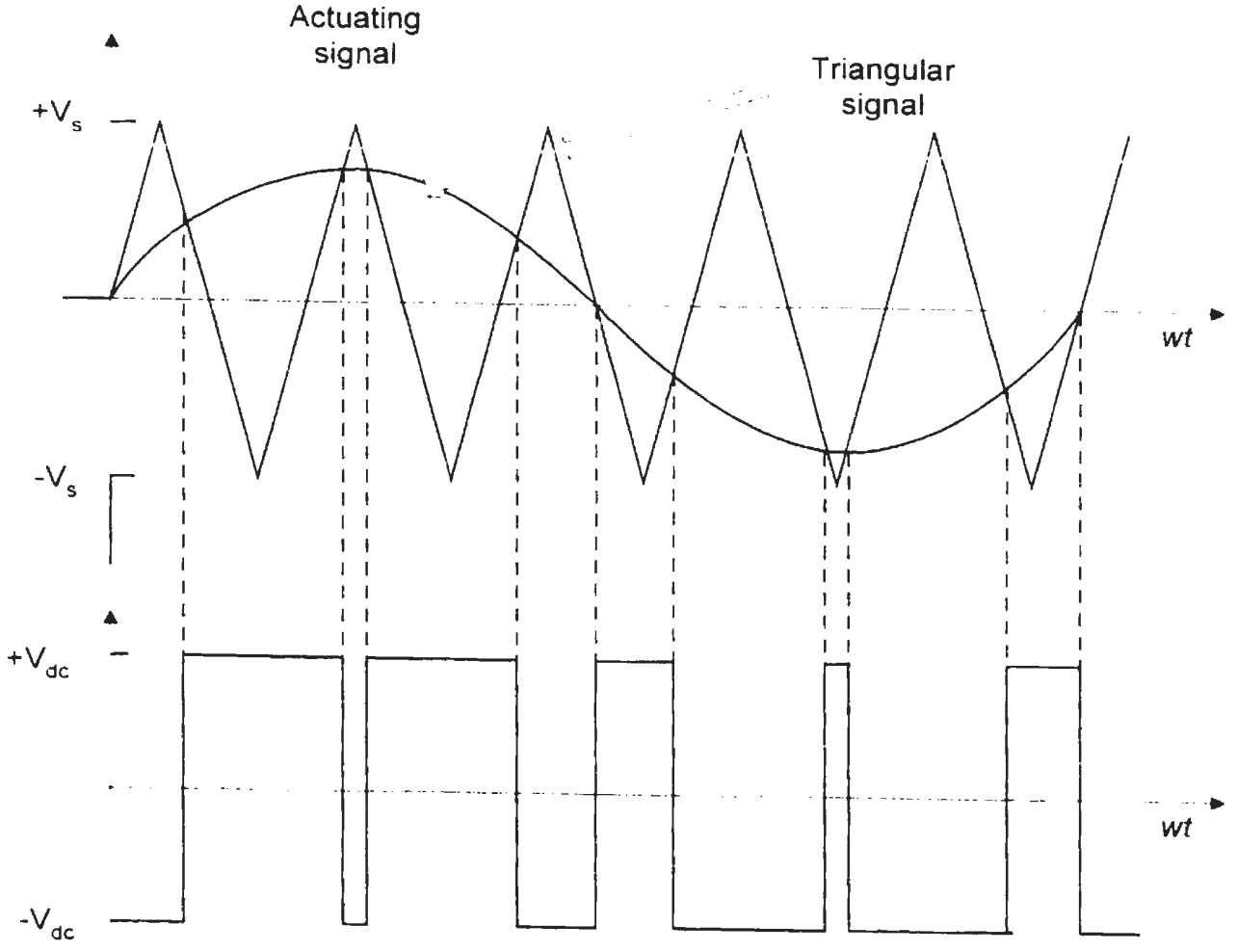

Figure 2.11: The fixed frequency PWM switching

In the basic control scheme, the current error signal constitutes the modulating signal. To keep up with the sinusoidal modulation, the signal is compared with a synchronized triangular carrier signal in the comparator which generate signals S_1 and S_2 for control of the inverter switches, Q_1 and Q_2 respectively.

In addition to the nonlinear switching controllers, there are also linear controllers which operate in association with the error signals. The control mechanism uses a linear proportional controller to condition the voltage and current errors. The use of a PI controller makes it possible, within a finite frequency band, to minimize the magnitude of the error in the output voltage. Even though the advantages of using PI controllers are known, proportional controllers are used in this preliminary study to develop the SIMULINK model of the basic control scheme.

The model of the inverter is obtained by assuming that the switches are ideal. In this case, the output of the inverter is an amplification of the PWM signal generated by the switching controller. The SIMULINK model of the switching controller and the inverter with an input dc voltage, V_{dc} of 100V is shown in figure 2.12. In the block diagram, the input 1 represents the current error signal, K_1=2 and K_2=1 provide bipolar output, switch 1 and switch 2 represent the transistors Q_1 and Q_2. The output represents the manipulated variable V_i. K=−1 ensures that switch 1 and switch 2 do not conduct at the same time. The bipolar dc voltage $\pm V_{dc}$ ($\pm$100V) is represented by constant 1 and constant 2 respectively.

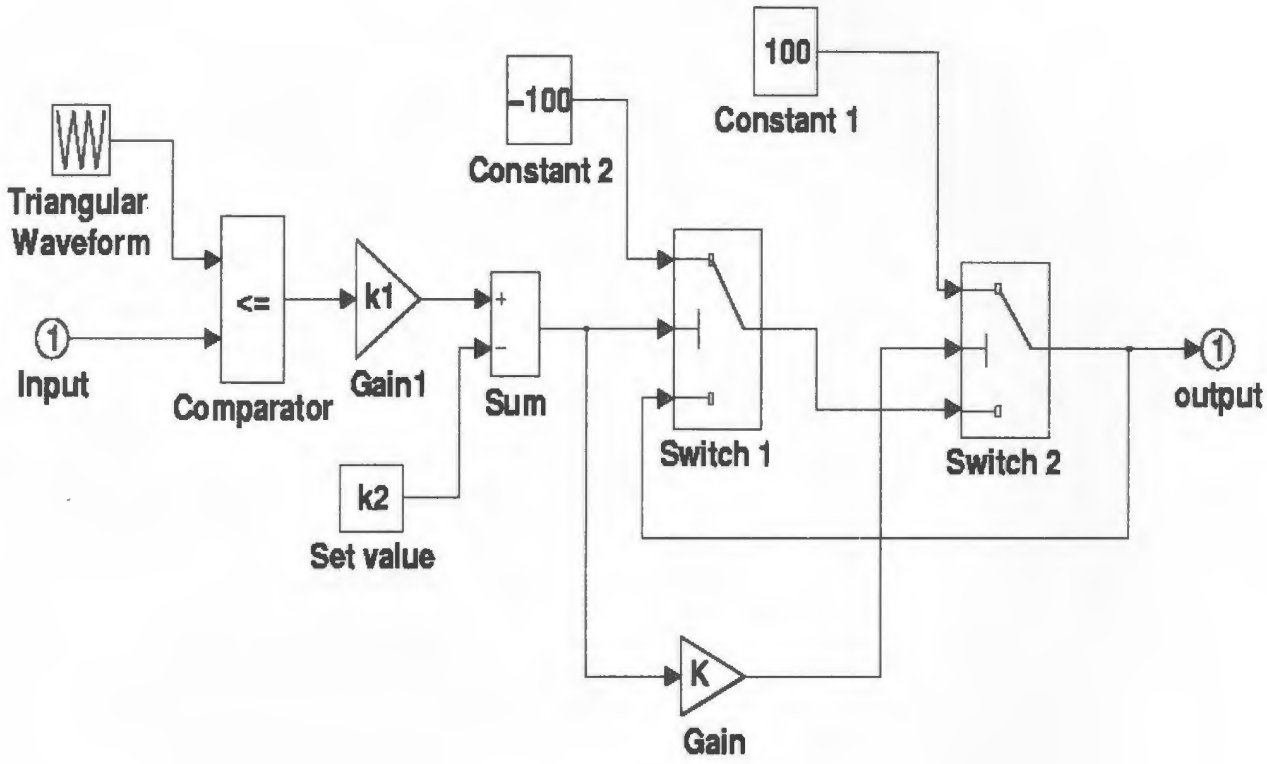

Figure 2.12: The model of switching controller and inverter

2.6.3 SIMULINK model of the basic control scheme

The SIMULINK model of the individual blocks in the basic control scheme are connected together to give the complete model of the basic control scheme as shown in figure 2.15. Two filters are used in the feedback paths to attenuate unwanted signals from the feedback variables. A small filter and proportional gain are used to condition the

primary variable error. To optimize the output voltage value, P controllers are used with higher gain. To match the performance of the controllers, different filter values are adjusted in the basic SIMULINK model. As a result, the combination of L_f and C_f is different from the previous study [38]. The following model parameters were used. The load consists of a series R-L circuit: R_l=20Ω, L_l=16mH. The ac filter values are L_f=7.5mH, C_f=130μF. The proportional gain of the linear controller 1(function 1) is K_{pv}=3.02V and for linear controller 2, the gain, K_{pc}=2.6. The switching frequency of the PWM2 block is f_s=4.2KHz. The inverter input dc voltage (V_{dc}) is 100V and the reference voltage and current command are 2V and 0.8V respectively.

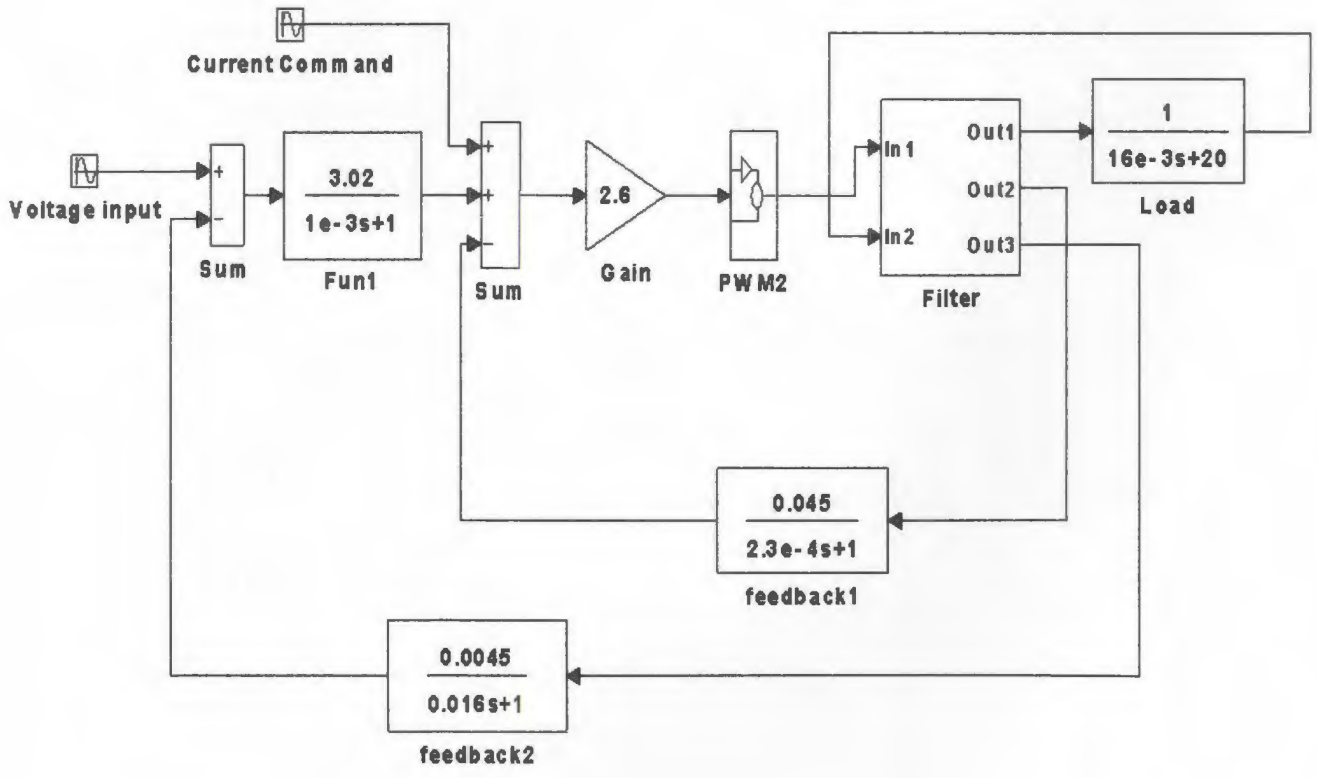

Figure 2.13: SIMULINK model of the basic control scheme

2.7 Validation of the SIMULINK Results

In this research, the output is simulated by a computer software SIMULINK. To verify the fidelity of the model, Bode diagram of the open-loop transfer function is made to compare with the published results [37][38]. Figure 2.14 shows the results presented in Reference 38. Figure 2.15 shows the results of the present model as represented by equation 2.2. Using the same parameters such as the filter values of L_f=5mH,C_f=100 μF, the load of Z_l=8.8 Ω and the voltage source of V_{dc}=100 V, and proportional controller K_{pc}=2, pf=0.7 (lagging), the present model has produced similar results in comparison with Reference 38. The system is also built stable in this research because its Bode diagram has the phase margin greater than 30° and gain margin larger than 8 dB as shown in Figure 2.15.

Furthermore, a SIMULINK run of the basic model with the same parameters as described before is performed. The results are shown in Figure 2.17. In the meanwhile, the results of Reference 38 are shown in Figure 2.16.

As it can be seen, the outputs of SIMULINK model, in terms of output voltage and capacitor current, exhibit similar waveforms, magnitude and frequency as compared to the experimental results obtained in Reference 38. In conclusion, the basic SIMULINK model is reliable.

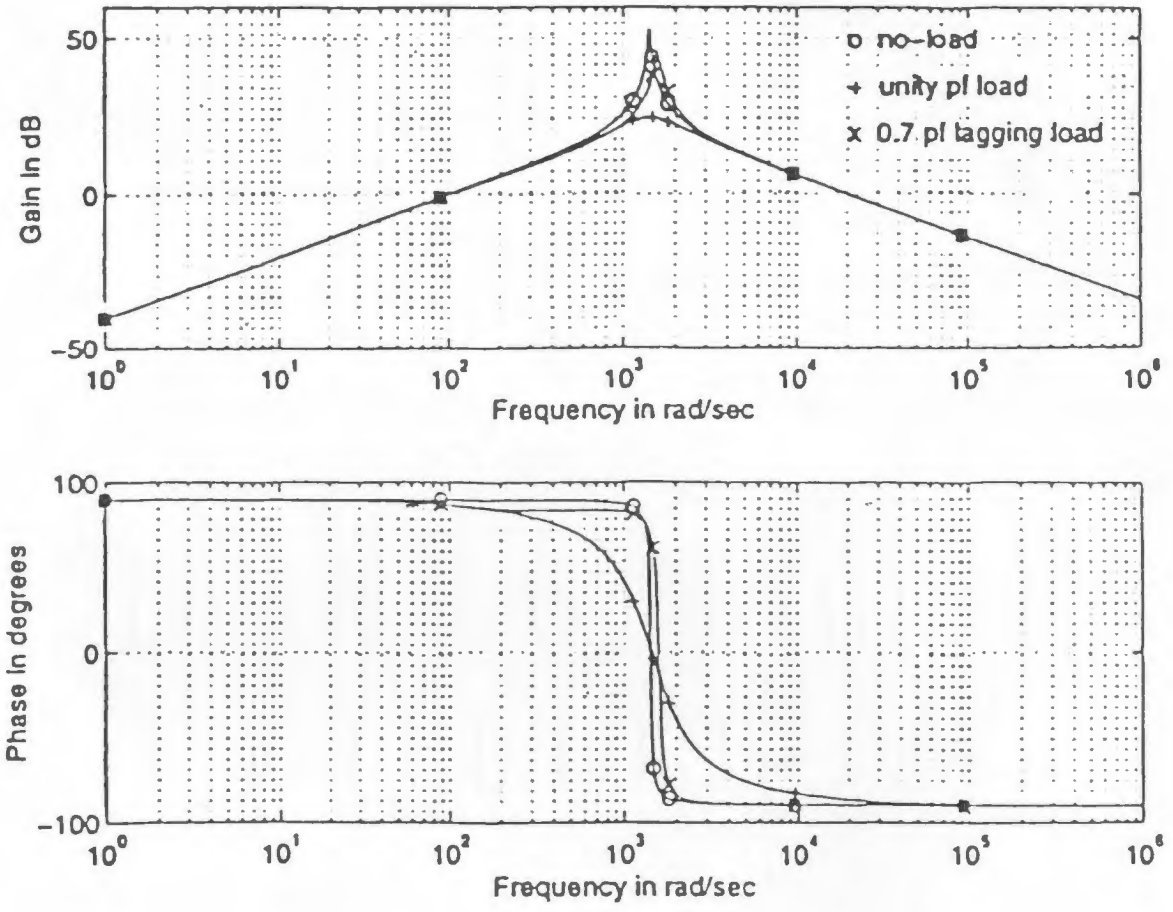

Figure 2.14: Bode diagram of the open-loop transfer function of the inner current loop of the UPS system in Reference 38: L_f=5.0 mH, C_f=100.0 μF, Z_l=8.8 Ω ,V_{dc}=100 V

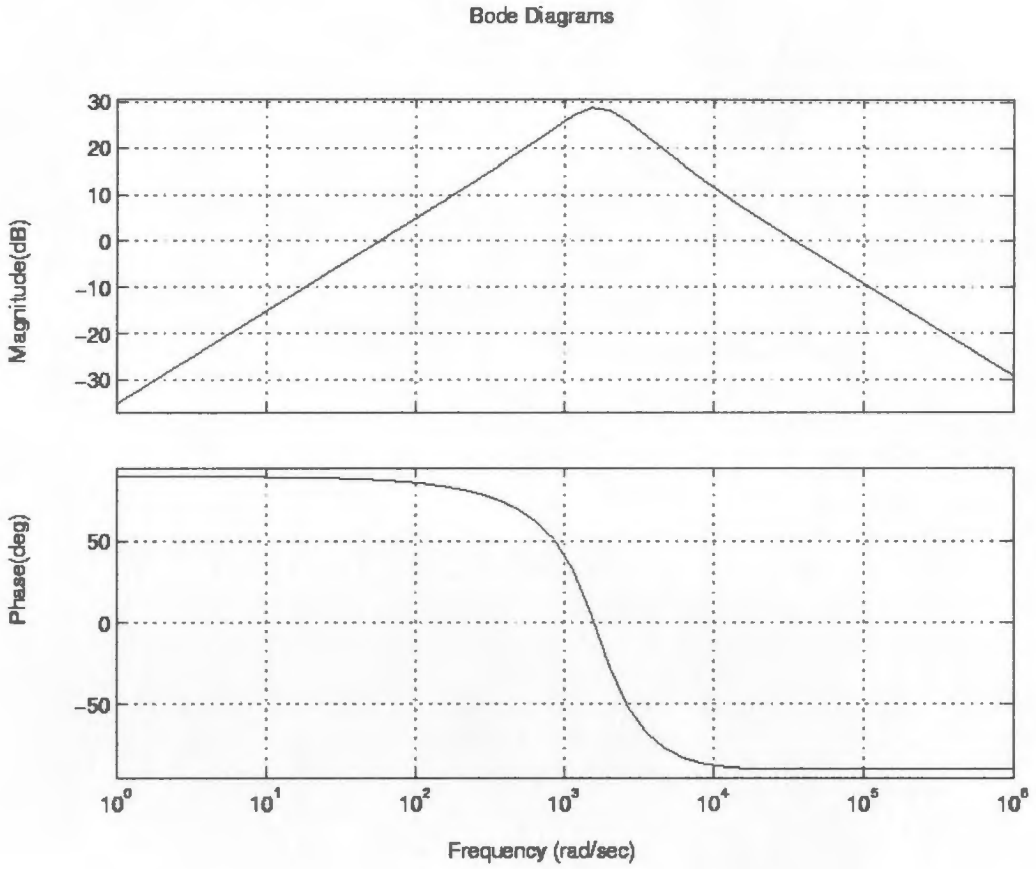

Figure 2.15: Bode diagram of the open-loop transfer function of the inner current loop of the basic SIMULINK model: L_f=5.0 mH, C_f=100.0 μF, Z_l=8.8 Ω ,V_{dc}=100 V, K_{pc}=2.0 and pf=0.7(lagging)

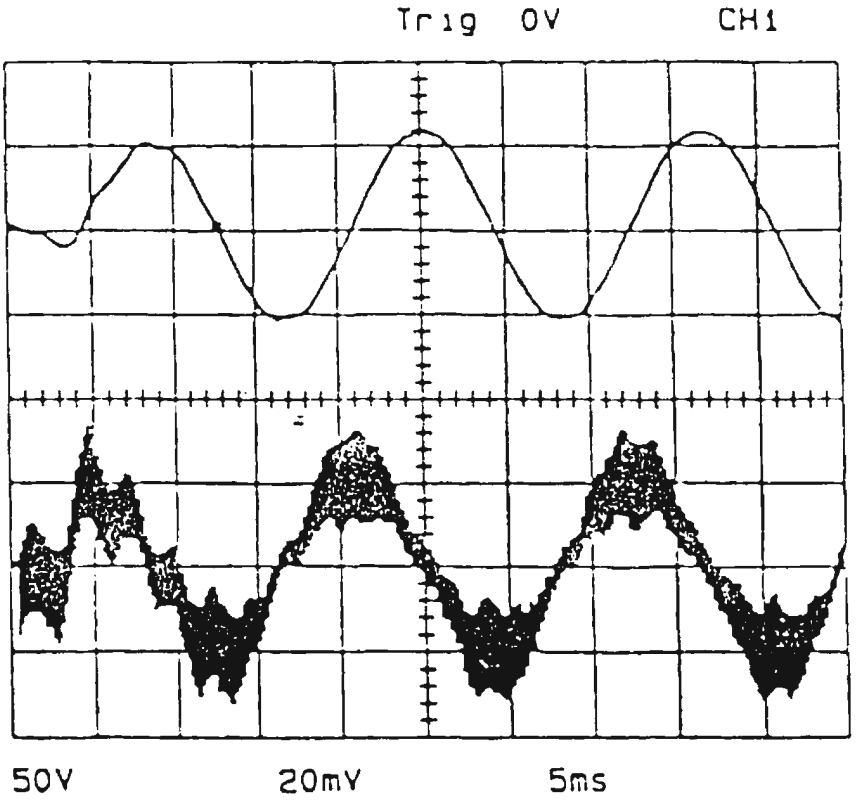

Figure 2.16: Capacitor voltage and current waveforms at 60Hz
(Experimental results in Reference 38)
Z_l=8.8Ω, L_f=5mH, C_f=100μF, V_{dc}=100V, K_{pc}=2.0
Pf=0.7 (lagging)

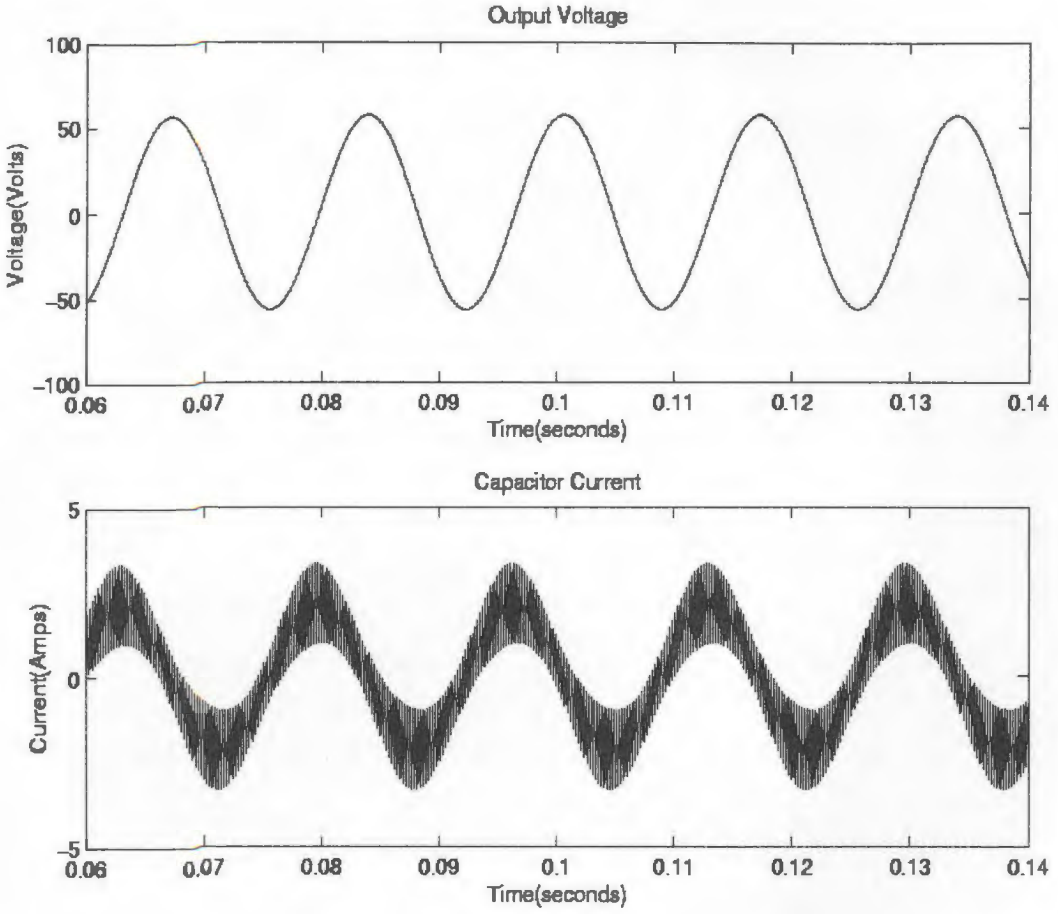

Figure 2.17: Output voltage and capacitor current waveforms at 60Hz (SIMULINK model used in validation)
Z_l=8.8 Ω, L_f=5 mH, C_f=100 μF, V_{dc}=100 V, K_{pc}=2.0
Pf=0.7 (lagging)

2.8 Performance of the Basic UPS Control Scheme

The performance of the basic UPS control scheme is investigated through simulation using the SIMULINK model developed in the previous section. One of the objectives of the study is to investigate the possibility of operating the UPS at a higher frequency (e.g.400Hz). As such, the preliminary study simulated the performance of the basic control scheme at the standard frequency of 60 Hz and at a higher frequency of 100Hz.

Figure 2.18 shows the output voltage and capacitor current waveforms at 60Hz. The waveforms illustrate that the basic control scheme can produce sinusoidal load voltage at 60Hz. For the same parameters, the model is simulated at a higher frequency of 100Hz. Figure 2.19 shows the output voltage and capacitor current waveforms. It is evident from the waveforms that the steady state load voltage is unstable.

Figure 2.20 shows the output voltages with respect to the output voltage reference signals at 60Hz and 100Hz. The waveforms show that although the load voltage at 60Hz is sinusoidal, and it tracks the reference voltage, a steady state phase error of about 2-3° exists. The steady-state phase error is pronounced at 100Hz. The results show the basic limitations of the fixed proportional controllers.

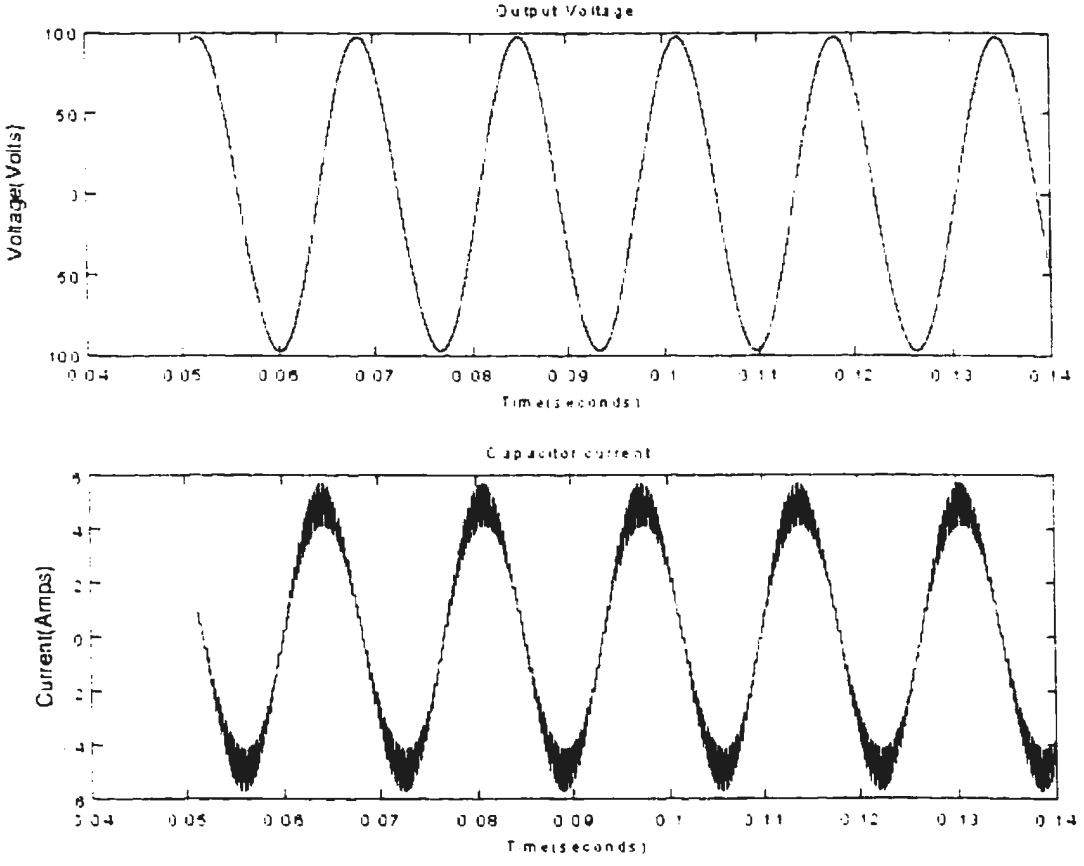

Figure 2.18: Output voltage and capacitor current waveforms at 60Hz
(Basic UPS control scheme)
(R_l=20Ω, L_l=16mH, L_f=7.5mH, C_f=130μF, V_{dc}=100V, f_s=4.2kHz)

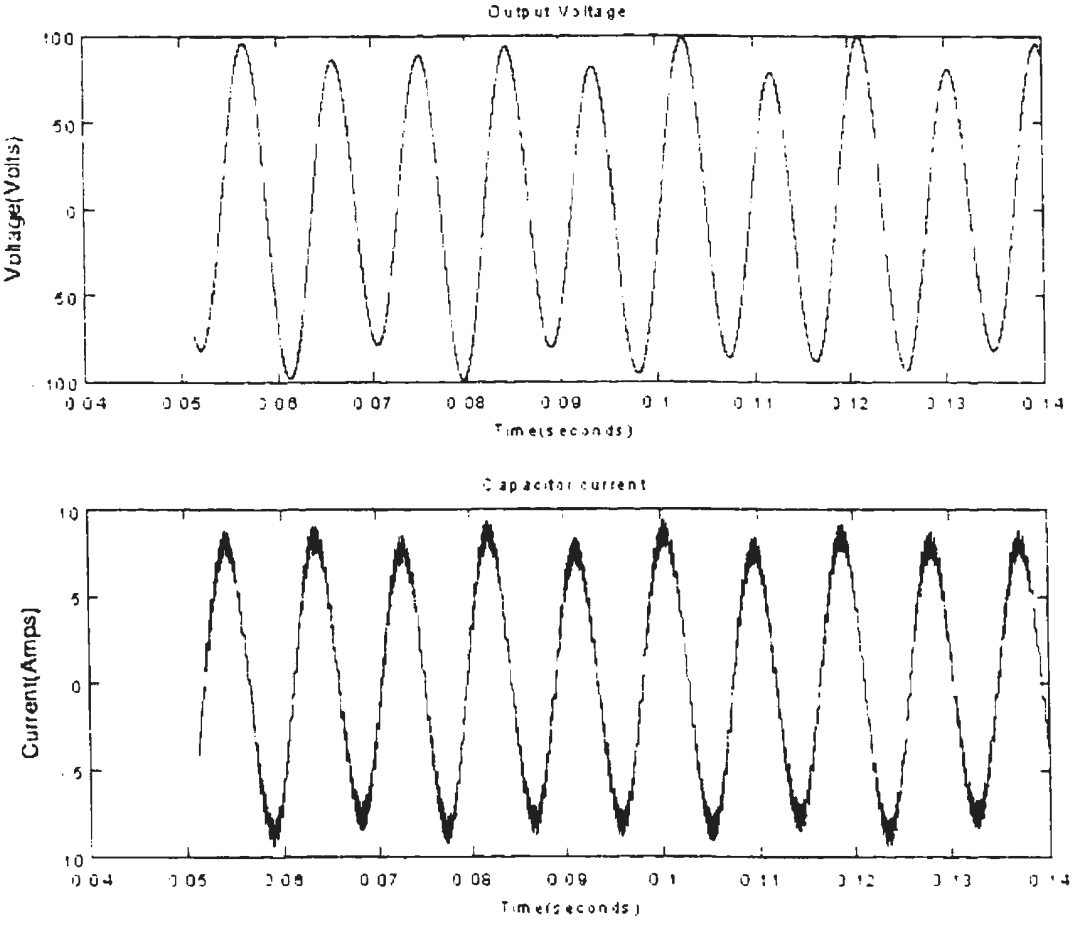

Figure 2.19: Output voltage and capacitor current waveforms at 100Hz (Basic UPS control scheme)
(R_f=20Ω, L_f=16mH, L_f=7.5mH, C_f=130μF, V_{dc}=100V, f_s=4.2kHz)

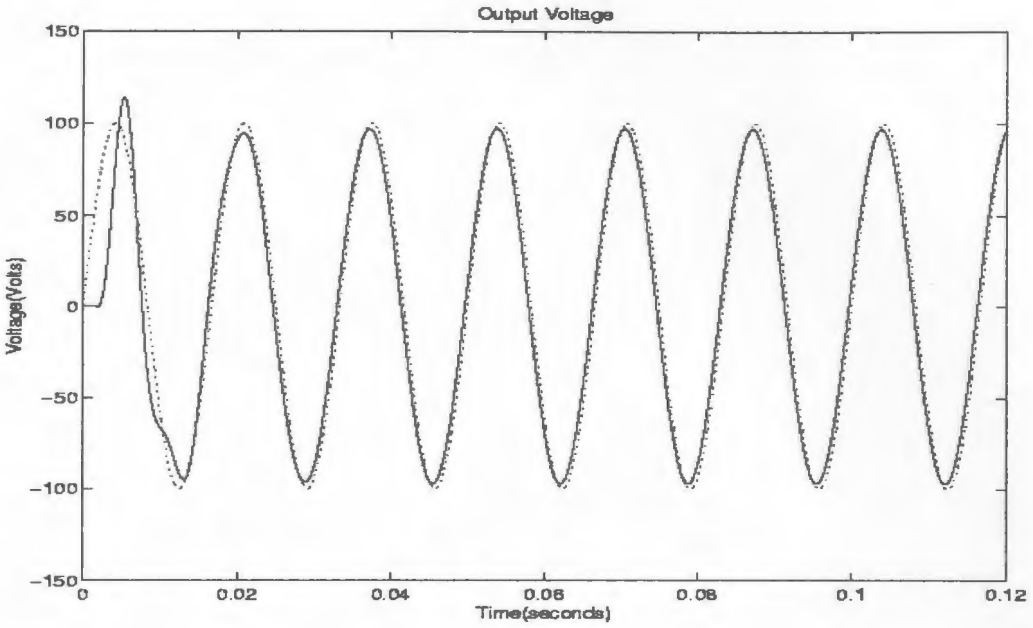

(a)

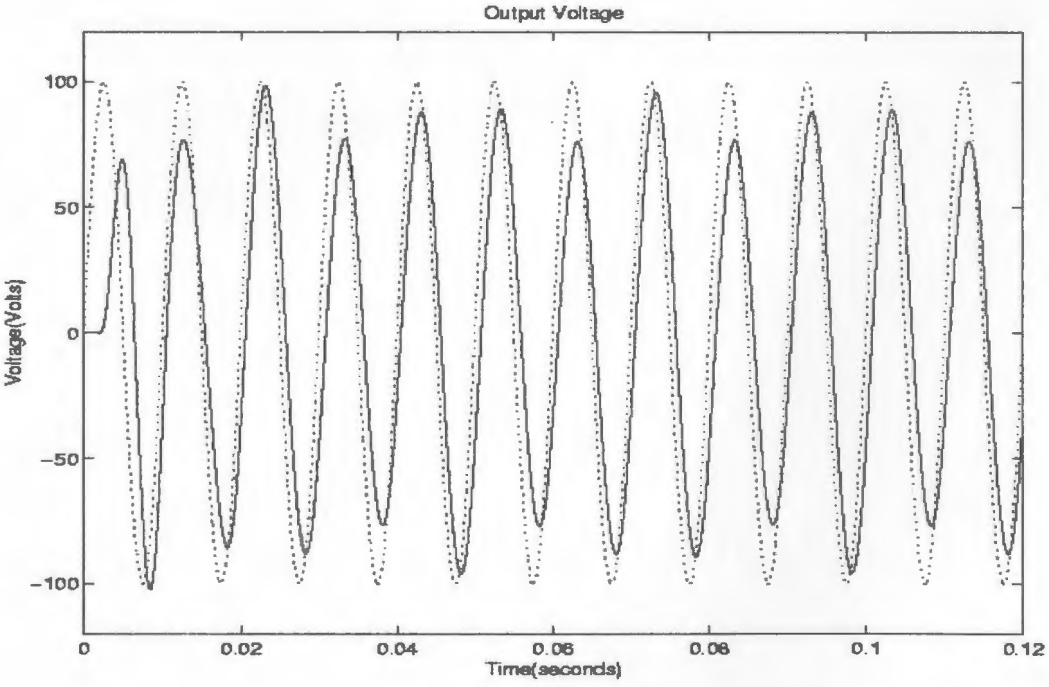

(b)

Figure2.20 (a) Output voltage with respect to reference signal at f=60Hz
(b) Output voltage with respect to reference signal at f=100Hz
(Basic control scheme)
(R_l=20Ω, L_l=16mH, L_f=7.5mH, C_f=130μF, V_{dc}=100V,
f_s=4.2kHz)

In order to improve the performance of the basic control scheme, a PI controller is introduced in the current loop. As a first step in investigating the performance of the basic control scheme with a PI controller, a PI controller of the form $K_{pc}+ K_{ic}/s$, where $K_{pc}=2.6$ and $K_{ic}=1090$ is chosen. All other system parameters are unchanged.

Figure 2.21 shows the stable output at f=60Hz. The signal has a perfect sinusoidal waveform. Figure 2.22 shows that the steady-state output signal is still unstable at a frequency of 100Hz. Figure 2.23 shows that the phase error is decreased at f=60Hz. However, the output voltage at f=100Hz indicates that although modified system has improved the phase error of the controlled variable, the output voltage remains unstable.

The results of the preliminary study of these basic models have shown that for an UPS system, a PI controller can significantly affect the performance of the control system. Therefore, more detailed analysis will be carried out in the following chapter to improve the performance of the UPS system.

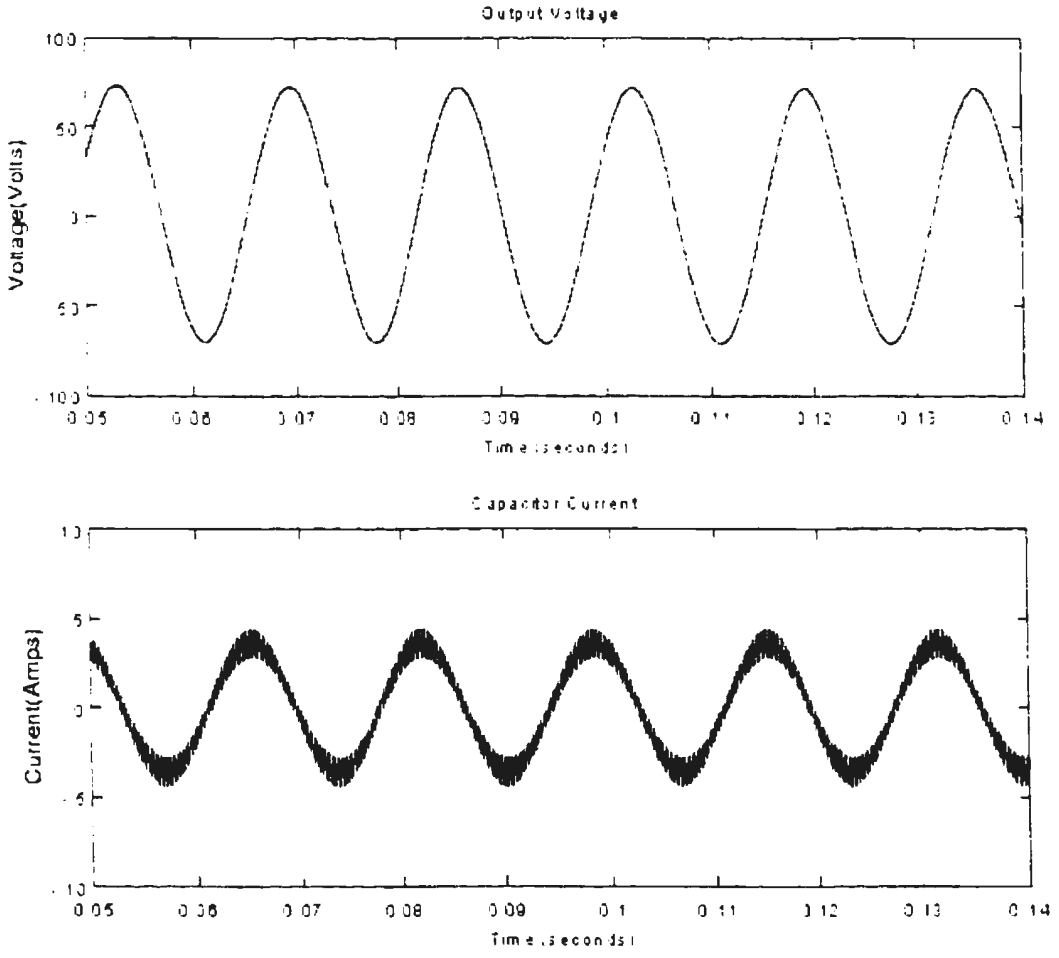

Figure 2.21:Output voltage and capacitor current waveforms at 60Hz (Modified basic UPS control scheme) (R_l=20Ω, L_l=16mH, L_f=7.5mH, C_f=130μF, V_{dc}=100V, f_s=4.2kHz)

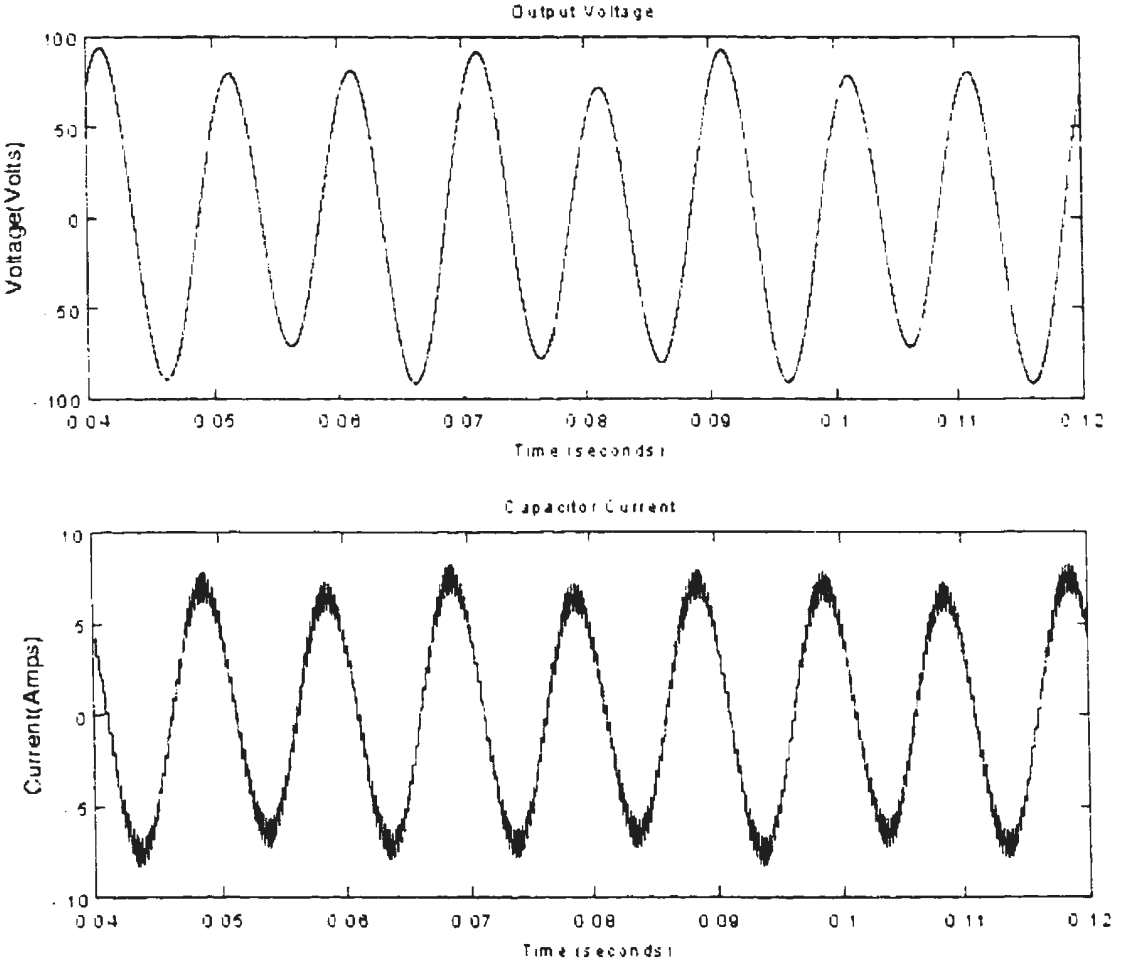

Figure 2.22: Output voltage and capacitor current waveforms at 100Hz
(Modified basic UPS control scheme)
(R_l=20Ω, L_l=16mH, L_f=7.5mH, C_f=130μF, V_{dc}=100V,
f_s=4.2kHz)

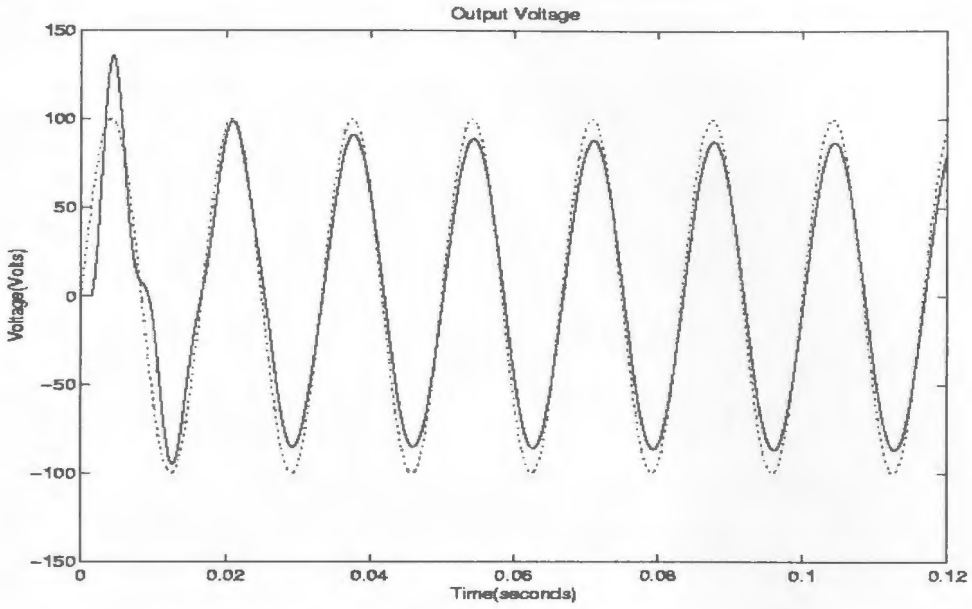

(a)

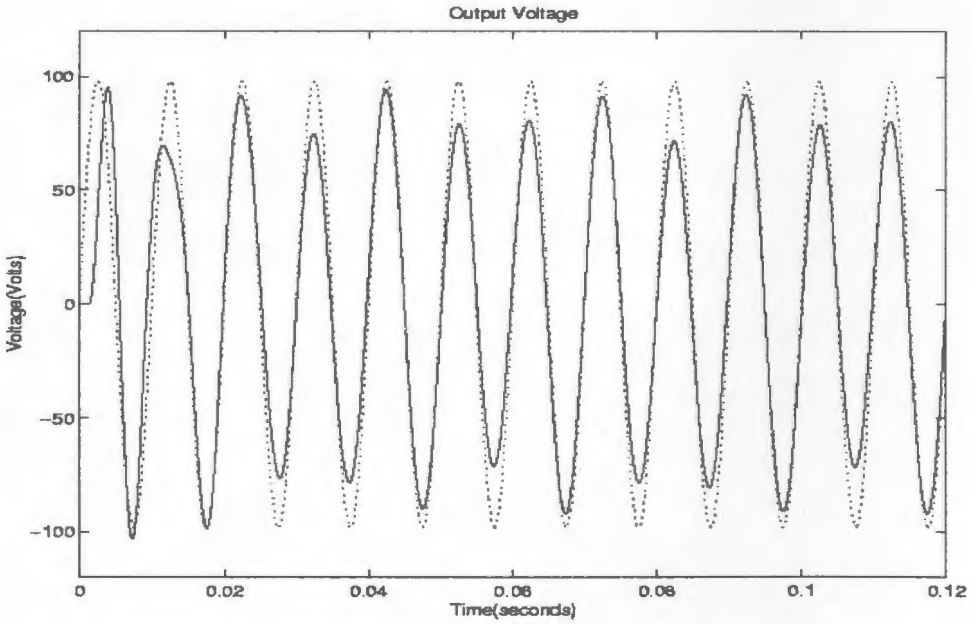

(b)

Figure2.23: (a) Output voltage with respect to reference signal at f_o==60Hz
(b) Output voltage with respect to reference signal at f_o=100Hz
(Modified basic control scheme)
(R_l=20Ω, L_l=16mH, L_f=7.5mH, C_f=130μF, V_{dc}=100V,
f_s=4.2kHz)

2.9 Summary

The basic UPS system, which employs outer voltage and inner capacitor current feedback signals to produce sinusoidal output voltage is presented in this chapter. A basic SIMULINK model of the control scheme is developed. Moreover, Validation is implemented to proof the reliability of the basic SIMULINK model. The performance of the system is investigated at a standard output frequency of 60 Hz and at a higher frequency. The results of the SIMULINK simulation show that the basic control scheme produces sinusoidal output voltage at 60Hz. However, at 100Hz, the output voltage is unstable. In order to improve the steady-state performance of the basic control scheme, a PI controller is introduced in the forward path of the inner current loop. The performance is slightly improved. These preliminary studies show that the basic control scheme is capable of producing sinusoidal output voltage at higher frequencies. However, a careful selection of the system parameters is required. In the next chapter, the detailed analysis of the system is carried out and suitable parameters are selected with a view to developing control strategies that will overcome the limitation of the basic control scheme.

Chapter 3
Transfer Functions of the UPS Systems

3.1 Introduction

This chapter presents the transfer functions of a single-phase voltage–source UPS system. In this study, a fixed-frequency current-controlled half-bridge inverter configuration is considered.

A small-signal model is developed to establish the transfer functions of the control variables. The model is at first represented by a set of equations involving discontinuous functions. The discontinuous functions are a result of the switching action of the inverter. According to Fourier analysis, a discontinuous signal consists of low-frequency and high-frequency continuous components. The high-frequency components are eliminated through signal modulation. Finally, a small signal model of the system is developed using perturbation analysis.

Studies in the previous chapter found out that proportional controllers do not satisfy the requirement of stable output voltage waveform over a wide frequency range. Therefore, in this chapter, suitable PI controllers with good performance in both current and voltage control loops are selected. Along with the controlled objects, frequency responses of PI controllers, as well as the calculation of steady-state error, are presented. Based on the results, suitable PI controllers are chosen, and filters in the

feedback paths are selected for the development of multiple feedback control strategies for UPS application.

3.2 State-Space Analysis of the UPS System

Figure 3.1 shows the equivalent circuit of the inverter supplying the filter–load combination. The system described in figure 3.1 contains the three basic components: the inverter, and the L_f–C_f filter and the R–L load. The three feedback variables chosen are the inductor current, capacitor current and capacitor voltage (load voltage). The state-space expression will therefore contain three variables (i_l, i_c, v_c).

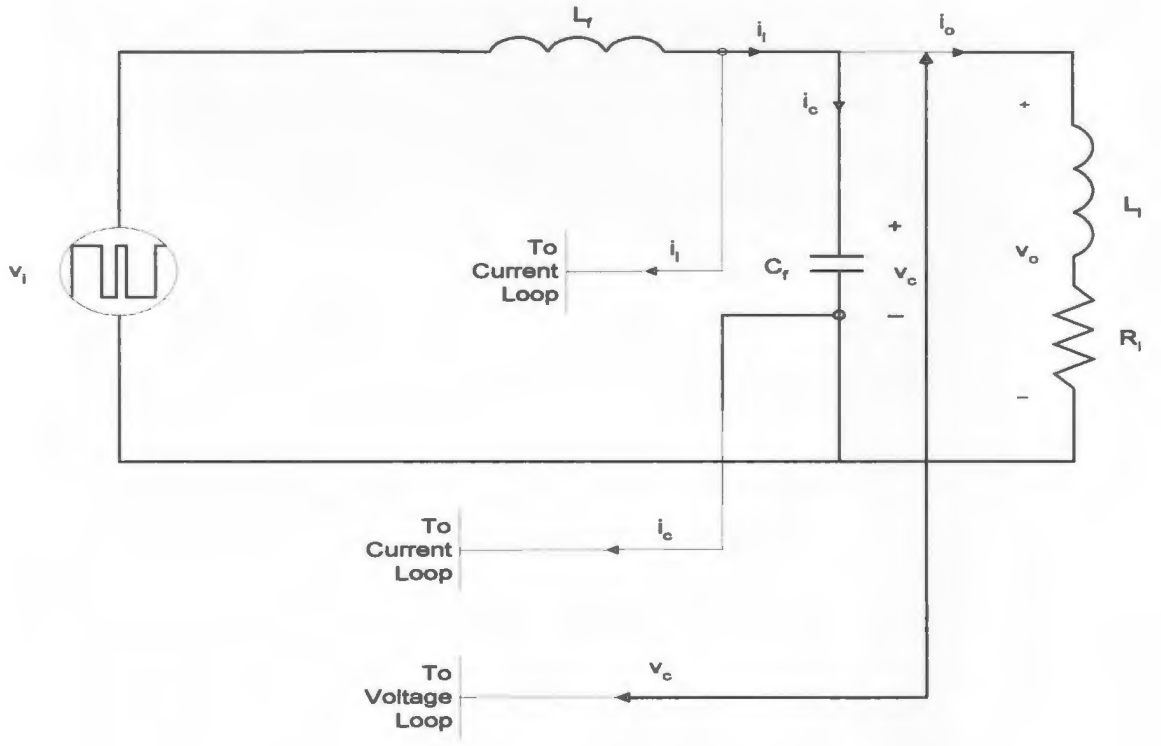

Figure 3.1 Equivalent circuit of the inverter-filter-load combination

As shown in the figure, the output voltage of the inverter, v_i is a PWM waveform. The resulting variables in the circuit will therefore be discontinuous in nature. But, a discontinuous signal can be expressed as a series of continuous signals according to Fourier analysis. Generally, any function can be expressed as a Fourier time series in the form of [18].

$$f(wt) = a_0 + \sum_{n=1}^{\infty} a_n \sin n\omega t + \sum_{n=1}^{\infty} b_n \cos n\omega t \tag{3.1}$$

In PWM switching, the controlled output signal has a low frequency, but the switching frequency is much higher than that of the output signal. Therefore, the modulating wave can be expressed in terms of the duty cycle, d. The coefficients in the Fourier series of equation (3.2) are given by [29].

$$a_0 = \frac{1}{2\pi} \int_{1-d1}^{1+d1} 1 \bullet d(\omega_S t) = d1 \tag{3.2}$$

$$a_n = 0 \tag{3.3}$$

$$b_n = (-1)^n \bullet \frac{2}{n\pi} \sin(n\, d_1 \pi) \tag{3.4}$$

Accordingly, the switching function can be expressed as

$$D = d_1 + \sum_{n=1}^{\infty} (-1)^n \bullet \frac{2}{n\pi} \sin(n\, d_1 \pi) \cos(n\omega_s t) \tag{3.5}$$

where d_1 is the time average or the duty cycle of the switching, and ω_s is the angular switching frequency.

The switching function includes both low and high frequency components. In a UPS application where the switching frequency is much higher than the output frequency, the components of the switching function can be neglected. Hence, only the fundamental frequency component is considered. State-space analysis is applied to controlled variables in a direct or indirect control. The state-space function reveals the relationship between these controlled variables and voltage source.

The half-bridge inverter has two switches, the upper one Q_1 and lower one Q_2. The two switches conduct alternately. When Q_1 is ON, Q_2 is OFF, and vice versa. Neglecting the higher frequency components, the output voltage of the inverter can be expressed in a continuous form as [37].

$$v_i = (2d_1 - 1)V_{dc} \tag{3.6}$$

The state–space analysis of the circuit shown in figure 3.1 results in the general state space representation.

$$\dot{x} = A\,x + B\,u \tag{3.7}$$

$$y = C\,x + D\,u \tag{3.8}$$

where the constant matrices, A, B, C, D are obtained as

$$A=\begin{bmatrix} -\frac{R_f}{L_f} & 0 & -\frac{1}{L_f} \\ 0 & -\frac{R_l}{L_l} & \frac{1}{L_l} \\ \frac{1}{C_f} & -\frac{1}{C_f} & 0 \end{bmatrix} \tag{3.9}$$

$$B=\begin{bmatrix} \frac{1}{L_f} & 0 & 0 \end{bmatrix}^T \tag{3.10}$$

$$C=\begin{bmatrix} 0 & 0 & 1 \end{bmatrix} \tag{3.11}$$

$$D=\begin{bmatrix} 0 \end{bmatrix} \tag{3.12}$$

The state variable, x represents the inductor current, output current and the capacitor voltage

$$\boldsymbol{x}=\begin{bmatrix} i_l & i_o & v_c \end{bmatrix}^T \tag{3.13}$$

and u presents the inverter output voltage. From equation 3.6, the u expression can be given by:

$$\boldsymbol{u}=v_i=\begin{bmatrix} 2d_1-1 \end{bmatrix}V_{dc} \tag{3.14}$$

The system output variable y is given by

$$\boldsymbol{y}=v_o \tag{3.15}$$

3.2.1 Small signal model of the inverter-filter load combination

In real-time control systems, there exist many disturbances that can influence the controlled variables. Disturbances can be caused by many factors such as load shifts, uncertain input signals and environment effects. These disturbances may drive the signal components of a control system to become worse, especially upon switching. The effects of those unwanted factors on the dynamic performance of the system should be studied. For this, equations are developed to determine which feedback-controlled variable would result in a successful operation of the system. Acceptable feedback variables should be chosen in the control regulator scheme. In the UPS system under consideration, it is assumed that the load voltage is to be maintained constant for variations in the load. Hence, a load current variable will not be suitable as a feedback variable. The disturbance signals are assumed to be superimposed on the steady-state variables and are expressed by a vector $\tilde{x}$. Thus equation (3.13) can be expressed as

$$x+\tilde{x}=\left[I_l+\tilde{i}_l \quad I_o+\tilde{i}_o \quad V_c+\tilde{v}_c\right] \tag{3.16}$$

where I_l, I_o and V_c represent the steady-state variables.

$$m=2d_1-1 \tag{3.17}$$

A modulating signal m corresponding to the duty cycle is expressed as [37]

Incorporating the small-signal variations in equation 3.14 gives

$$u+\tilde{u}=(m+\tilde{m})\left(V_{dc}+\tilde{V}_{dc}\right) \tag{3.18}$$

In equations 3.16 and 3.18 the disturbance signals are denoted by "~". When the above equations in vector form are written in algebraic forms, the disturbance signals exist in each algebraic equation. The equations become even more complex when the load disturbance and load current are considered, and it is almost impossible to solve these equations analytically.

The small-signal model of the inverter-filter-load combination is obtained by setting the steady-state variables to zero. The resulting small-signal model representation of the combination is given by the state-space equation.

$$\dot{\tilde{x}} = A_s \tilde{x} + B_s \tilde{m} \tag{3.19}$$

where $A_s = A$, $B_s = B$.

3.2.2 Transfer functions of the inverter-filter-load combination

From equation 3.19, the Laplace transform of the state-space vector in relation to the modulating signal can be obtained as the following equations:

$$G_p(s) = \frac{\tilde{x}(s)}{\tilde{m}(s)} = \left[sI - A_s \right]^{-1} B_s \tag{3.20}$$

From equation 3.20 the transfer functions of the feedback variables are obtained as:

$$\frac{\tilde{i}_c(s)}{\tilde{m}(s)} = \frac{V_{dc}}{L_f} \frac{s\left(s + \dfrac{R_l}{L_l} \right)}{s^3 + \dfrac{R_l}{L_l} s^2 + \dfrac{1}{C_f}\left(\dfrac{1}{L_f} + \dfrac{1}{L_l} \right) s + \dfrac{R_l}{L_l L_f C_f}} \tag{3.21}$$

$$\frac{\tilde{i}_l(s)}{\tilde{m}(s)} = \frac{V_{dc}}{L_f} \frac{s^2 + \frac{R_l}{L_l}s + \frac{1}{L_l C_f}}{s^3 + \frac{R_l}{L_l}s^2 + \frac{1}{C_f}\left(\frac{1}{L_l} + \frac{1}{L_f}\right)s + \frac{R_l}{L_f L_l C_f}} \tag{3.22}$$

$$\frac{\tilde{v}_c(s)}{\tilde{m}(s)} = \frac{V_{dc}}{L_f C_f} \frac{s + \frac{R_l}{L_l}}{s^3 + \frac{R_l}{L_l}s^2 + \frac{1}{C_f}\left(\frac{1}{L_f} + \frac{1}{L_l}\right)s + \frac{R_l}{L_l L_f C_f}} \tag{3.23}$$

As expected, the small signal transfer functions are the same as the transfer functions obtained in chapter 2.

3.3 Selection of PI Controllers

3.3.1 Frequency-Response of PI Controllers

As indicated in the previous chapter, the P-type linear controller results in steady-state error in the output voltage waveform. A PI-type controller is selected to modify the control system, and hence, improve the steady-state performance.

Consider the simple control system shown in figure 3.2. Formally, the design procedure for the cascade compensator $G_c(s)$ is more direct than that for the feedback compensator, $H_c(s)$.

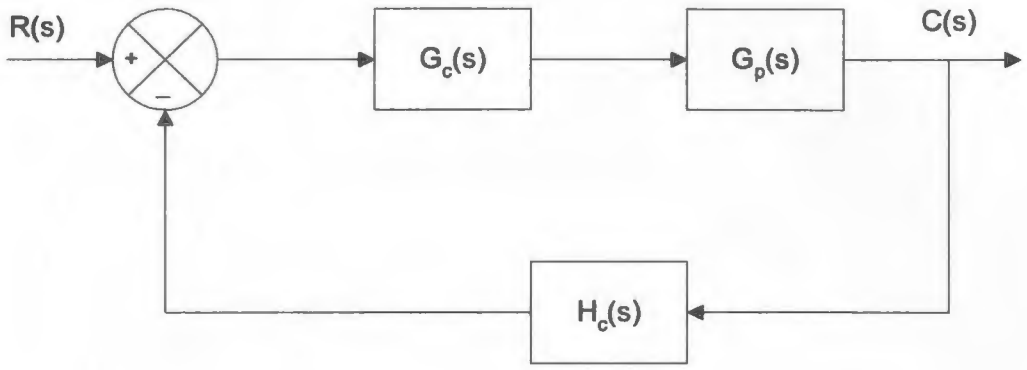

Figure 3.2: Basic control system

In UPS applications, the signal flow in the forward path goes from low to high energy level, while the signal goes back from high to low energy level in a feedback loop. Thus the forward path generally requires an amplifier for gain and/or isolation. The noise can be reduced by a greater amplifier gain in the forward compensator. The system developed in this thesis has a multiple loop control. The advantage of the multiple loop control is the capability of isolating a portion of a control system from the whole system. Also, some of the variables can be used to enforce stability. The control scheme under investigation has a current loop, which provides rapid changes during dynamic operation. Accurate and stable operation of the control system requires a proper compensator in the forward path.

The PI controller is less affected by small steady-state error since its value continues to increase with the existence of error, while the proportional controller cannot eliminate the steady-state error. When the input and output become equal in a PI controller, the error is to become zero.

Controller type 1 is the standard PI controller.

$$G_{c1}(s)=a_1+\frac{b_1}{s} \tag{3.24}$$

Controller type II is the second order PI controller.

$$G_{c2}(s)=\frac{c_2 s+d_2}{a_2 s^2+b_2 s+1} \tag{3.25}$$

Controller type III is a cascade of two second order PI controllers

$$G_{c3}(s)=\left(\frac{c_3 s+d_3}{a_3 s^2+b_3 s+1}\right)\times\left(\frac{c_4 s+1}{a_4 s^2+b_4 s+1}\right) \tag{3.26}$$

In a conventional control system, one technique used to measure the performance of the system is frequency response. The frequency response reflects the control system's behavior in the frequency-domain. Based on the frequency response, the noise will be removed to improve the performance of the control system. To reproduce the true signal and attenuate the noise, the compensators are designed to be band-pass or low-pass.

Figure 3.3 shows the characteristics for controller type I in the frequency-domain. The figure shows that the frequency bandwidth is narrow and the system is stable.

Figure 3.4 shows the characteristics for the controller type II in the frequency-domain. The figure shows that the controller is suitable for a wide frequency range with higher gain. And the phase value is between $\pm 90^{o}$ that can protect the control system from instability. Because of the wide range of frequency bandwidth, it is easy for noise

to invade the control system; feedback with other controllers is needed to minimize this noise.

Figure 3.5 shows the frequency-response for the controller type III. There is a wide frequency with a low-gain. In the designed control system, other compensators are needed to help in preventing the noise entrance by increasing the signal-to-noise ratio. The gain could be increased by adding a proportional controller K, which results in a multiplier factor corresponding to the gain of the controller and need a compensator for phase margin.

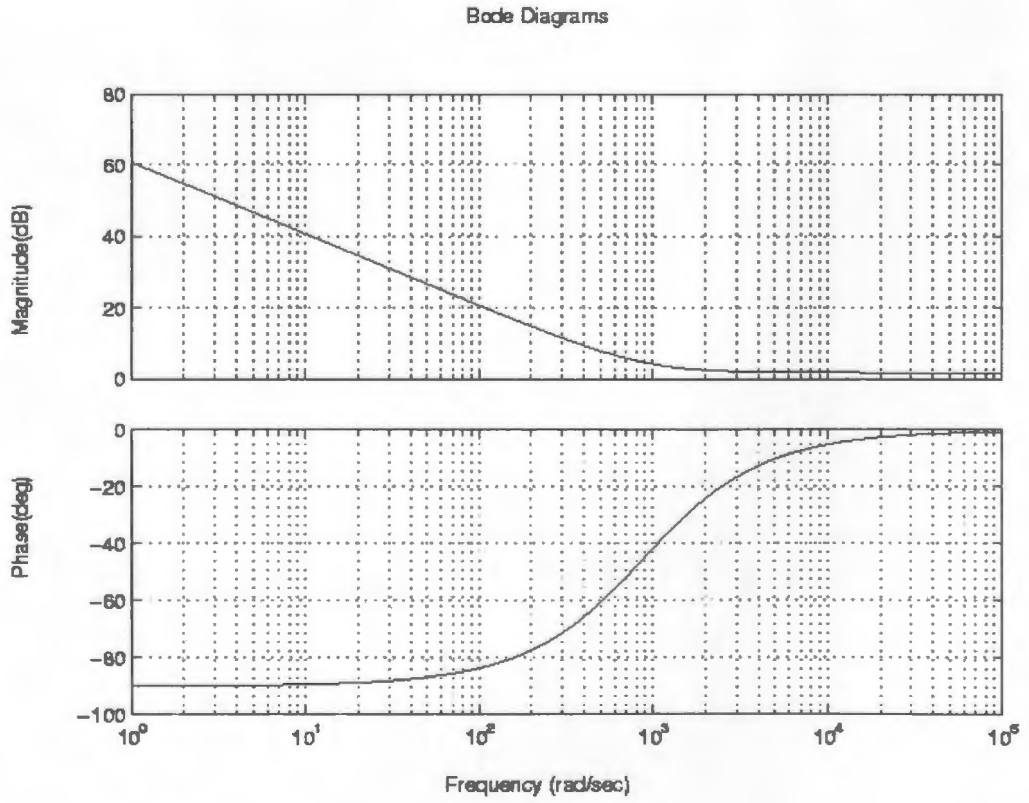

Figure 3.3: Frequency-Response for Controller Type I
a_1=1.23, b_1=1091

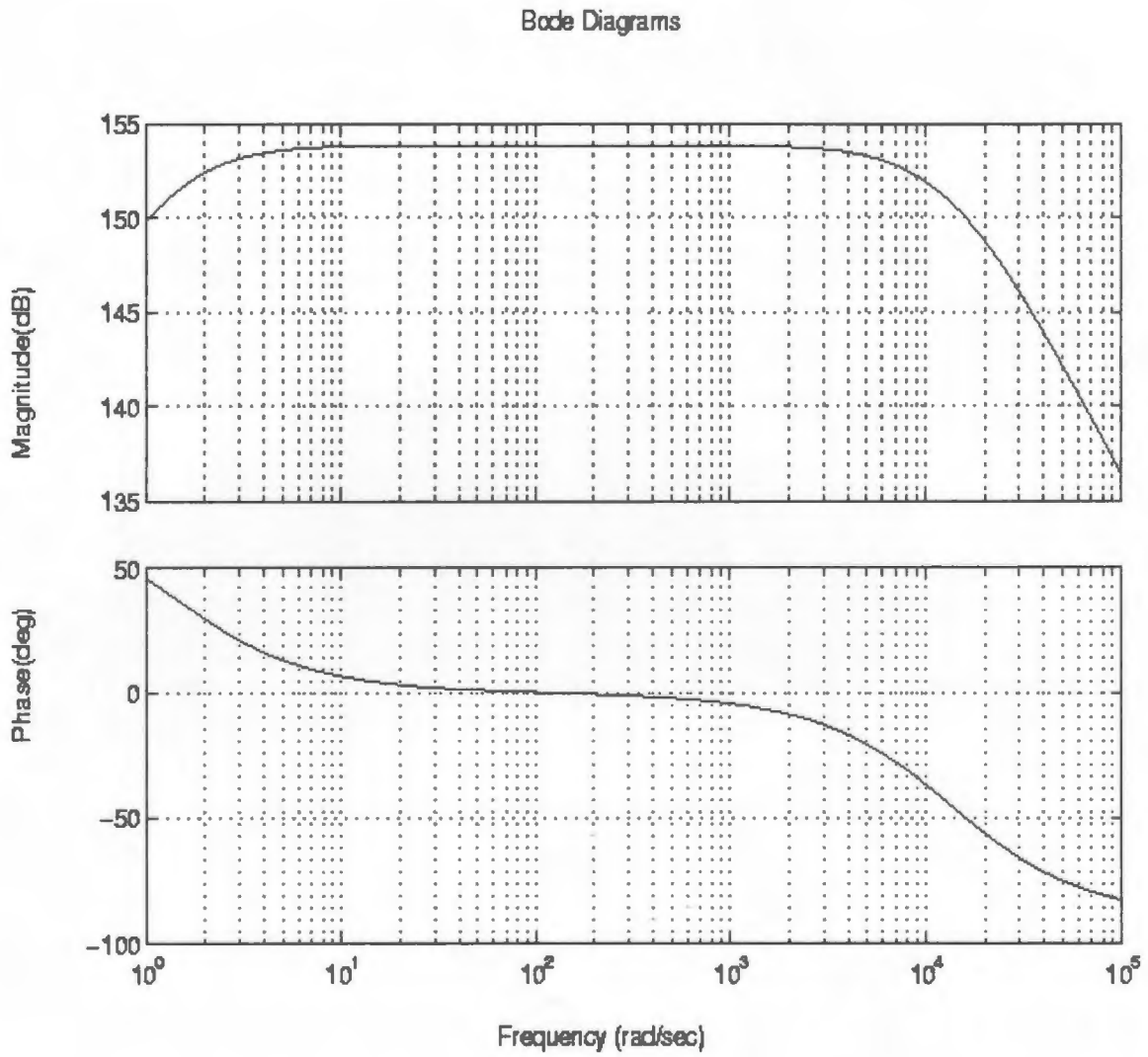

Figure 3.4: Frequency Response for Controller Type II
a_2=5.93e-5, b_2=0.7974, c_2=3.952e+7, d_2=3.6499e+5

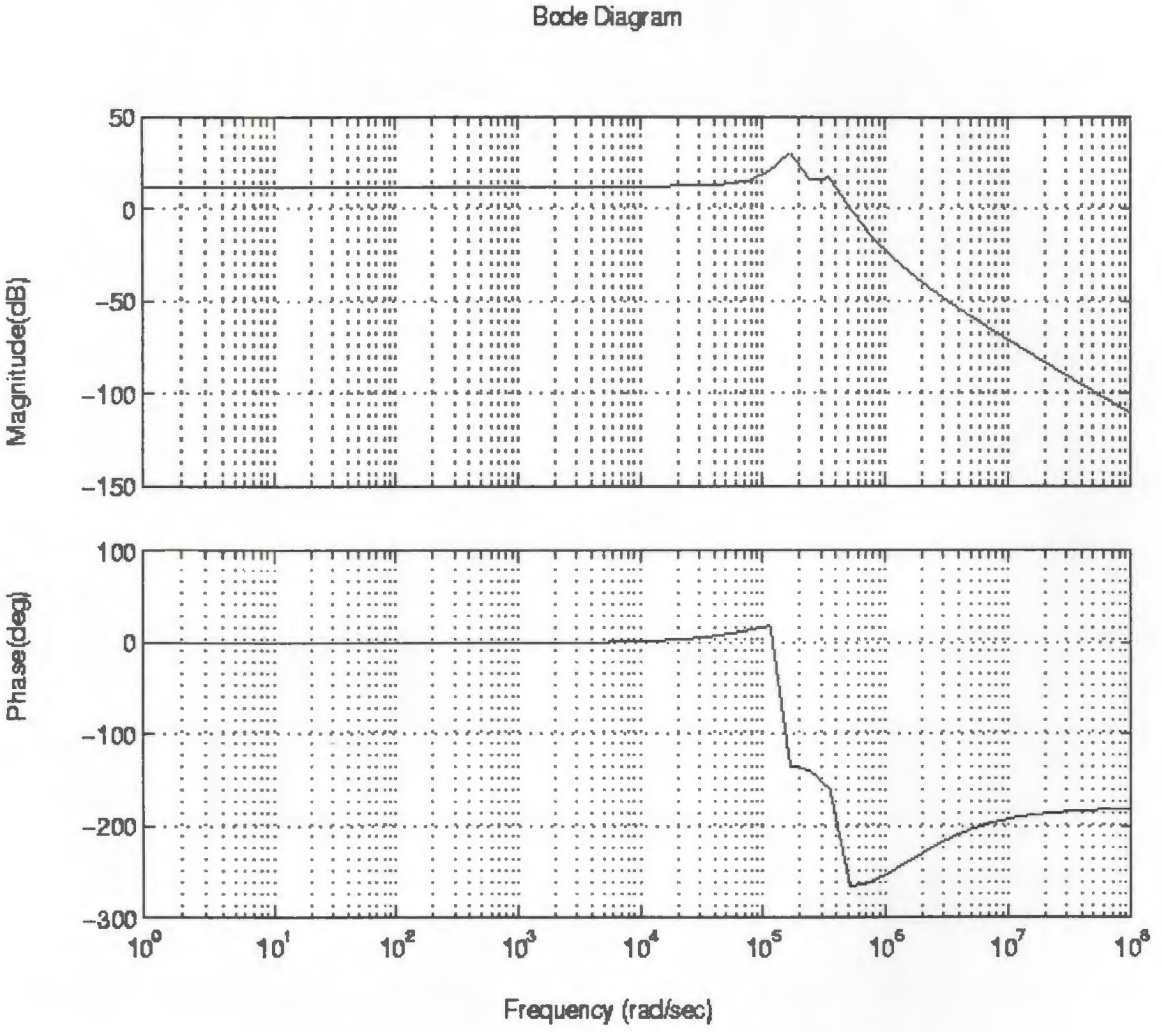

Figure 3.5: Frequency-Response for Controller Type III
a_3=6.6e-12, b_3=4.43e-7, c_3=2.2e-6, d_3=4.22
a_4=4.15e-11, b_4=2.74e-7, c_4=3.58e-6

3.3.2 Selection of PI Controllers for the UPS System

The steady-state errors of the various controllers are examined, and based on the results, a suitable controller is selected. The steady-state error is calculated for the combined transfer function, consisting of the transfer functions of the controller and the inverter-filter load combination, assuming the worse-case condition of a unit-step input.

The steady-state error is calculated as follows, assuming unity feedback (i.e. $H_c(s)=1$)

$$e_{ss} = \lim_{s\to\infty} s\left[\frac{1}{1+G(s)}\right]\frac{1}{s} \tag{3.27}$$

The following parameters are used in the calculation: L_f =3.8mH, C_f=83.3 μF, L_l=9.5mH, R_l=16Ω, V_{dc}=100 volts, f= 200 Hz. The combined transfer function G(s) is given by.

$$G(s)=G_c(s)\times\frac{\tilde{i}_c(s)}{\tilde{m}(s)} \tag{3.28}$$

$$G(s)=G_c(s)\times\frac{\tilde{V}_c(s)}{\tilde{m}(s)} \tag{3.29}$$

$$G(s)=G_c(s)\times\frac{\tilde{i}_l(s)}{\tilde{m}(s)} \tag{3.30}$$

where $G_c(s)$ represents the transfer function of the various controllers defined in equations 3.24 to 3.26.

The steady-error is calculated using Maple [27] correspond to $\tilde{v}_c(s)/\tilde{m}(s)$, $\tilde{i}_c(s)/\tilde{m}(s), \tilde{i}_l(s)/\tilde{m}(s)$. These values are shown in Table 3.1

Table 3.1: Steady-state error of different controllers

Controllers	$\tilde{v}_c(s)/\tilde{m}(s)$	$\tilde{i}_c(s)/\tilde{m}(s)$	$\tilde{i}_l(s)/\tilde{m}(s)$
Controller Type I a_1=1.23, b_1=1091	0	0.052	0
Controller Type II a_2=5.93e-5,b_2=0.7974,c_2=3.952e+7, d_2=3.6499e+5	$0.14*10^{-7}$	1	$0.22*10^{-6}$
Controller Type III a_3=6.6e-12, b_3=4.43e-7, c_3=2.2e-6, d_4=4.22 a_4=4.15e-11, b_4=2.74e-7, c_4=3.58e-6	0.0012	1	0.019

Based on the results of Table 3.1, controller type I produces the lowest value of steady-state error. However, the gain and bandwidth of the controller are small. Controller type II has very small steady-state errors for inductor current and capacitor voltage transfer functions. Since the controller has high gain and wide bandwidth, it is chosen as the PI Controller for the UPS system.

The parameters of the controller are chosen as:

a_2= 5.93*10^{-5}, b_2=0.7974, c_2=3.952*10^7, d_2=364990

As shown in Table 3.1, the steady-state error of this controller for capacitor current transfer function is rather high. This will be further investigated.

Controller type II is also chosen for the forward path of the outer voltage control loop in order to further minimize the amplitude and phase errors in the output voltage. The transfer function of the controller is expressed as

$$G_v(s)=\frac{c_5 s+d_5}{a_5 s^2+b_5 s+1} \tag{3.31}$$

These parameters in the expression are selected as: a_5=6.6*10^{-5}, b_5=0.44015, c_5=1.6575, d_5=107.5.

The open-loop transfer function of inner current loop can be written as

$$G_c(s)= G_{c2}(s)\times\frac{\tilde{i}_c(s)}{\tilde{m}(s)} \tag{3.32}$$

where $\frac{\tilde{i}_c(s)}{\tilde{m}(s)}$ is transfer function of output part and $G_{c2}(s)$ represents the transfer function of PI controller II.

The stability feature of this inner-loop is shown in Figure 3.6. It can be seen that the open-loop system has sufficient stability margin as: gain margin> 8 dB and phase margin > 30°. In particular, the bandwidth is expanded, which facilitates passing higher frequency signals. These parameters of the system are L_f= 3.8 mH, C_f =83.3 μF, Z_l=20 Ω and V_{dc}=100 V.

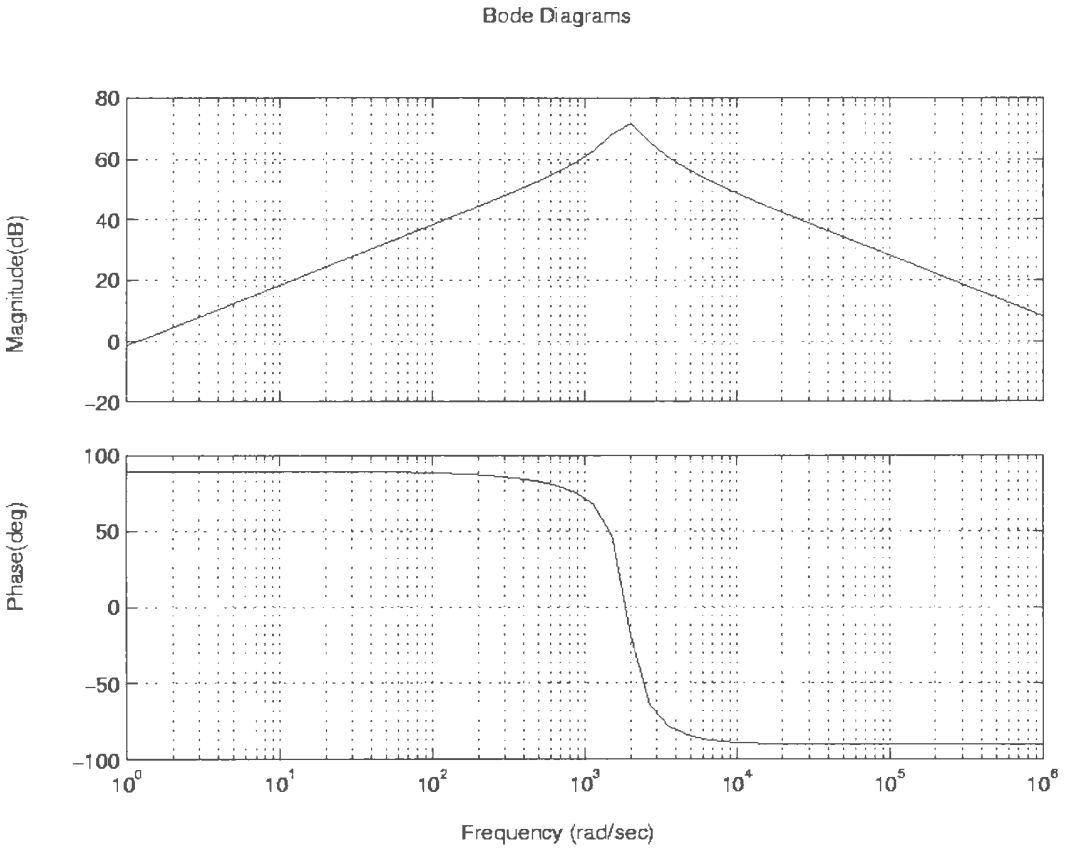

Figure 3.6: Bode diagram of the open-loop transfer function of the inner current loop of the UPS system: L_f=3.8 mH, C_f= 83.3 μF, Z_l= 20 Ω and V_{dc}=100 V.

3.3.3 Selection of feedback compensators

The choice of a feedback compensator is based on the complexity of the basic system, the accessibility of insertion points, the form of the signal being fed back, the signal being compared, and the desired improvement. In this study, the feedback channels mainly consist of filters. A suitable type of feedback filter which improves the performance of the control system is discussed below.

The need to determine the number of differentiating terms in the feedback compensator is permitted in the numerator of $H_c(s)$ in the feedback loop with lag-lead compensator. The lag compensator can attenuate the high frequency signal and noise and improve the steady-state accuracy. The lead compensator can improve the stability of the system. The lag-lead compensator results in good steady-state response. It has a large increase in the undamped natural frequency.

As a result, the feedback compensator can be expressed in a general form as

$$H_c(s)=\frac{c_6 s+e_6}{a_6 s^2+b_6 s+d_6} \tag{3.33}$$

As shown in Table 1, the steady state error of $\tilde{i}_c(s)/\tilde{m}(s)$ in controller II is high. In this section, the steady-state error is calculated by considering the transfer functions of the feedback compensator, the PI controller and the inverter-filter-load combination (plant). These transfer functions are denoted as $H_c(s)$, $G_c(s)$, $G_p(s)$ in figure 3.2. The transfer function of the control system shown in figure 3.2 is given by [24]:

$$\frac{C(s)}{R(s)}=\frac{G(s)}{1+G(s)H_c(s)} \tag{3.34}$$

$$\frac{E(s)}{R(s)}=1-\frac{G(s)}{1+G(s)H_c(s)} \tag{3.35}$$

The steady-state error of the system is given by

$$e_{ss}=\lim_{s\to 0} s\times\frac{1+G(s)(H_c(s)-1)}{1+G(s)H_c(s)} \tag{3.36}$$

where G(s) is the transfer function of the compensator and the plant.

Table 2 shows the effect of the feedback compensator parameters on the steady-state error for the plant transfer function, $\tilde{i}_c(s)/\tilde{m}(s)$. The parameters of the PI controller are given in Table 3.1. The parameters of the transfer function G(s) and the feedback compensator $H_s(s)$ are used in equations 3.36 to calculate the steady-state error. Maple is used to compute the results.

Table 3.2 Steady-state error with feedback compensator for $\tilde{i}_c(s)/\tilde{m}(s)$

Feedback compensator parameters	Steady-state error
a_0=6.72e-8, b_0=7.69e-5, c_0=1, d_0=1, e_0=0.	-17.2
a_0=6.72e-8, b_0=7.69e-5, c_0=4.99e-5, d_0=1, e_0=1	0.052
a_0=6.72e-8, b_0=7.69e-5, c_0=0, d_0=3, e_0=1	-1.57

As shown in Table 3.2, the steady state error for certain controller parameters is less than unity when the feedback compensator is considered. The following parameters are selected for the feedback compensator.

a_0= 6.72*10^{-8}, b_0=7.69*10^{-5}, c_0=4.99*10^{-5}, d_0=1, e_0=1.

3.4 Summary

In this chapter, a general and dynamic model of the inverter-filter-load combination (plant) is developed using the state-space analysis techniques. The model is used to obtain the transfer functions of the plant in terms of three possible feedback variables, namely capacitor current, capacitor voltage (output voltage) and filter-inductor current.

In order to select a suitable PI controller for the control of the UPS system, the frequency response characteristics of three-types of controllers are examined. Also the

steady-state error of the compensators with the three transfer functions of the plant are investigated. It is shown that the second order PI controller results in a wide frequency bandwidth and negligible small steady-state error for the output voltage and inductor current transfer functions. Suitable parameters of the PI controller are selected and used in conjunction with the transfer functions of the capacitor current and a second order feedback compensator filter to examine the steady- state error. It is shown that using a second order controller in the feedback path significantly reduces the steady-state error associated with the capacitor current transfer function.

The models and configurations of the PI controllers and feedback compensators are used to develop various control strategies for the UPS system in the next chapter.

Chapter 4

Control Strategies for the UPS System

4.1 Introduction

In this chapter, three control strategies that provide sinusoidal output voltage waveforms are presented. The basic differences between the control strategies are discussed by comparing the outputs at different frequencies. The feasibility of the strategies is demonstrated by simulation using SIMULINK, and their inherent features are discussed.

4.2 Two-Loop Control Strategy

The basic two-loop control scheme presented in chapter 2 is modified to include P controllers and feedback compensators. The structure of the control strategy is shown in Fig. 4.1. It consists of an inner capacitor current loop which includes a feedback compensator and a PI controller in the forward path. The load voltage constitutes the outer loop, which contains a feedback compensator and a second order compensator in the forward path. The strategy also incorporates a current command. The details of the

SIMULINK model and the parameters of the individual blocks in the control strategy are given in Appendix A, and the simulation procedure is exhibited in Appendix C.

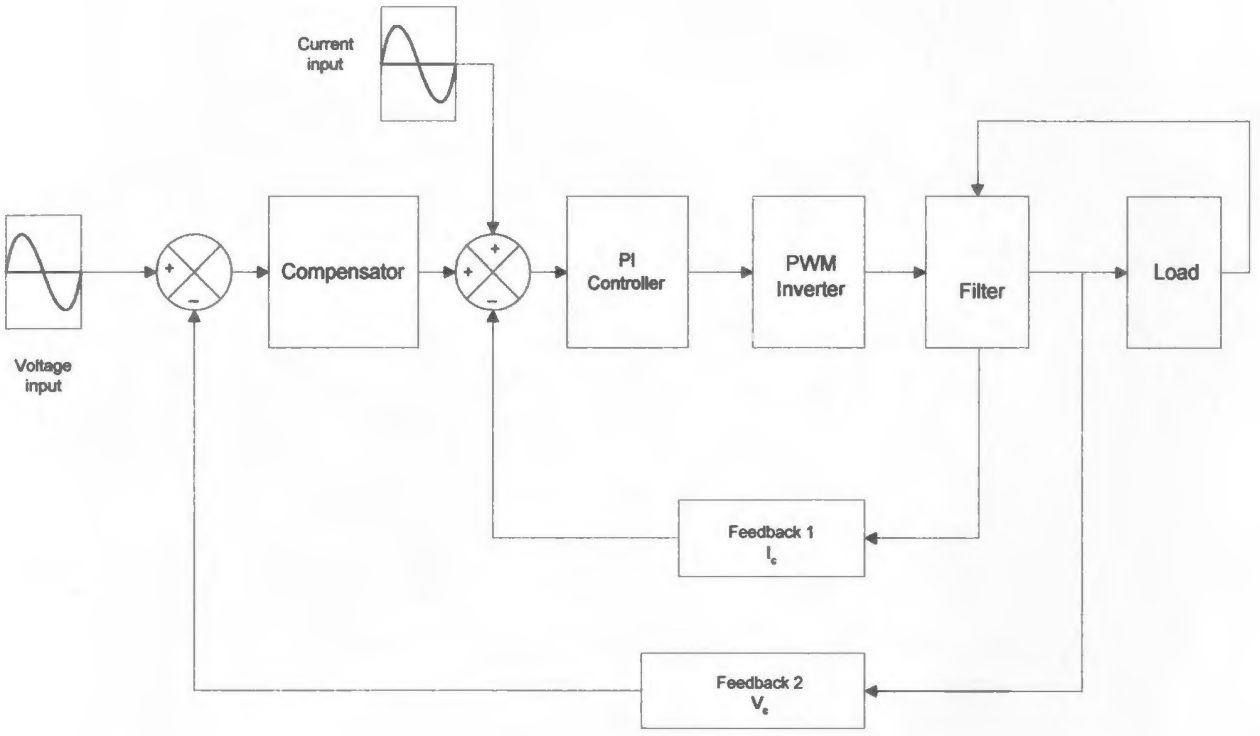

Figure 4.1: The structure of the two-loop control strategy

The control strategy is simulated at two different frequencies, f=60Hz and f=400Hz for the following inverter-filter-load parameter, V_{dc} = 100 Volts, L_f = 7.5 mH, C_f = 71.4 μF, R_l = 16 Ω, L_l = 4.7 mH. PI controllers are used in this two-loop control model. Again, L_f and C_f value need to be adjusted to yield the optimum output

performance. Compared with the basic SIMULINK model, C_f value is reduced to 71.4 μF allowing the passing of the high frequency signals.

Figure 4.2 shows the output voltage and capacitor current waveforms at f=60Hz. It is observed that both the output voltage and capacitor current waveforms are highly distorted. The waveforms show that for the selected parameters, the performance of the control strategy is poor.

Figure 4.3 shows the output voltage and capacitor current waveforms at f=400Hz. With the introduction of PI controllers and feedback compensators, the waveforms indicate that stable operation at higher frequencies is feasible. The quality of the waveforms are improved at this frequency.

The output voltage waveforms at the two frequencies indicate that the voltage utilization factor of the control strategy U_v, (defined as the peak value of the output voltage expressed as a percentage of the dc voltage V_{dc}), is very low. For f=60Hz, U_v=74.3%, and for f=400Hz, U_v=51.9%. This indicates that the efficiency of the control strategy is very low.

The quality of waveforms at f=60Hz can be improved by changing the parameters of the L-C filter. Figures 4.4 and 4.5 show the output voltage and capacitor current waveforms at f=60Hz and f=400Hz respectively for L_f=3.8mH and C_f=83.3μF. It is seen that the voltage utilization at f=60Hz is improved from U_v=74.3% to U_v=75.7%, while the quality of the waveforms at f=400Hz is degraded and the voltage utilization is improved from U_v=51.9% to U_v=71.8%. Hence, changing the parameters of the L-C filter only is not enough to achieve an improved performance at the two frequencies. It

may be necessary to adjust the parameters of the controllers to achieve acceptable performance at the two frequencies.

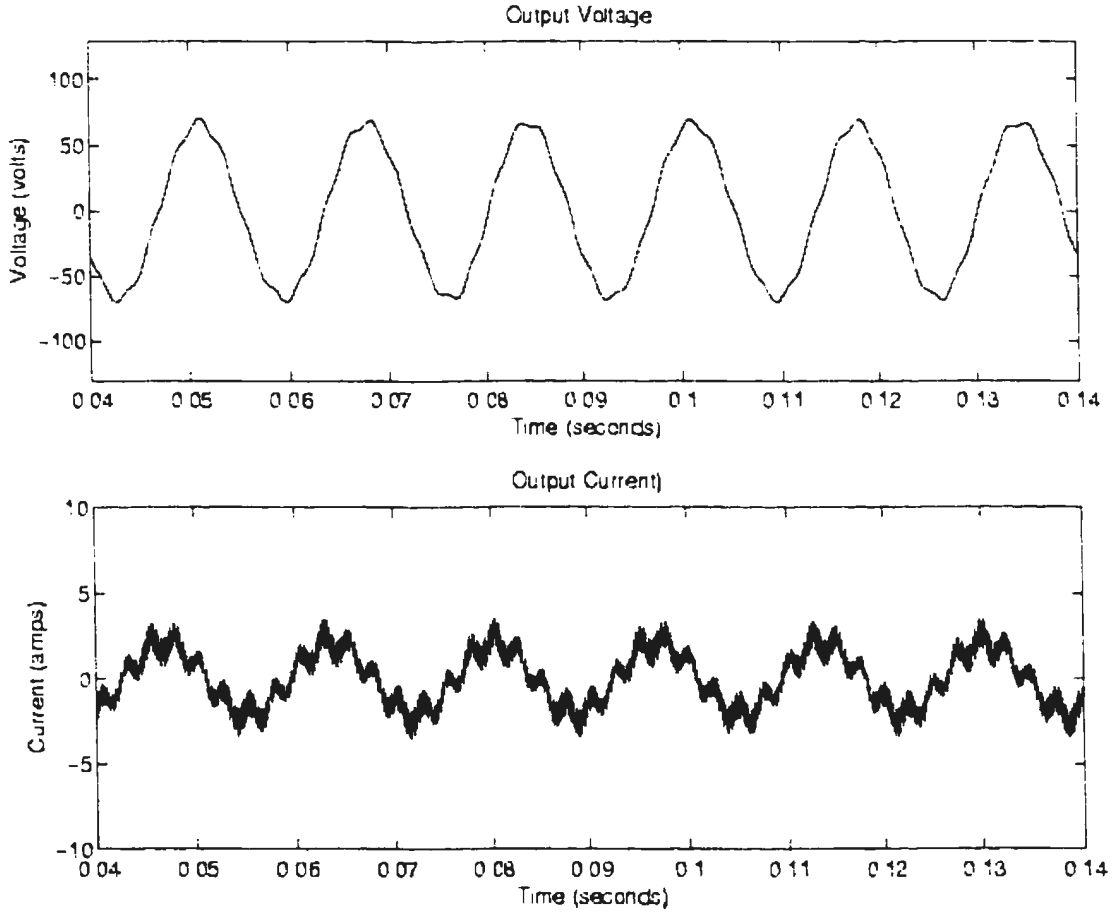

Figure 4.2: Output voltage and capacitor current waveforms at 60Hz (Basic two-loop control)
(R_l=16Ω, L_l=4.7mH, L_f=7.5mH, C_f=71.4μF, V_{dc}=100V, f_s=4.2kHz)

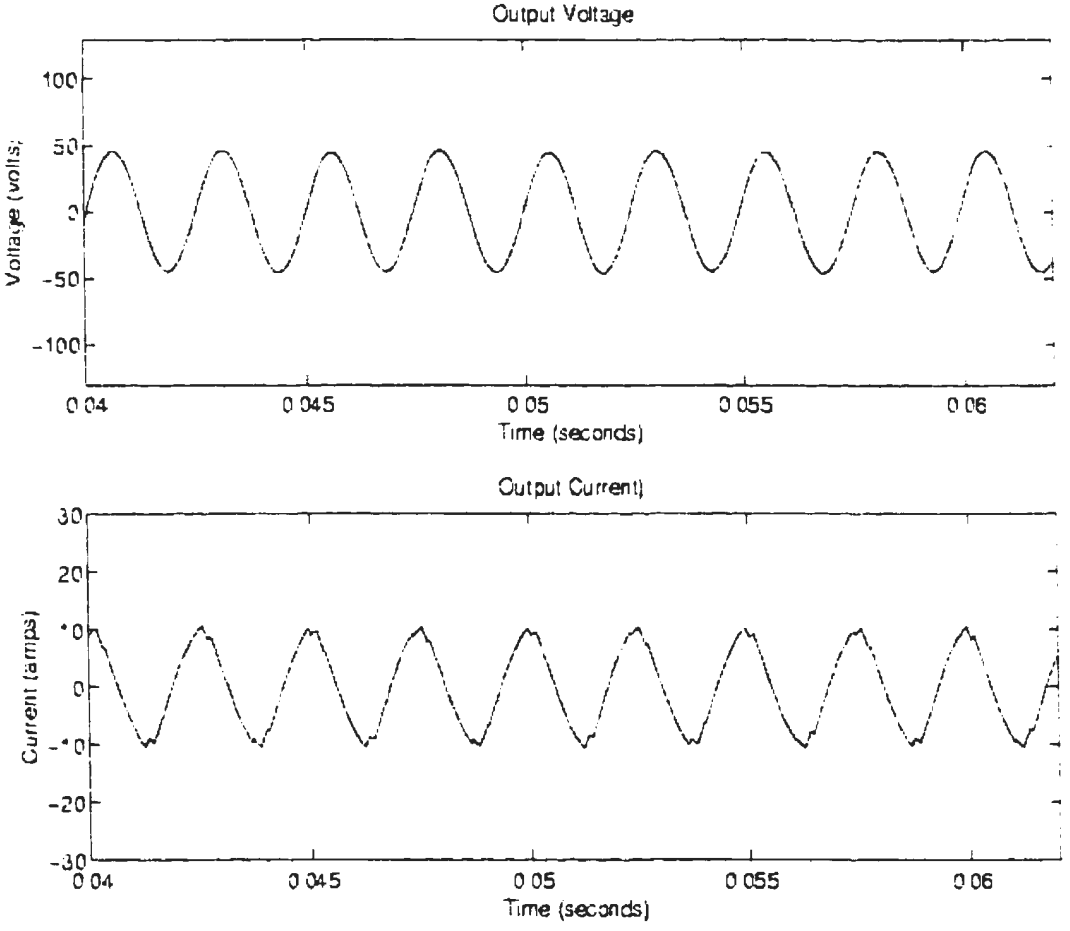

Figure 4.3: Output voltage and capacitor current waveforms at 400Hz
(Basic two-loop control)
(R_l=16Ω, L_l=4.7mH, L_f=7.5mH, C_f=71.4μF, V_{dc}=100V, f_s=4.2kHz)

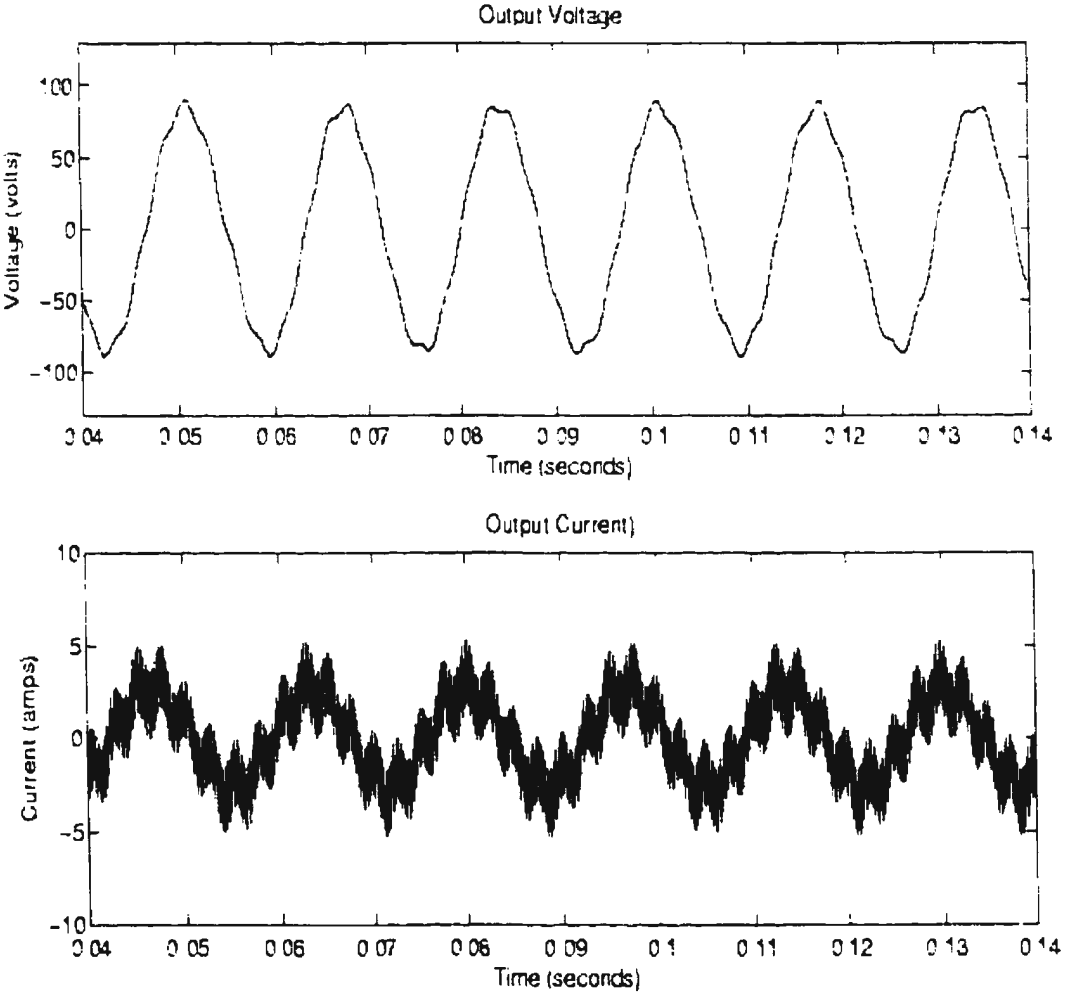

Figure 4.4: Output voltage and capacitor current waveforms at 60Hz
(Basic two-loop control(changed))
(R_l=16Ω, L_l=4.7mH, L_f=3.8mH, C_f=71.4μF, V_{dc}=100V, f_s=4.2kHz)

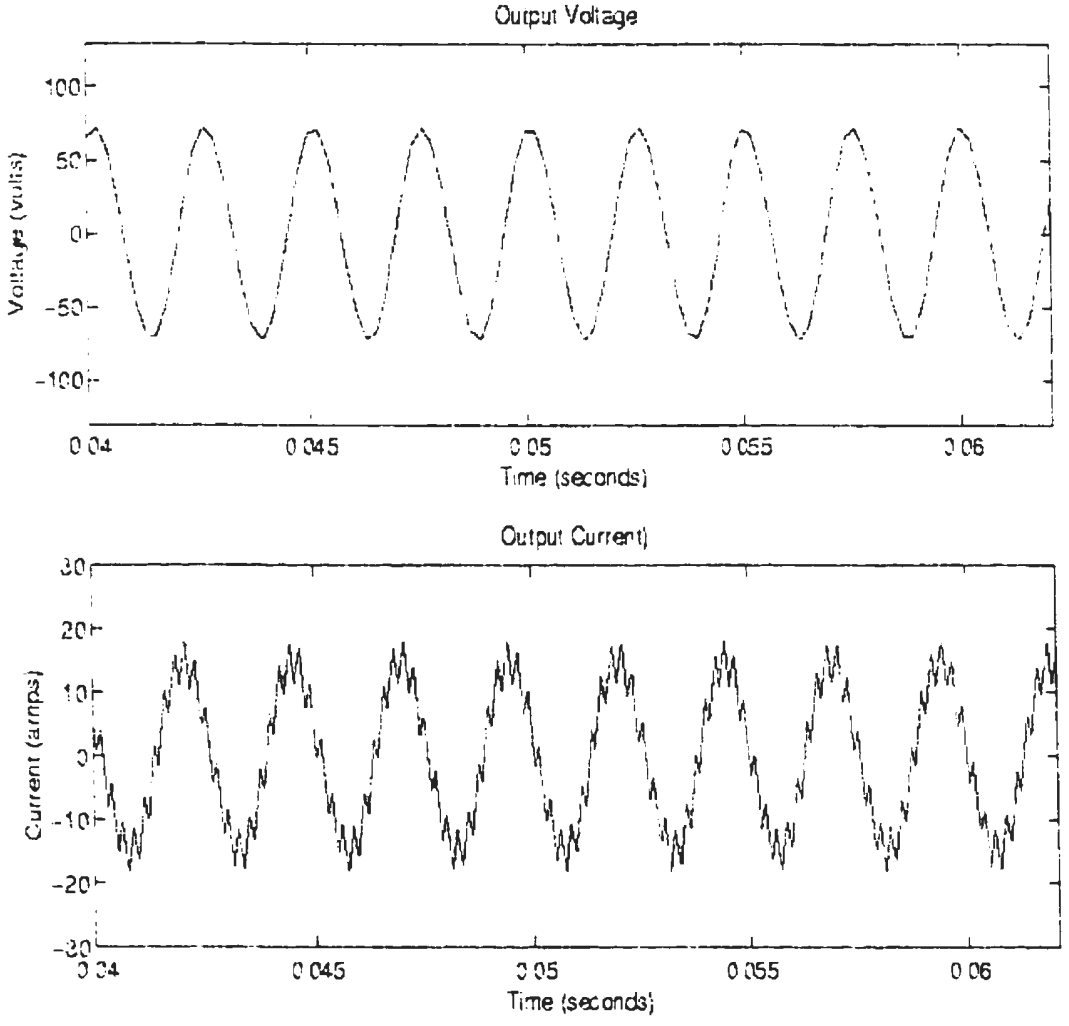

Figure 4.5: Output voltage and capacitor current waveforms at 400Hz
(Basic two-loop control (changed))
(R_l=16Ω, L_l=4.7mH, L_f=3.8mH, C_f=71.4μF, V_{dc}=100V,
f_s=4.2kHz)

4.3 The Modified Two-loop Control Strategy

The simulation for the previous two-loop control strategy has shown that only adjusting L-C filter values cannot achieve optimum output at both frequency ends (60 Hz and 400 Hz) which suggest that controllers have to be changed in order to optimize the performance. For this reason, PI controllers with higher gain and bandwidth used in the modified two-loop control strategy as shown in Figure 4.6. The strategy includes PI controllers in the forward path of the output voltage and capacitor current loops. The details of SIMULINK model are shown in Appendix A. Unlike the basic two-loop control strategy, this scheme does not employ an external current signal for the following reasons:

1. Although the external current command can help the control system to provide a high quality output voltage, it is not easy to implement.
2. When the input voltage command and the external current command are derived from the same signal, the external current command arrives at the input of the inner current loop earlier that the compensated error signal from the outer voltage loop. The delays caused by the PI controller causes steady-state phase errors in the output.

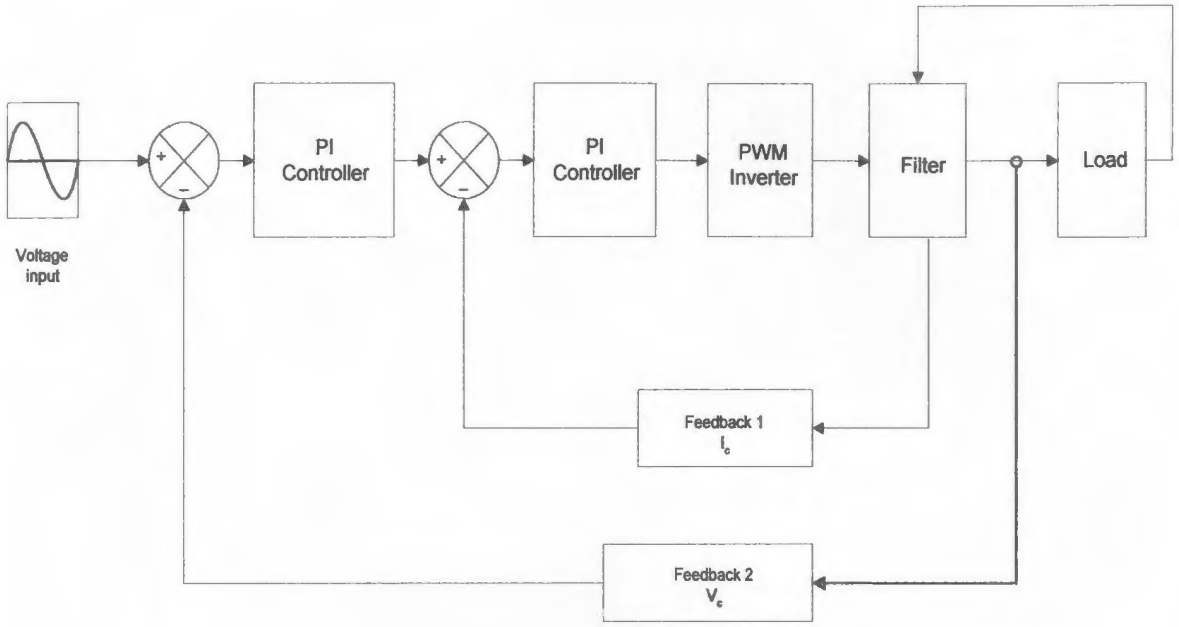

Figure 4.6: The structure of modified two-loop control strategy

Again, since different controllers are employed, a new set of L-C filter of SIMULINK is tried out as follows.

Z_l=20 Ω (load impedance as same in following part)

V_{dc}=100 V, f_s=4.2 kHz,

L_f= 3.8mH, C_f =83.3μF,

R_l = 16Ω, L_l = 31.85mH, (f=60Hz)

R_l = 16Ω, L_l =4.8 mH, (f=400Hz)

The details of the SIMULINK model and the parameters of the individual blocks and given in Appendix A

The control strategy is simulated at two frequencies, f=60Hz and f=400Hz. Figures 4.8 and 4.9 show the output voltage and capacitor current waveforms at f=60Hz and f=400Hz respectively. The waveforms reveal that the control strategy produces high quality output voltage waveforms at the two frequencies. In addition, the control strategy results in a higher uniform voltage utilization at the two frequencies (U_v=88.3% for f=60Hz and U_v=88.8% for f=400Hz)

4.4 The Three-Loop Control Strategy

The choice presented in chapter 3 showed that it is possible to employ the three variables associated with the load filter in a control strategy to improve the performance of the UPS system. The structure of the three-loop control strategy is shown in Fig 4.7. The strategy uses the filter inductor current as a second inner current loop in addition to the inner capacitor current loop and the output voltage loop. Hence the term, three-loop control strategy. The strategy also incorporates PI controllers in the forward path of the current loops and the voltage loop, as well as feedback compensators. The details of the SIMULINK model and the parameters of the control strategy are given in Appendix A.

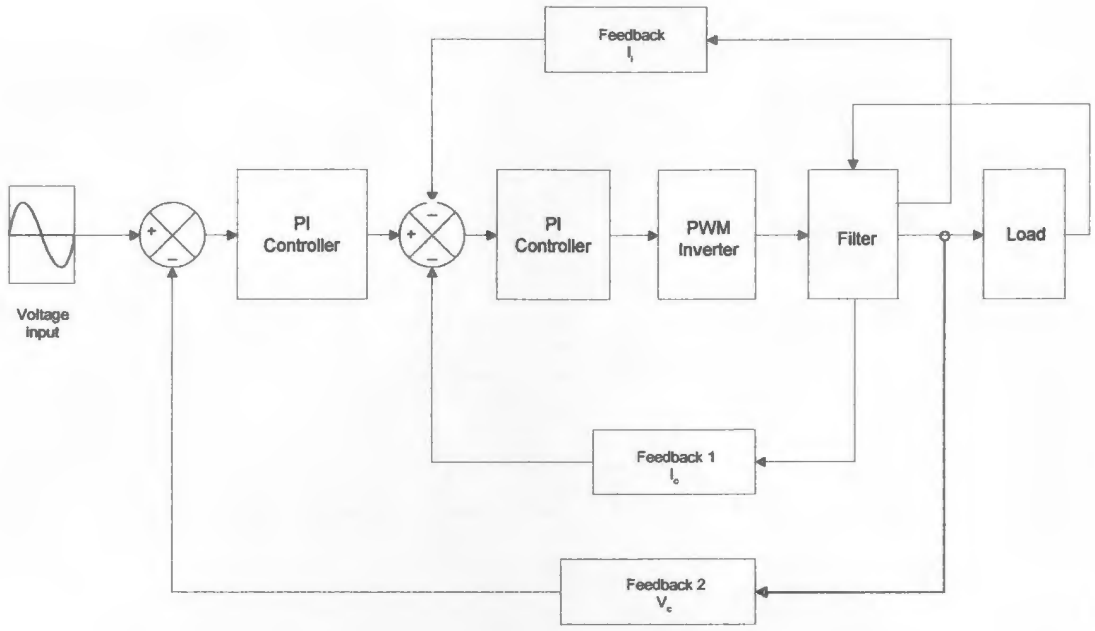

Figure 4.7: The structure of three-loop control strategy

The control strategy is simulated at two frequencies, f=60Hz and f=400Hz for the same load impedance of Z_l=20Ω. The following parameters of the inverter-filter-load circuit of the control strategy are used for the SIMULINK simulation.

V_{dc}=100 V, f_s=4.2 kHz,

L_f=3.8mH, C_f= 83.3μF,

R_l = 16Ω, L_l = 31.85mH, (f=60Hz)

R_l=16Ω, L_l = 4.7mH, (f=400Hz)

Figures 4.10 and 4.11 show the output voltage and capacitor current waveforms at f=60Hz and f=400Hz respectively. The waveforms reveal that the control strategy produces high quality output voltage waveforms at the two frequencies. The voltage utilization factors are U_v=100 % for f=60Hz and U_v=99.6% for f=400Hz. Additional

waveforms for different load parameters are given in Appendix B. These waveforms confirm the feasibility of the three-loop control strategy and its robustness for variations in load parameters.

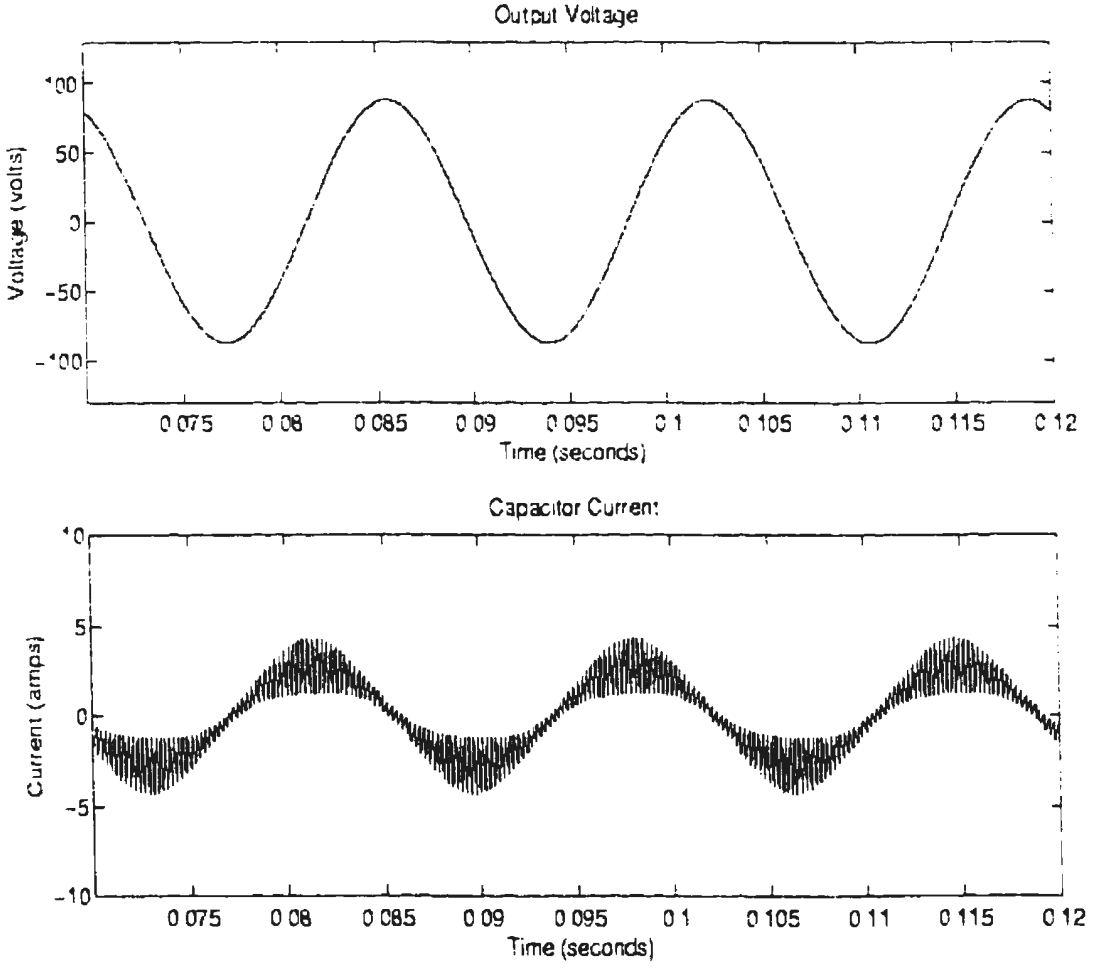

Figure 4.8: Output voltage and capacitor current waveforms at 60Hz
(Modified two-loop control)
(R_l=16Ω, L_l=31.85mH, L_f=3.8mH, C_f=83.3μF, V_{dc}=100V, f_s=4.2kHz)

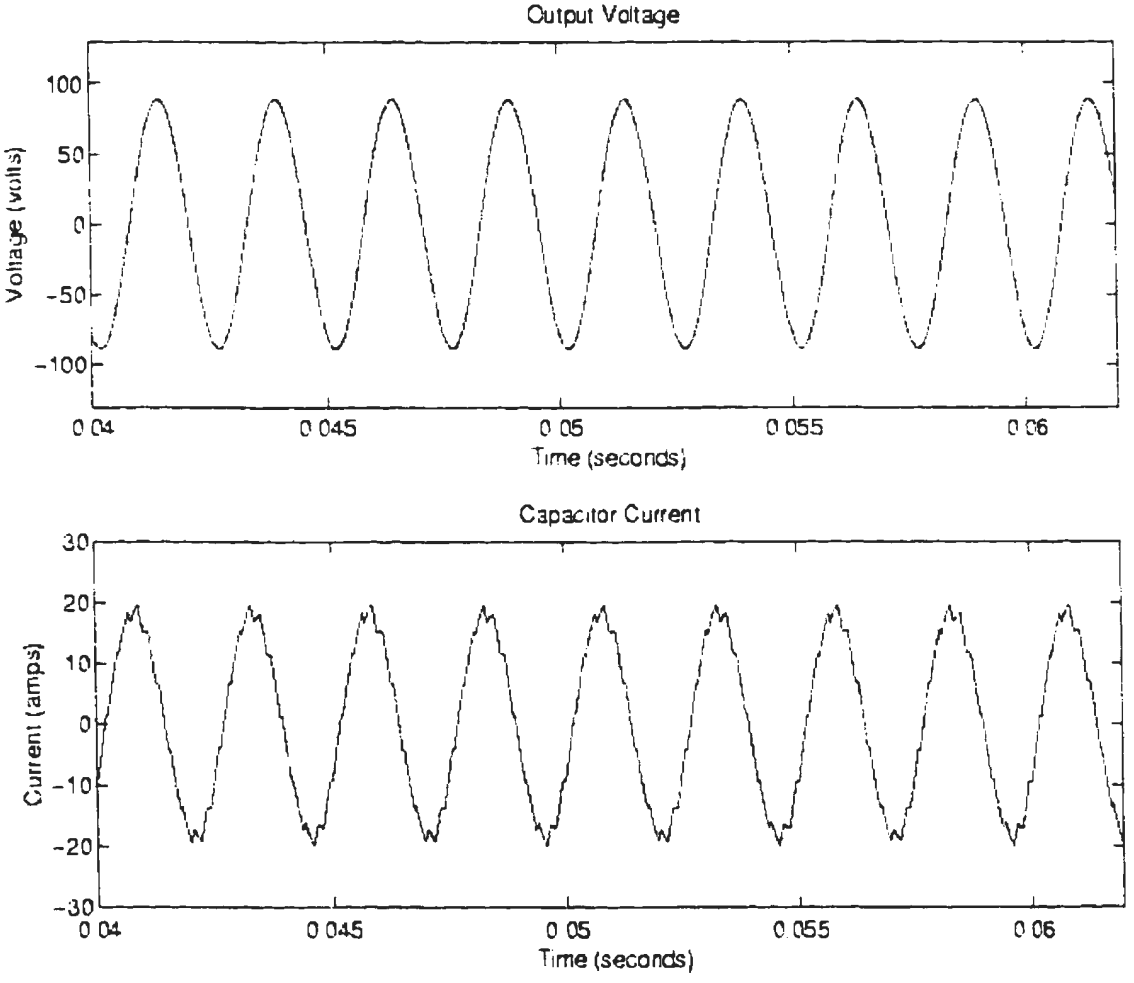

Figure 4.9: Output voltage and capacitor current waveforms at 400Hz
(Modified two-loop control)
(R_l=16Ω, L_l=4.8mH, L_f=3.8mH, C_f=83.3μF, V_{dc}=100V, f_s=4.2kHz)

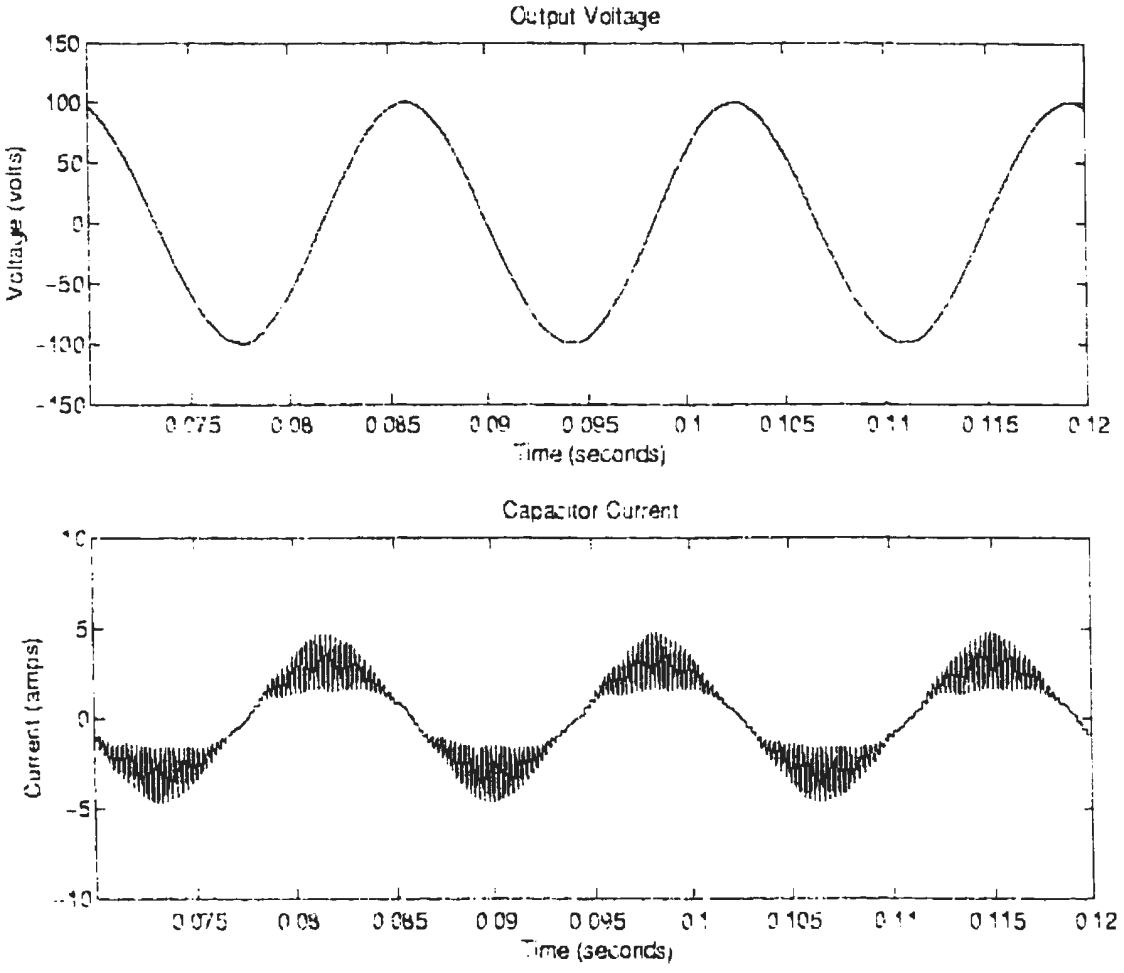

Figure 4.10: Output voltage and capacitor current waveforms at 60Hz (Three-loop control)
(R_l=16Ω, L_l=31.85mH, L_f=3.8mH, C_f=83.3μF, V_{dc}=100V, f_s=4.2kHz)

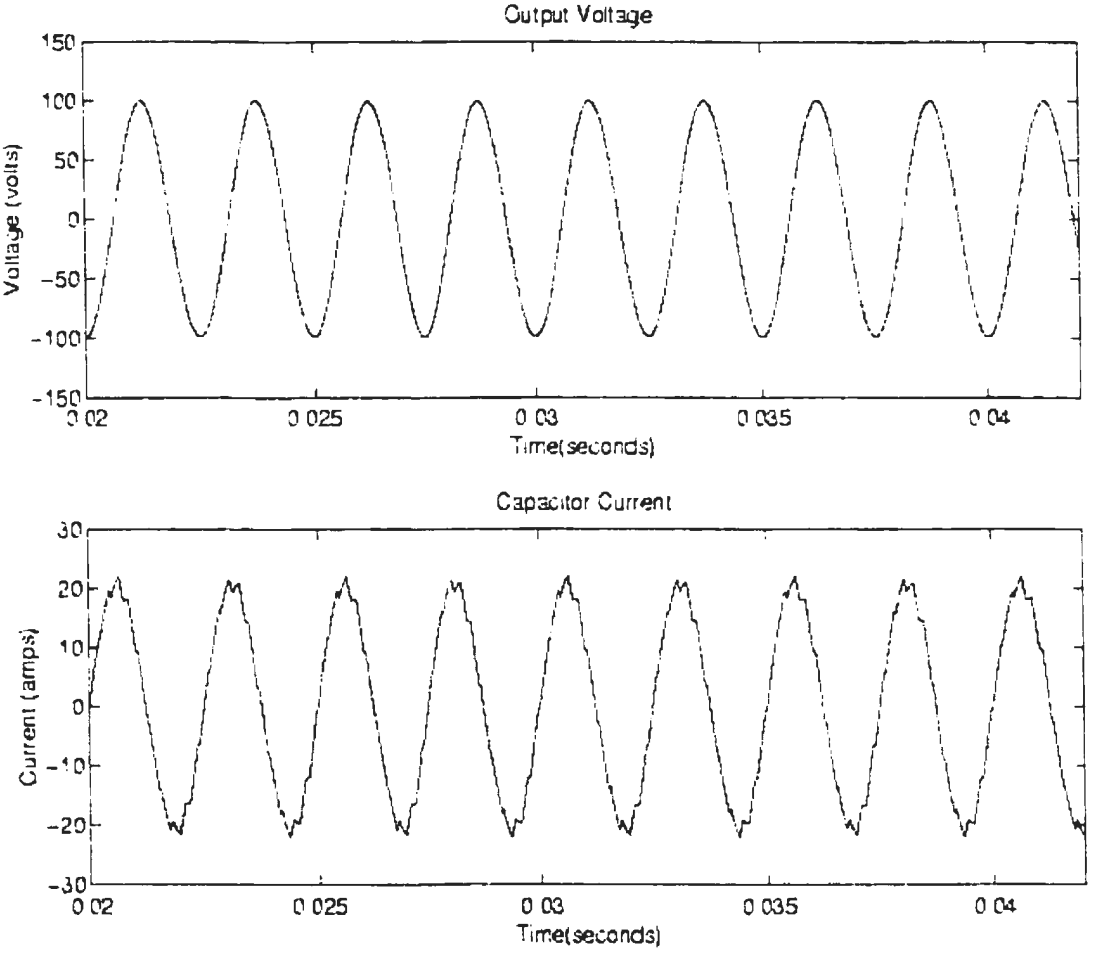

Figure 4.11: Output voltage and capacitor current waveforms at 400Hz (Three-loop control)
(R_l=16Ω, L_l=4.8mH, L_f=3.8mH, C_f=83.3μF, V_{dc}=100V, f_s=4.2kHz)

4.5 Summary

In this chapter, the feasibility of three control strategies for the UPS system was demonstrated through SIMULINK simulation. The basic two-loop control strategy needed an external current to achieve a high quality voltage waveform, although the strategy could not provide uniform performance at the two standard frequencies of 60Hz and 400Hz. In addition, the control strategy required a large output filter to achieve a high quality output voltage waveform and the voltage utilization was found to be poor. The modified two-loop control strategy provided performance improvement in voltage utilization and reduced filter rating. Further improvements were obtained in the three-loop control strategy. These improvements were achieved at the expense of an additional current sensor. The performance of the modified and three-loop control strategies is investigated further in the next chapter.

Chapter 5

Performance Evaluation of the UPS System

5.1 Introduction

In chapter 4, three control strategies for the UPS system were developed, and their feasibility was demonstrated at the two standard frequencies. This chapter focuses on the performance of two of the control models. The goal is to achieve a control strategy capable of operating at a high frequency with rapid dynamic response. To reach this goal, the operation of the control models at various frequencies and the characteristics of the control models under steady state and dynamic operations are studied in this chapter. In addition, the effects of the control parameters on the performance of the modified two-loop and three-loop control strategies are investigated. The models of the control strategies are implemented in SIMULINK. The results of the simulation are presented in the chapter. It is shown from the results that the three-loop control strategy has a robust performance.

5.2 Simulation Set-up

Figure 5.1 shows the general structure of a multiple feedback control system for UPS. The control system consists of the following components: a current loop and a voltage loop (for the three-loop control strategy, an inductive loop is added as the third loop (represented by dashed line), a PI controller for voltage adjustment (PI_v), a PI controller for current adjustment (PI_c), a comparator, a voltage-source PWM inverter, a L_f –C_f filter, a resistive-inductive load R_l – L_l and filters F_1, F_2 and F_3 in the inductor, capacitor current and load voltage feedback paths respectively. The SIMULINK models of the individual blocks in the system have been discussed in the previous chapters. A typical SIMULINK model of the system is given in Appendix A.

The simulation results for steady state operation are obtained for a fixed load of Z_l=20Ω at a power factor of 0.8 lagging for the two standard frequencies. For f=60Hz, R_l=16Ω and L_l=31.83mH, and for f=400Hz, R_l=16Ω and L_l=4.8mH. The inverter and filter parameters are V_{dc}=100V, f_s=4.2kHz and L_f=3.8mH, C_f=83.3μF.

5.3 Performance of the Modified two-loop Control Strategy

In this section, the simulation results for the output voltage and capacitor current, THD values, and dynamic responses at the two frequencies (f=60Hz and f=400Hz) in the

modified two-loop control strategy for a linear R-L load are presented. The characteristics of the two-loop control scheme are demonstrated.

5.3.1 Output Voltage and Capacitor Current Waveforms

Figures 5.2 and 5.3 show the waveforms of the inner-loop current and the outer-loop voltage at f=60Hz and f=400Hz, respectively. The control system operated successfully at these standard frequencies. The voltage utilization was found to be 88.3% at f=60Hz and 88.6% at f=400Hz. It is found that there is a larger peak-peak variation in the inductor current. This can cause higher current stress on the switching devices and produce voltage loss.

Figures 5.4 and 5.5 show the load voltage waveforms with respect to the reference signals at f=60Hz and f=400Hz. The addition of PI controllers has reduced the phase error to less than 0.1 degrees at f=60Hz and f=400Hz. However, there is an appreciable amplitude error.

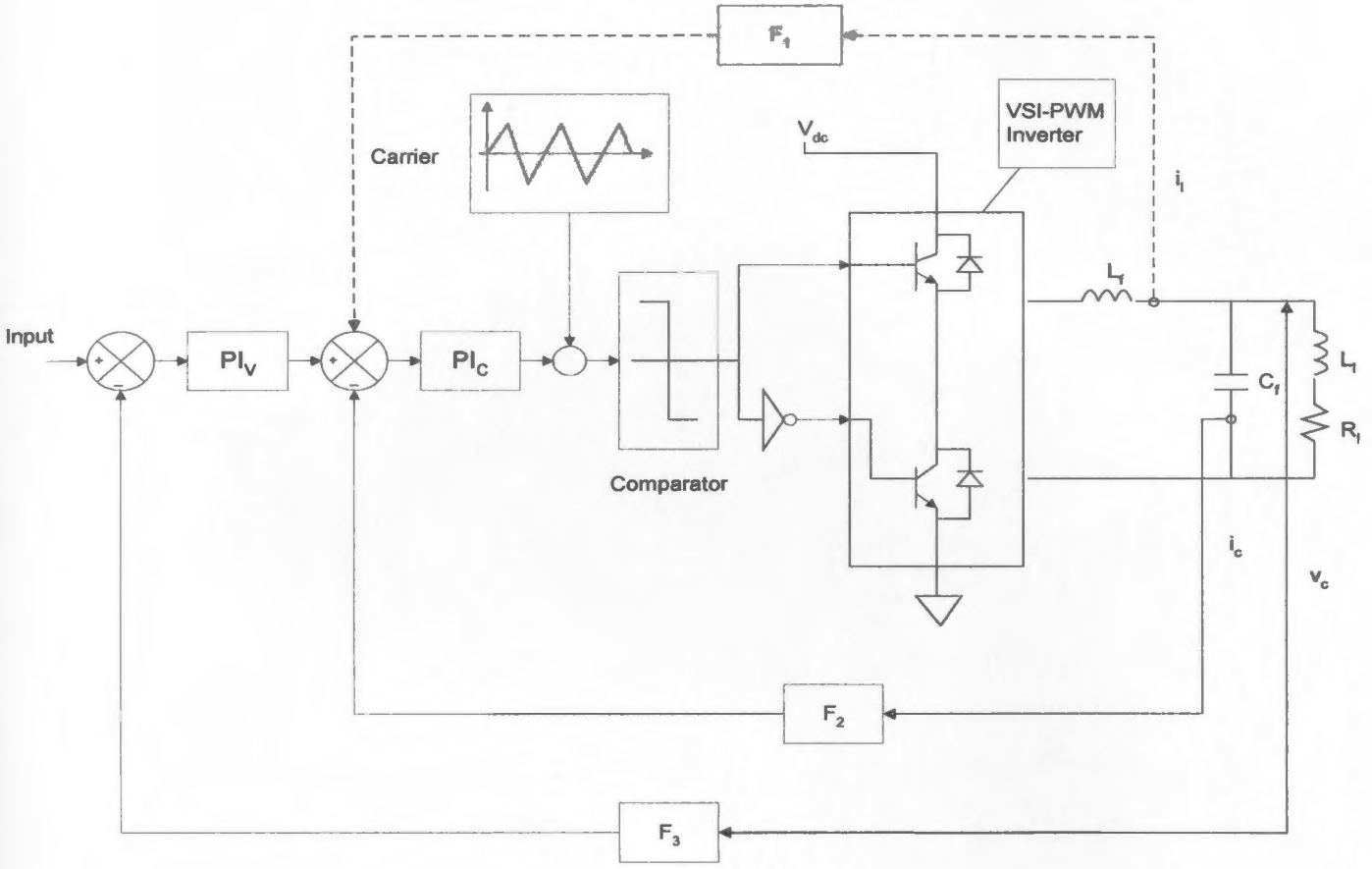

Figure 5.1: The general structure of the multiple feedback control system for UPS

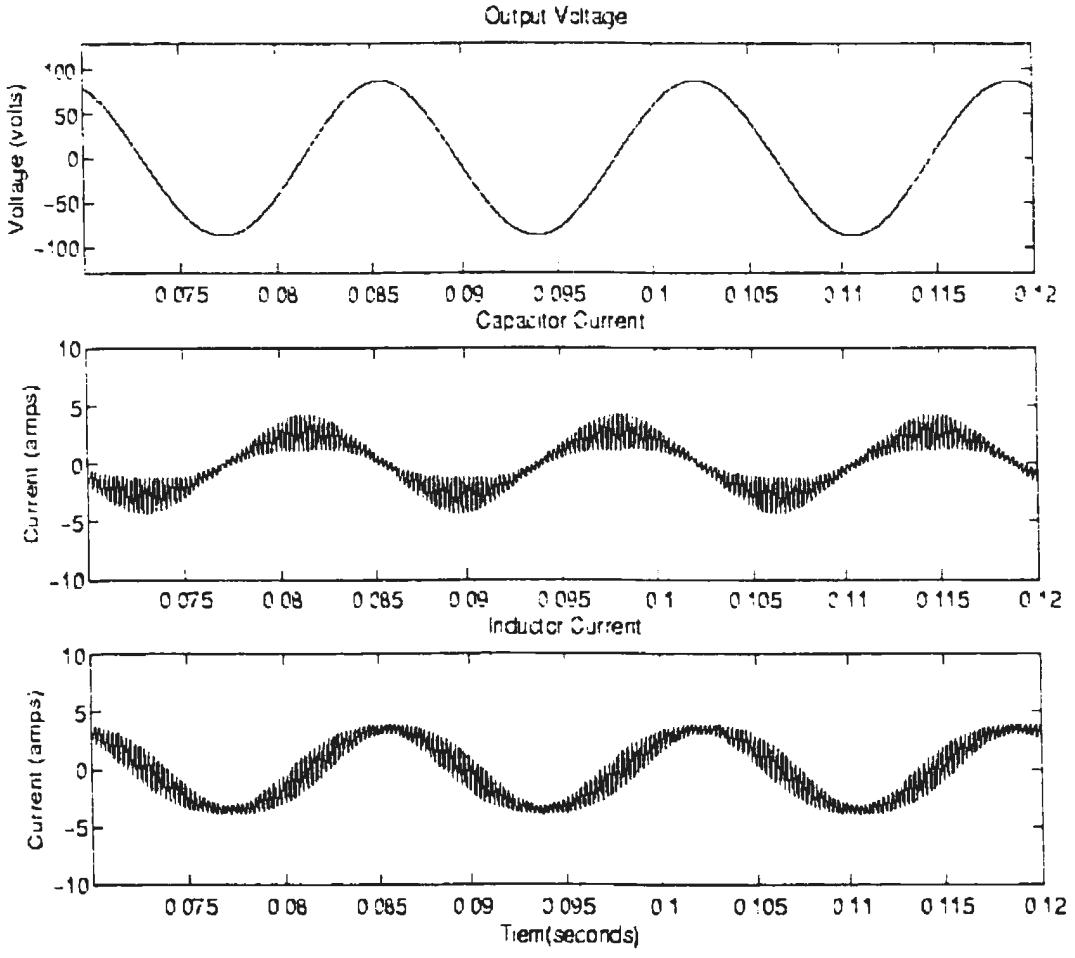

Figure 5.2: Output voltage and capacitor and inductor current waveforms at 60Hz (Modified two-loop control)
(R_l=16Ω, L_l=31.85mH, L_f=3.8mH, C_f=83.3μF, V_{dc}=100V, f_s=4.2kHz)

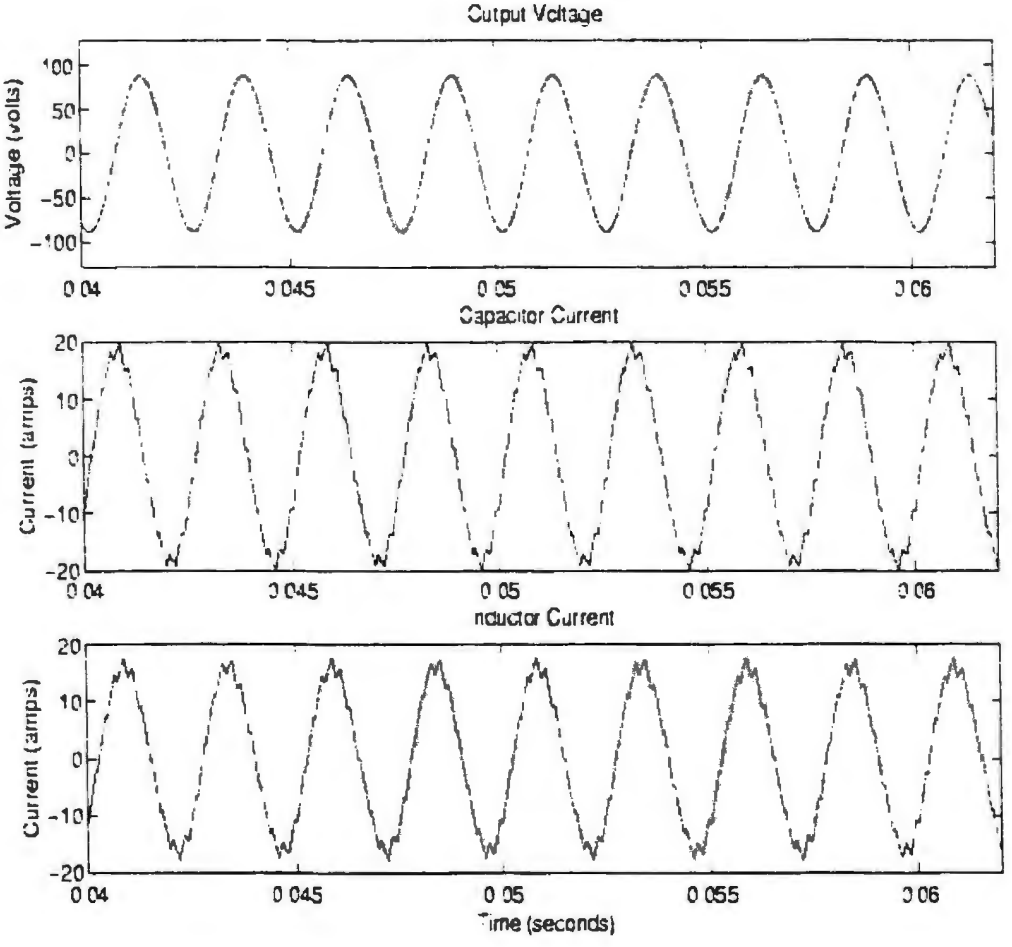

Figure 5.3: Output voltage and capacitor and inductor current waveforms at 400Hz (Modified two-loop control)
(R_l=16Ω, L_l=4.8mH, L_f=3.8mH, C_f=83.3μF, V_{dc}=100V, f_s=4.2kHz)

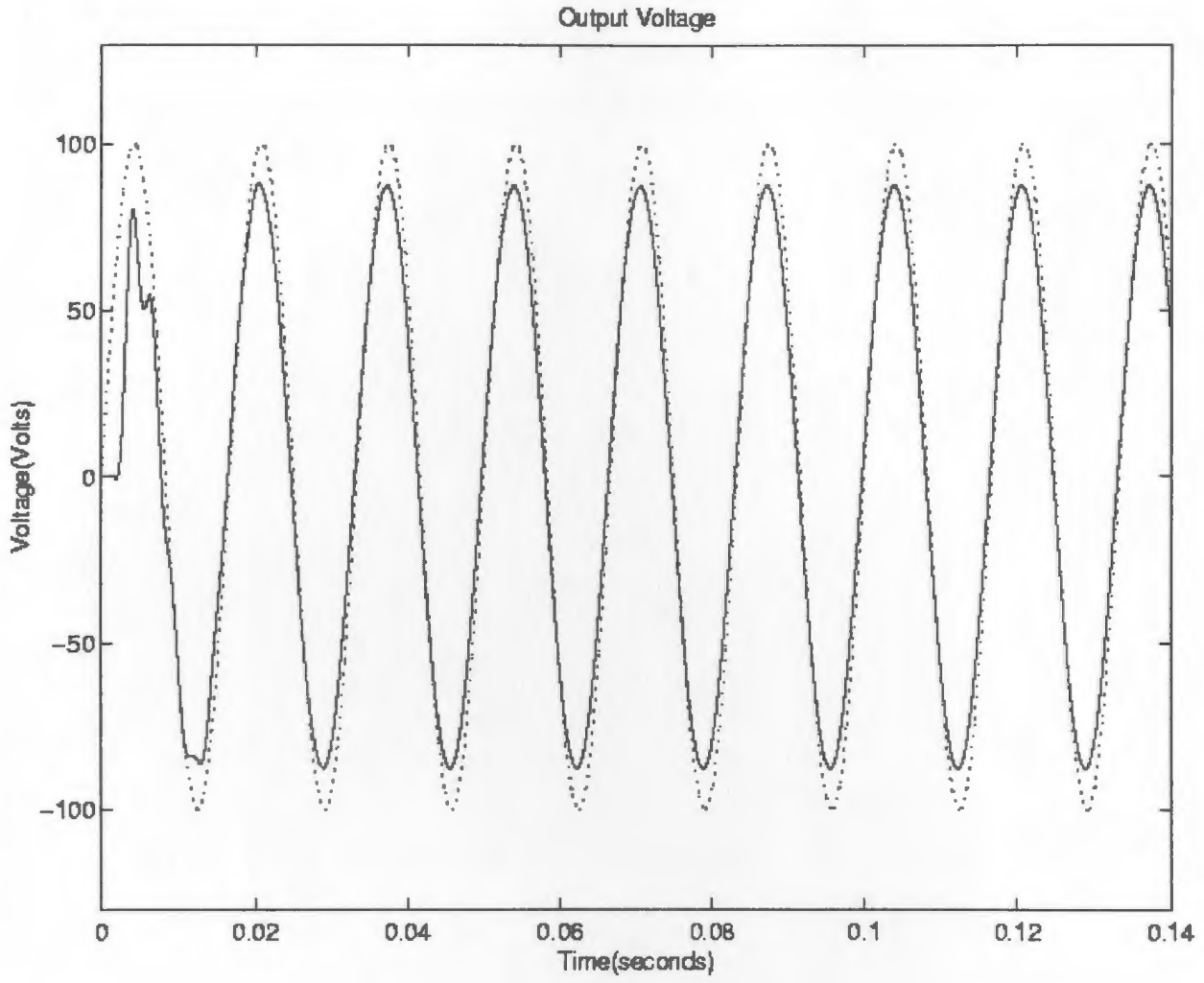

Figure 5.4: The load voltage with respect to the reference signal at f=60Hz (Modified two-loop control)
(R_l=16Ω, L_l=31.85mH, L_f=3.8mH, C_f=83.3μF, V_{dc}=100V, f_s=4.2kHz)

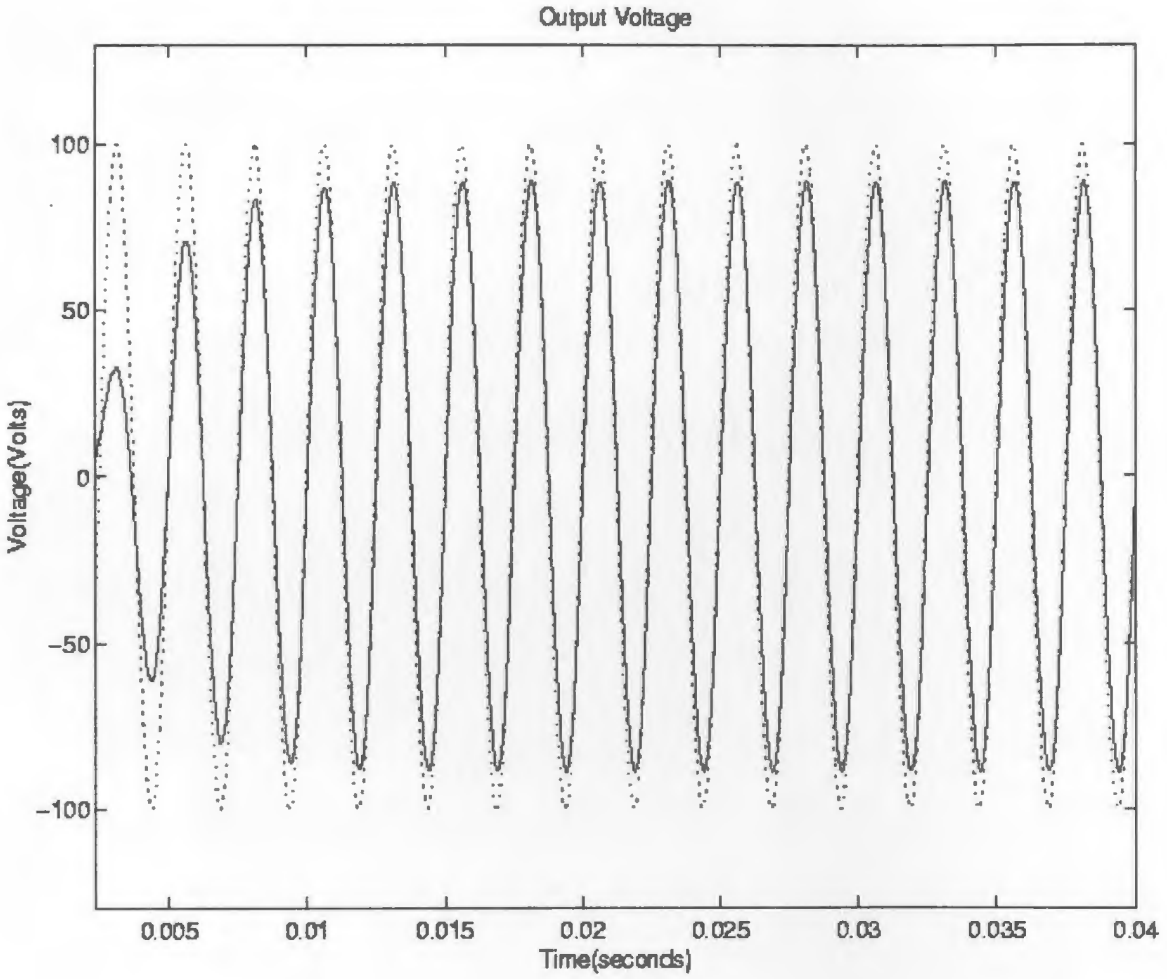

Figure 5.5: The load voltage with respect to the reference signal at f=400Hz (Modified two-loop control)
(R_l=16Ω, L_l=4.8mH, L_f=3.8mH, C_f=83.3μF, V_{dc}=100V, f_s=4.2kHz)

5.3.2 Total harmonic distortion and voltage utilization

The THD value is a measure of the quality of a waveform. Normally, waveforms with THD less than 5% are acceptable [18]. The THD for the output voltage waveform is defined as [18].

$$THD(\%)=\frac{\left(\sum_{h=2}^{\infty} V_h^2\right)}{V_1}\times 100 \tag{5.5}$$

where V_h is the rms value of the harmonic voltage and V_1 is the rms value of the fundamental component.

Figure 5.4 shows the THD values as a function of the output frequencies which include the standard frequencies. It can be seen that at any frequency the THD of the output voltage waveform is less than 4%. At the standard frequencies, the THD values are less than 2.2%. Hence, it is shown that the unwanted components in the output waveform have been almost eliminated and the output voltage can be considered as a sinusoidal signal. The figure also shows that the control scheme is capable of maintaining constant output voltage at the two standard frequencies. However, the system exhibits a significant increase in THD and a decrease in the voltage utilization for frequencies above 420 Hz.

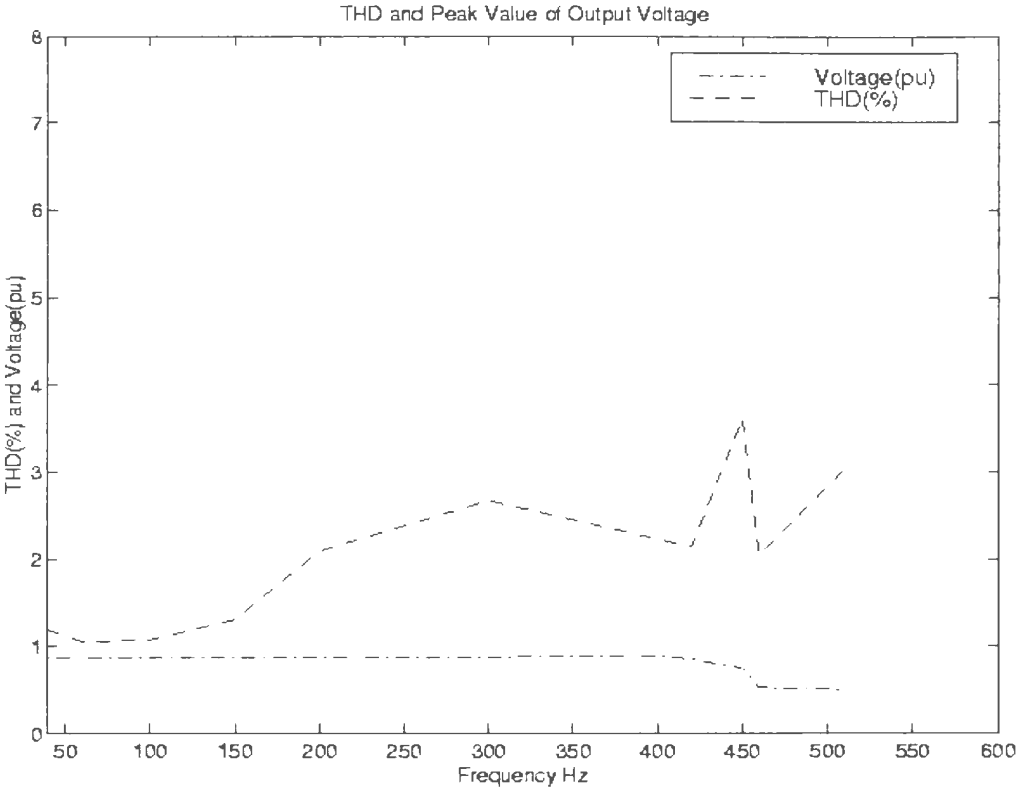

Figure 5.6: THD and peak value of output voltage as a function of frequency.
(Modified two-loop control).
(V_{dc}=100V, f_s=4.2kHz, L_f=3.8mH, C_f=83.3μF, Z_l=20Ω)

5.3.3 Dynamic Response

The transient response is investigated at the two standard frequencies to verify the performance of the control system under varying load.

Figures 5.7 and 5.8 show respectively the dynamic responses of the load current and load voltage at f=60 Hz for a 100% step change in load. As shown in the figures, the transient response lasts for about half of the cycle before reaching the steady state. The control strategy therefore provides a fast transient response to load changes. As well, the load voltage is maintained almost constant during the load changes indicating that the UPS system operates as a stiff voltage source at 60Hz.

Figures 5.9 and 5.10 exhibit the dynamic responses to the loading and unloading at f=400 Hz. Figure 5.9 shows the case of unloading (removing the load from the control system). The adjusting time of the control system was found to be 23ms (from 0.042 seconds to 0.065 seconds). When the load was removed from the system, the output voltage was suddenly increased. The control system was able to adjust the output immediately until the output voltage reached the steady state. Figure 5.10 shows the case of loading (applying a load to the control system). The adjusting time of the control system was found to be only 7ms (from 0.042 seconds to 0.049 seconds). When the load was applied to the control scheme, the output voltage dropped. However, it recovered its steady state value after 3 cycles. These test results indicate that the control system is capable of delivering and maintaining the desired output following load changes at 400Hz. However, a careful scrutiny of Figures 5.9 and 5.10 reveals that the dynamic

responses are slightly different upon applying and removing a load. The recovery time following the removal of load is longer than the sudden application of load.

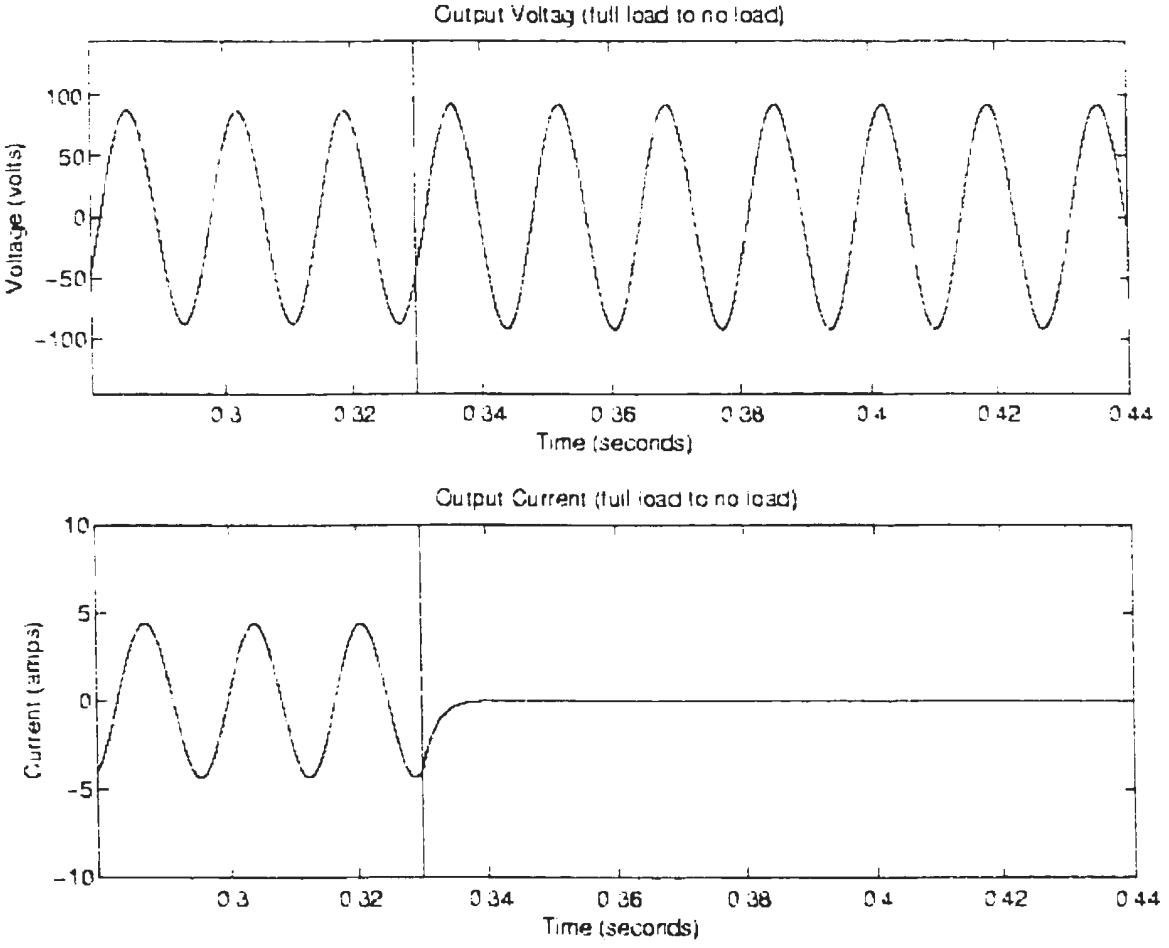

Figure 5.7: Dynamic response from full load to no load at 60Hz
(Modified two-loop control)
(R_l=16Ω, L_l=31.85mH, L_f=3.8mH, C_f=83.3μF, V_{dc}=100V, f_s=4.2kHz)

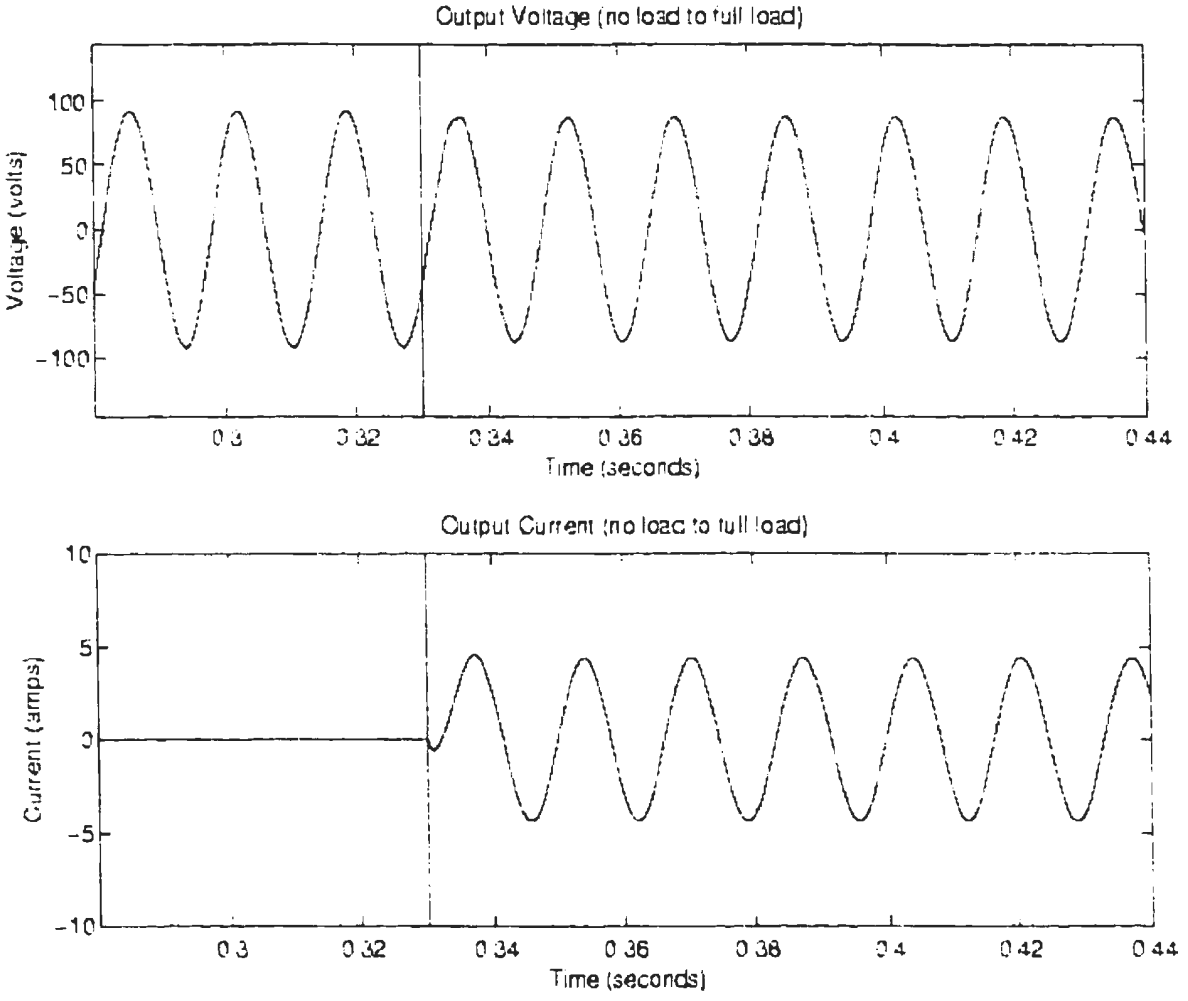

Figure 5.8: Dynamic response from no load to full load at 60Hz
(Modified two-loop control)
(R_l=16Ω, L_l=31.85mH, L_f=3.8mH, C_f=83.3μF, V_{dc}=100V, f_s=4.2kHz)

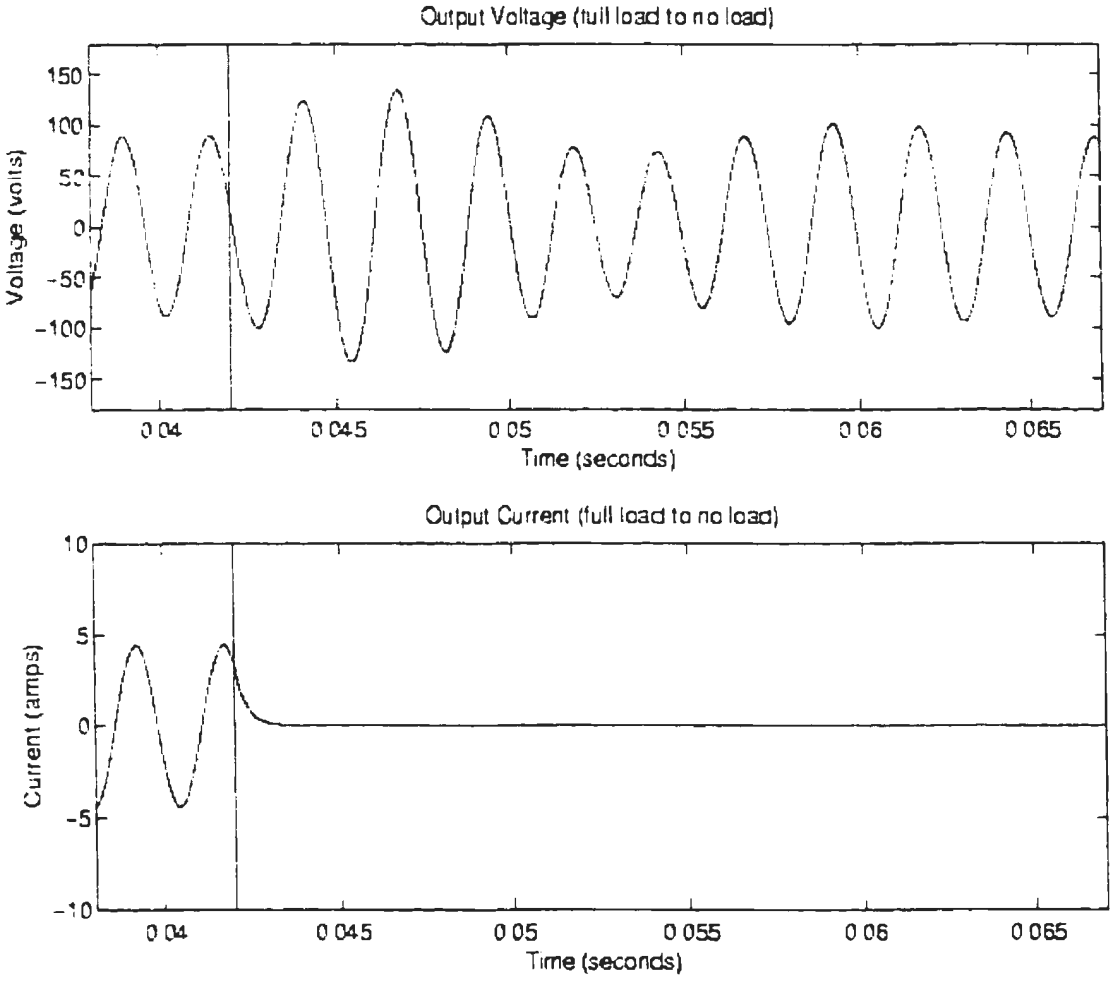

Figure 5.9: Dynamic response (full load to no load) at 400Hz
(Modified two-loop control)
(R_l=16Ω, L_l=4.8mH, L_f=3.8mH, C_f=83.3μF, V_{dc}=100V, f_s=4.2kHz)

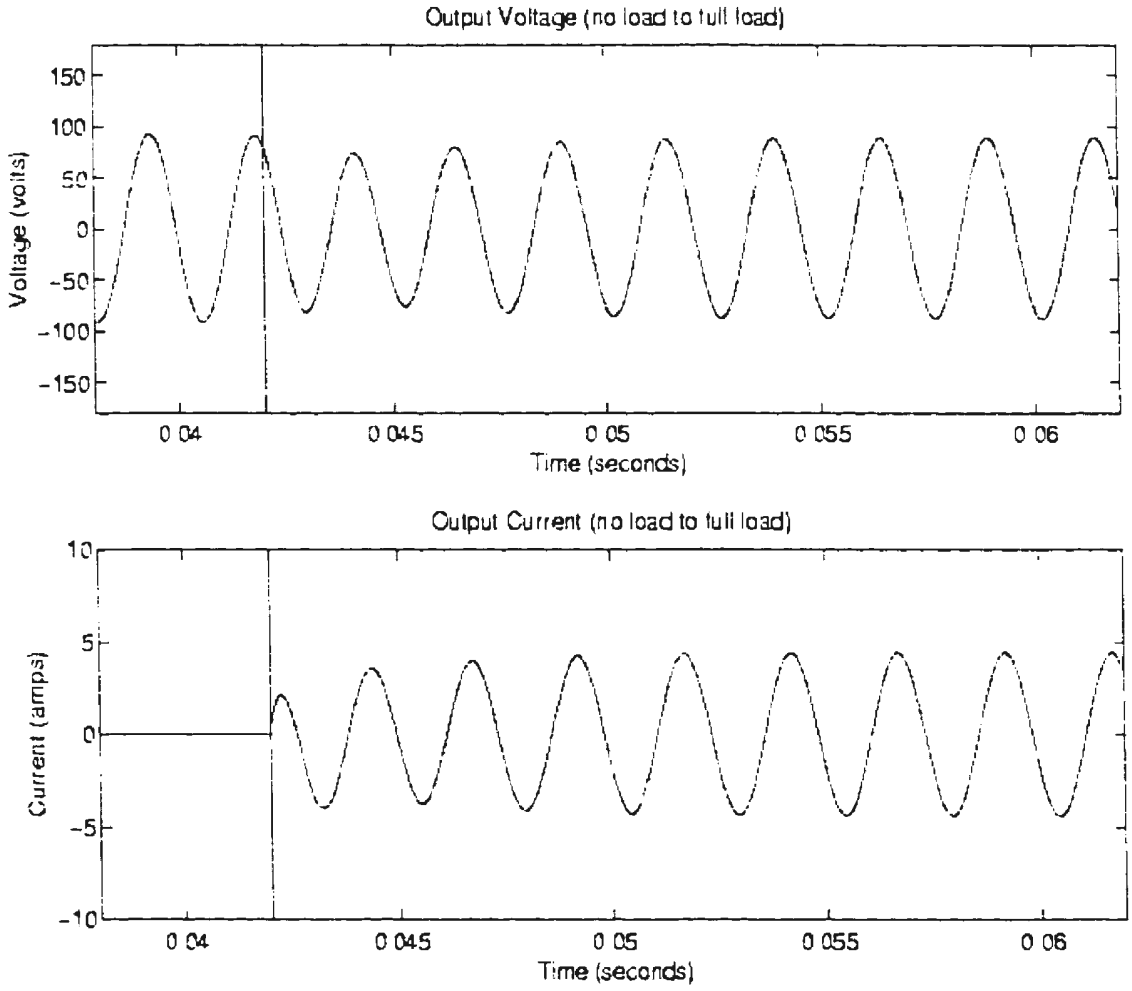

Figure 5.10: Dynamic response (no load to full load) at 400Hz
(Modified two-loop control)
(R_l=16Ω, L_l=4.8mH, L_f=3.8mH, C_f=83.3μF, V_{dc}=100V, f_s=4.2kHz)

5.4 Performance of the Three-Loop Control Strategy

In this section, the simulation results for the output voltage and capacitor current, THD values, and dynamic responses at the two frequencies (f=60Hz and f=400Hz) in the three-loop control strategy for a linear R-L load are presented. The characteristics of the three-loop control scheme are demonstrated.

5.4.1 Output voltage, capacitor current and inductor current waveforms

Figures 5.11 and 5.12 show the waveforms of the control variables: load voltage, capacitor current and inductor current at 60Hz and 400Hz respectively. The voltage utilization is found to be 100% at f=60Hz and 99.6% at f=400Hz. There is a slight reduction in the current variation at the peak of the inductor current, and at near the zero crossings of the capacitor current. This results in a decrease in the stresses on the switching devices.

Figures 5.13 and 5.14 show the waveforms of the load voltage with respect to reference signals at f=60Hz and f=400Hz. The resulting output voltage waveform has negligible phase and amplitude errors.

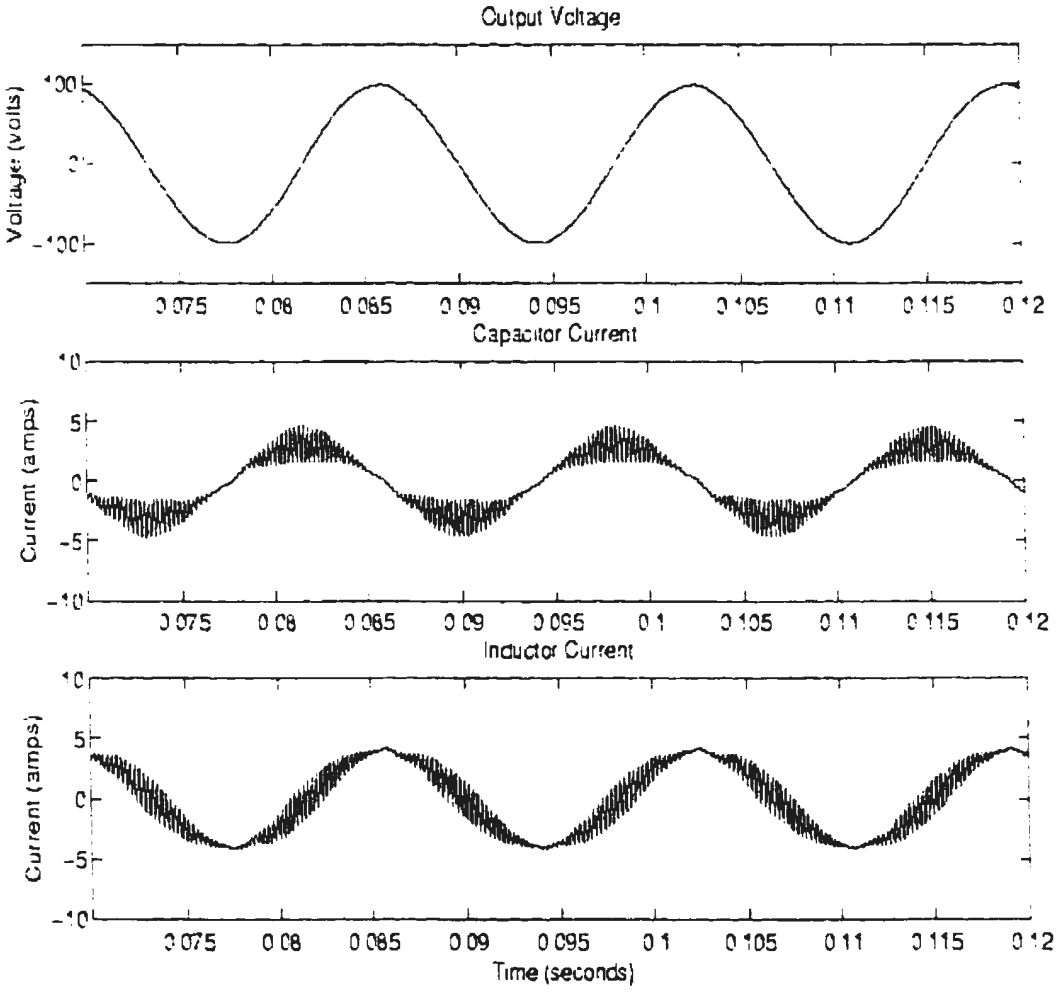

Figure 5.11: Output voltage and capacitor and inductor current waveforms at 60Hz
(Three-loop control)
(R_l=16Ω, L_l=31.85mH, L_f=3.8mH, C_f=83.3μF, V_{dc}=100V, f_s=4.2kHz)

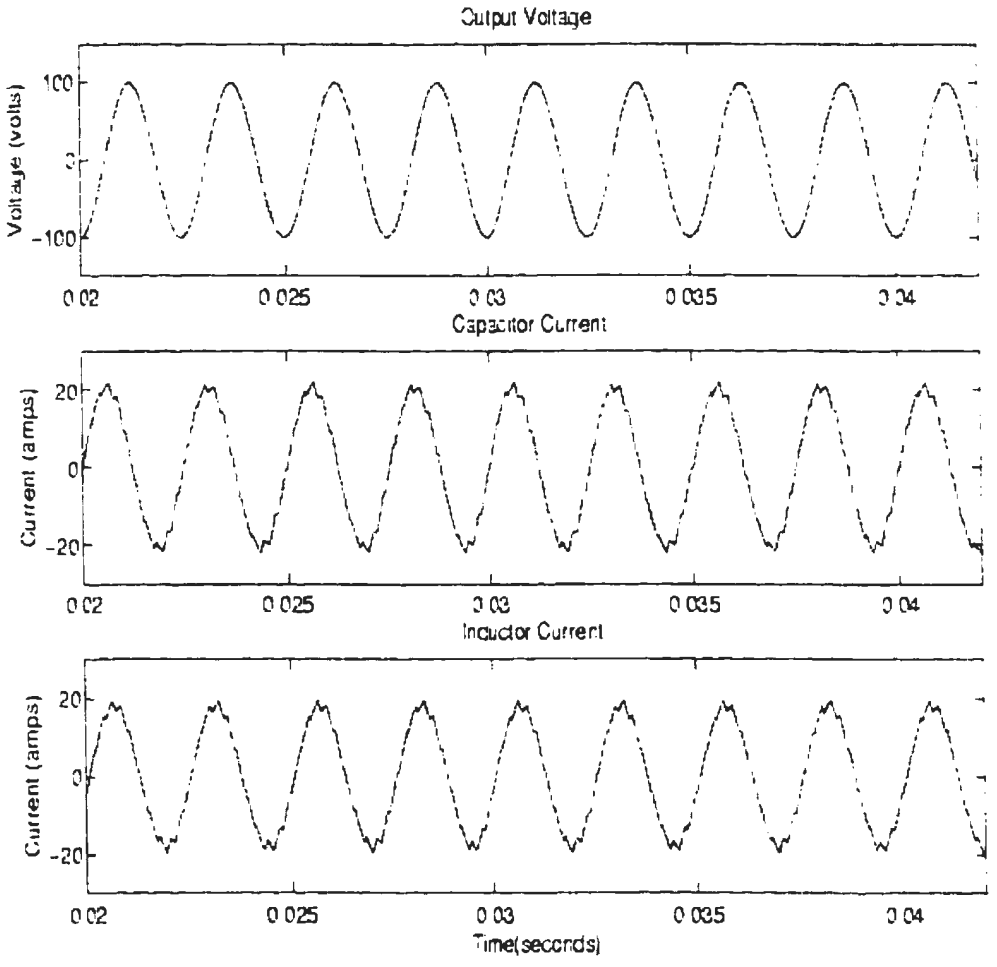

Figure 5.12: Output voltage and capacitor and inductor current waveforms at 400Hz
(Three-loop control)
(R_l=16Ω, L_l=4.8mH, L_f=3.8mH, C_f=83.3μF, V_{dc}=100V, f_s=4.2kHz)

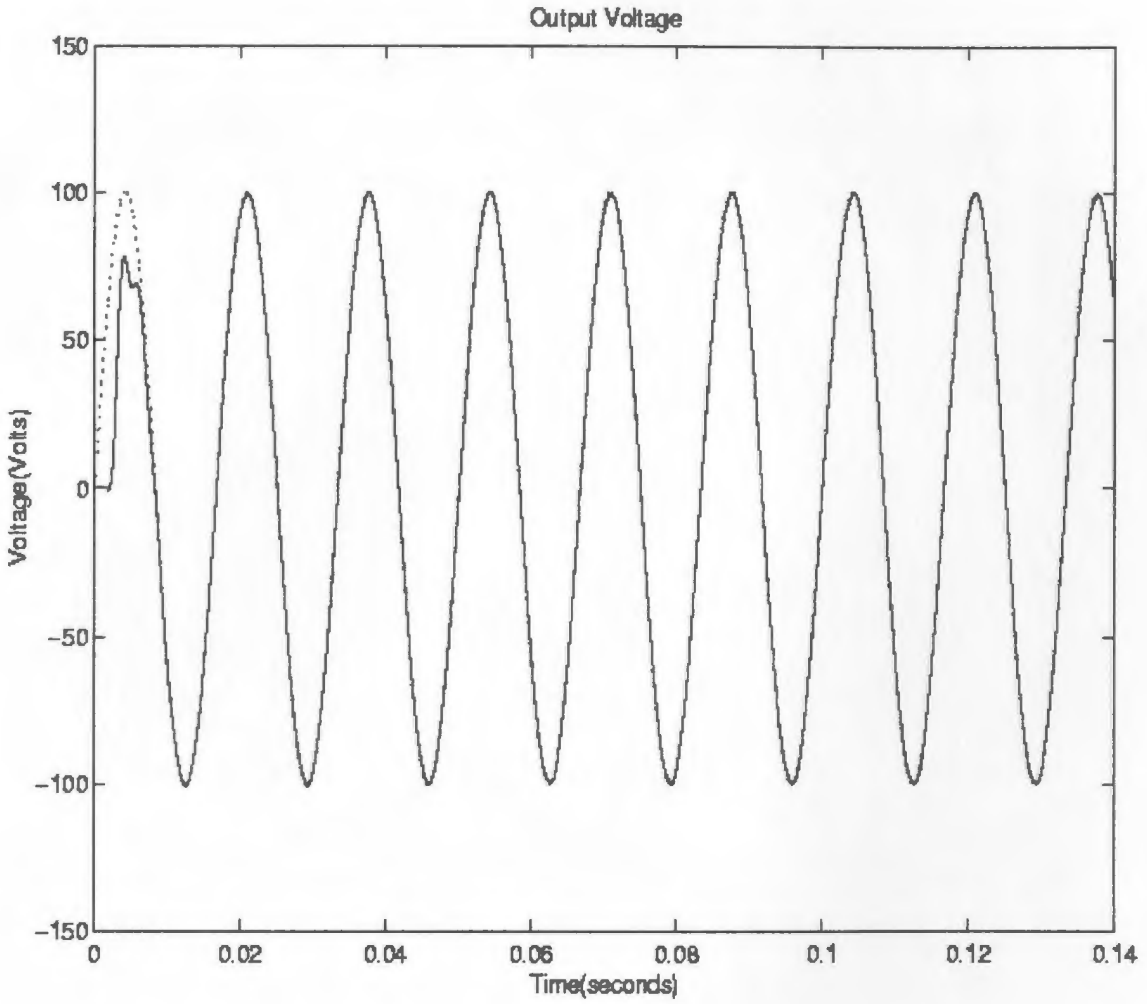

Figure 5.13: The load voltage with respect to the reference signal at f=60Hz (Three-loop control)
(R_l=16Ω, L_l=31.85mH, L_f=3.8mH, C_f=83.3μF, V_{dc}=100V, f_s=4.2kHz)

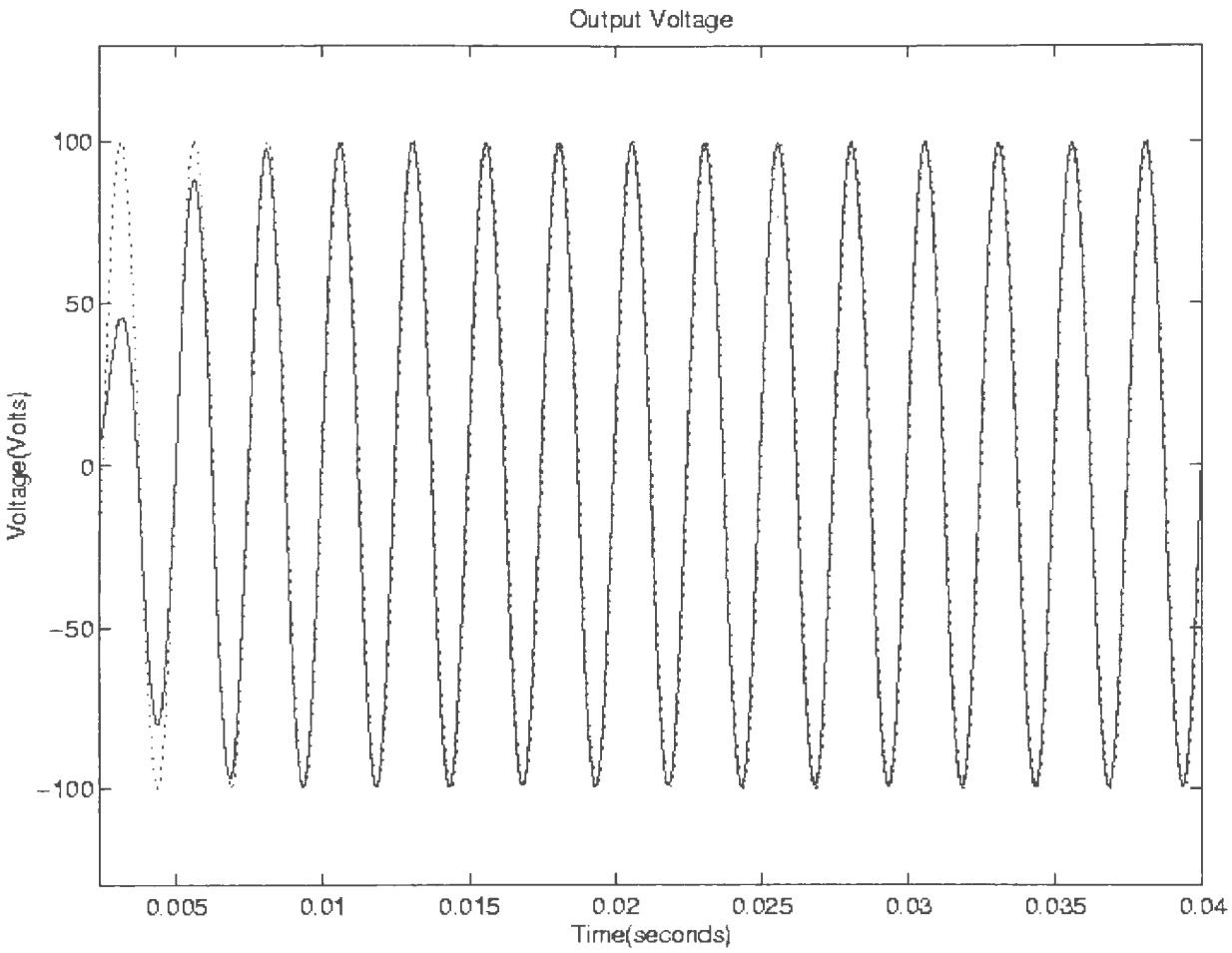

Figure 5.14: The load voltage with respect to the reference signal at f=400Hz (Three-loop control)
(R_l=16Ω, L_l=4.8mH, L_f=3.8mH, C_f=83.3μF, V_{dc}=100V, f_s=4.2kHz)

5.4.2 Total Harmonic Distortion and Voltage Utilization

Figure 5.15 shows the THD values in the frequency bandwidth which includes the standard frequencies. The THD values for the three-loop system are found to be less than 1.7%. In addition, the figure shows that the three-loop control scheme is capable of maintaining constant voltage at the two standard frequencies. The system presents a low THD value and higher voltage utilization for frequencies above 400Hz at the system parameters used.

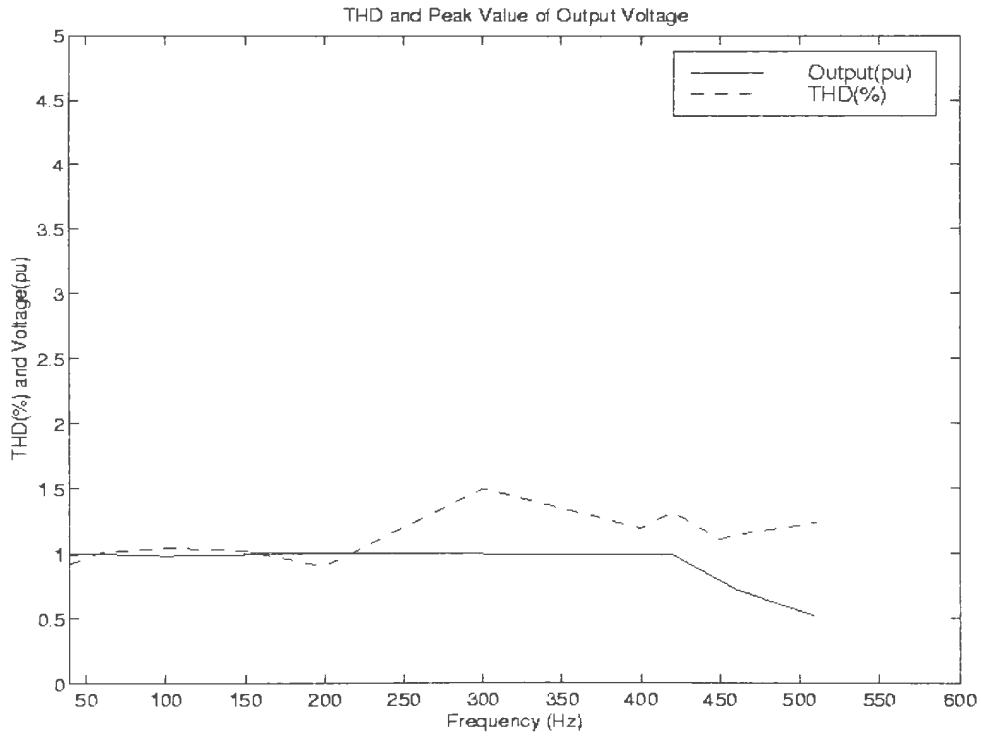

Figure 5.15: THD and peak value of output voltage as a function of frequency
(Three-loop control scheme)
(V_{dc}=100V, f_s=4.2kHz, L_f=3.8mH, C_f=83.3μF, Z_l=20Ω)

5.4.3 Dynamic Response

Figures 5.16 and 5.17 show the transient responses of the three-loop control system for a 100% step change in load. The transient period is a little less than half of a cycle, before the system reaches the steady state. The control strategy therefore provides a fast transient response to load changes. As well, the load voltage is maintained almost constant during the load changes.

Figures 5.18 and 5.19 show the transient responses at f=400 Hz for step changes in load. Figure 5.18 shows the case of removing the load from the system. The adjusting time of the control system was found to be 22ms (from 0.042 seconds to 0.064 seconds). It is shown in figure 5.19 that the transient period is 6ms (0.042 seconds to 0.048 seconds). When the load was applied to the system, the output voltage dropped but steady state was reached after three cycles. As shown, the transient time of the three-loop system decreased slightly in comparison with that of the two-loop system. These figures demonstrate that, when load is applied and removed at any time, the control system can adjust the parameters immediately to meet the steady-state requirements and maintaining the desired output. In fact, the dynamic responses are slightly different upon applying and removing 100% step change in load. The recovery time following the removal of load is longer than that for the sudden application of load.

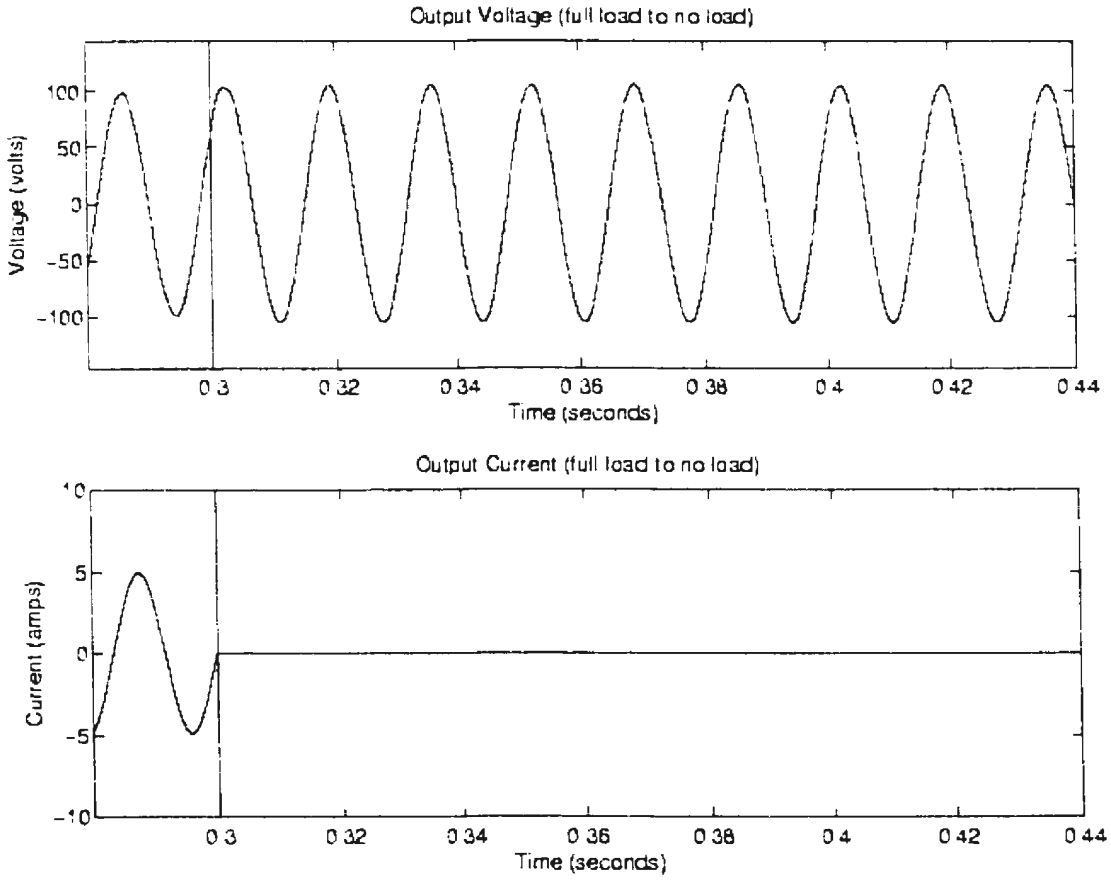

Figure 5.16: Dynamic response (from full load to no load) at 60Hz
(Three-loop control)
(R_l=16Ω, L_l=31.85mH, L_f=3.8mH, C_f=83.3μF, V_{dc}=100V, f_s=4.2kHz)

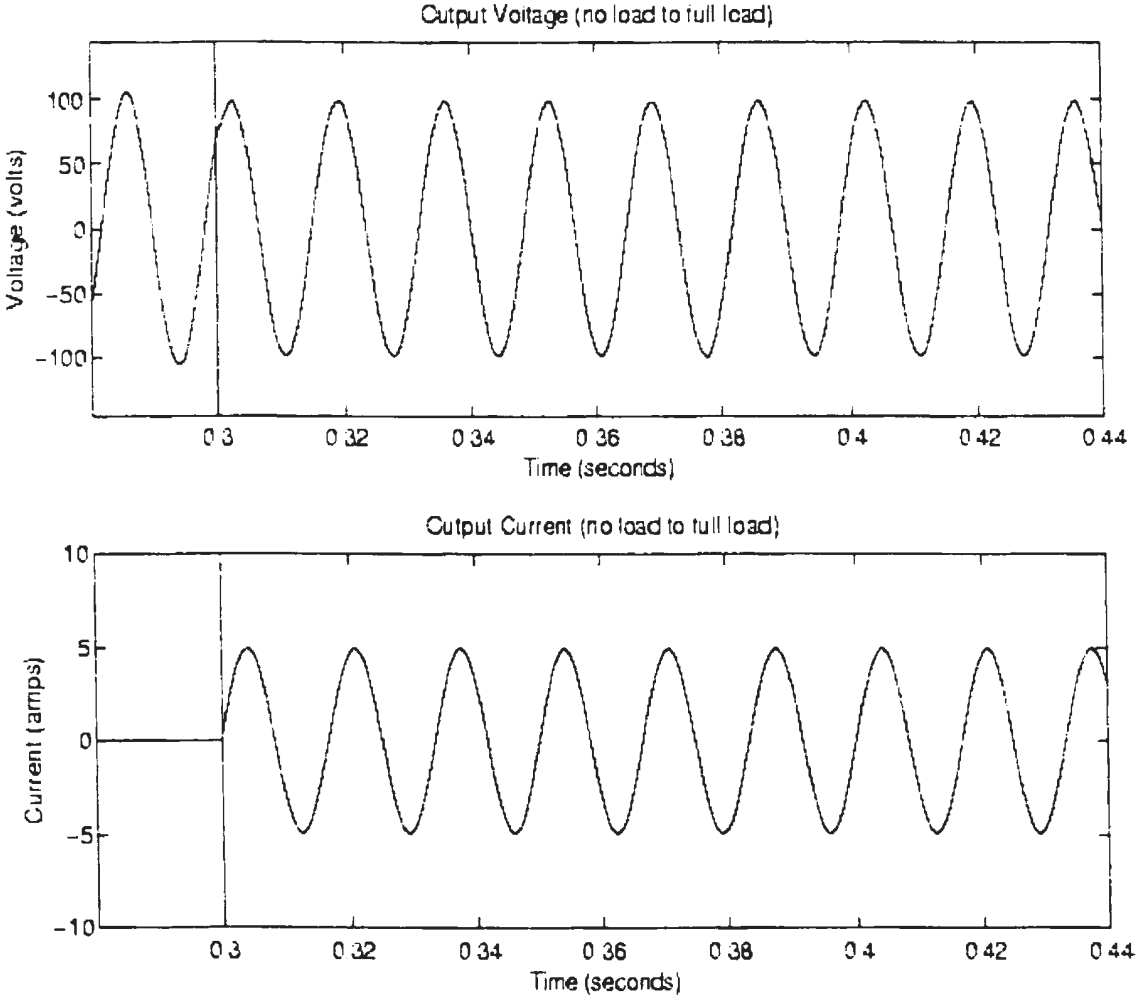

Figure 5.17: Dynamic response (from no load to full load) at 60Hz (Three-loop control)
(R_l=16Ω, L_l=31.85mH, L_f=3.8mH, C_f=83.3μF, V_{dc}=100V, f_s=4.2kHz)

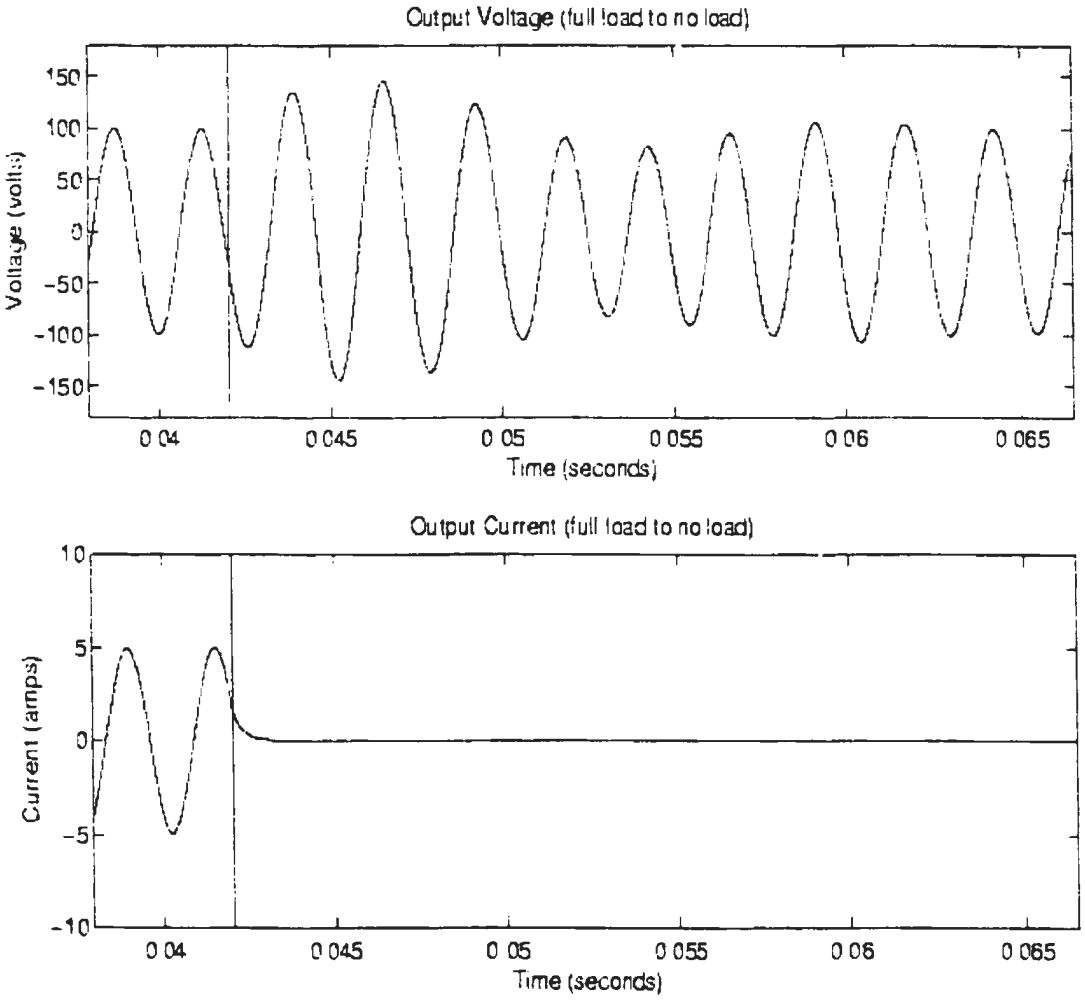

Figure 5.18: Dynamic response (full load to no load) at 400Hz
(Three-loop control)
(R_l=16Ω, L_l=4.8mH, L_f=3.8mH, C_f=83.3μF, V_{dc}=100V, f_s=4.2kHz)

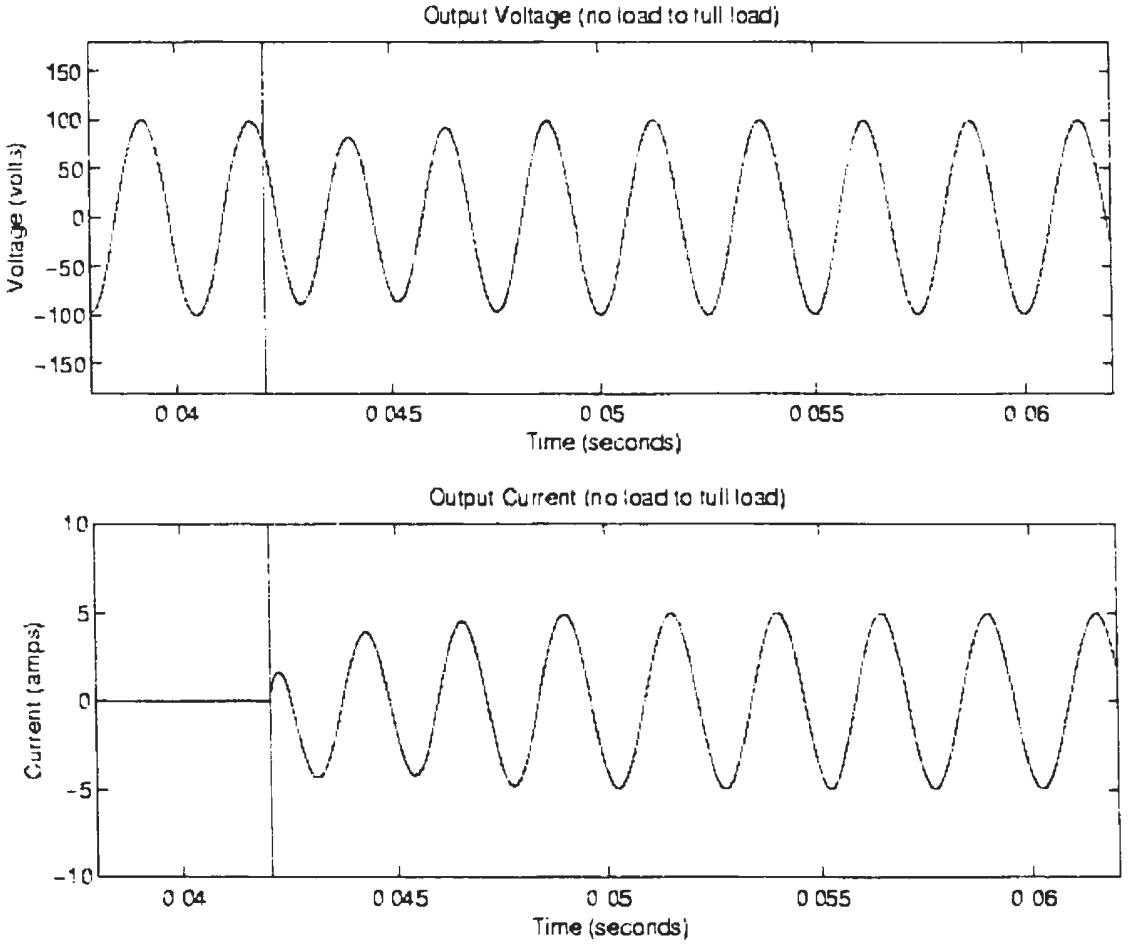

Figure 5.19: Dynamic response (full load to no load) at 400Hz
(Three-loop control)
(R_l=16Ω, L_l=4.8mH, L_f=3.8mH, C_f=83.3μF, V_{dc}=100V, f_s=4.2kHz)

5.5 Effect of System Parameters on The Performance of The Three-Loop Control Strategy

The results of the previous sections indicate that the three-loop control strategy results in improved performance. In this section, the performance of the three-loop control strategy is further investigated by examining the effects of load power factor variation and switching frequency on the THD and voltage utilization of the UPS system.

Figures 5.20 and 5.21 show the THD and the voltage utilization as a function of the load power factor at 60Hz and 400Hz respectively. The figures show that the output voltage remains constant as the load power factor varies from pf=0.6 (lagging) to pf=0.9(lagging). For 60Hz operation, the THD is low (1.1%) and changes slightly for the range of power factor. At 400Hz, the THD is worse (1.83%) at low power factors but decreases steadily with increasing power factor.

Furthermore, the effect of switching frequency is studied for the three-loop control system. Three switching frequencies of f_s =4.2kHz, f_s=3.2kHz and f_s=2.2kHz were selected. It is shown in figure 5.22 that higher switching frequencies improve the quality of the output voltage. Normally, the switching frequency is much higher than the output frequency. When the switching frequency is decreased, the output harmonics would increase because the PWM cannot remove the harmonics which are too large compared to the fundamental frequencies. However, in an application, the switching frequency cannot be chosen to be too high because of the increased losses in the inverter devices at higher switching frequencies. Figure 5.23 shows the effect of the switching

frequency on the output voltage. It is shown that the output voltage is not affected by the switching frequency.

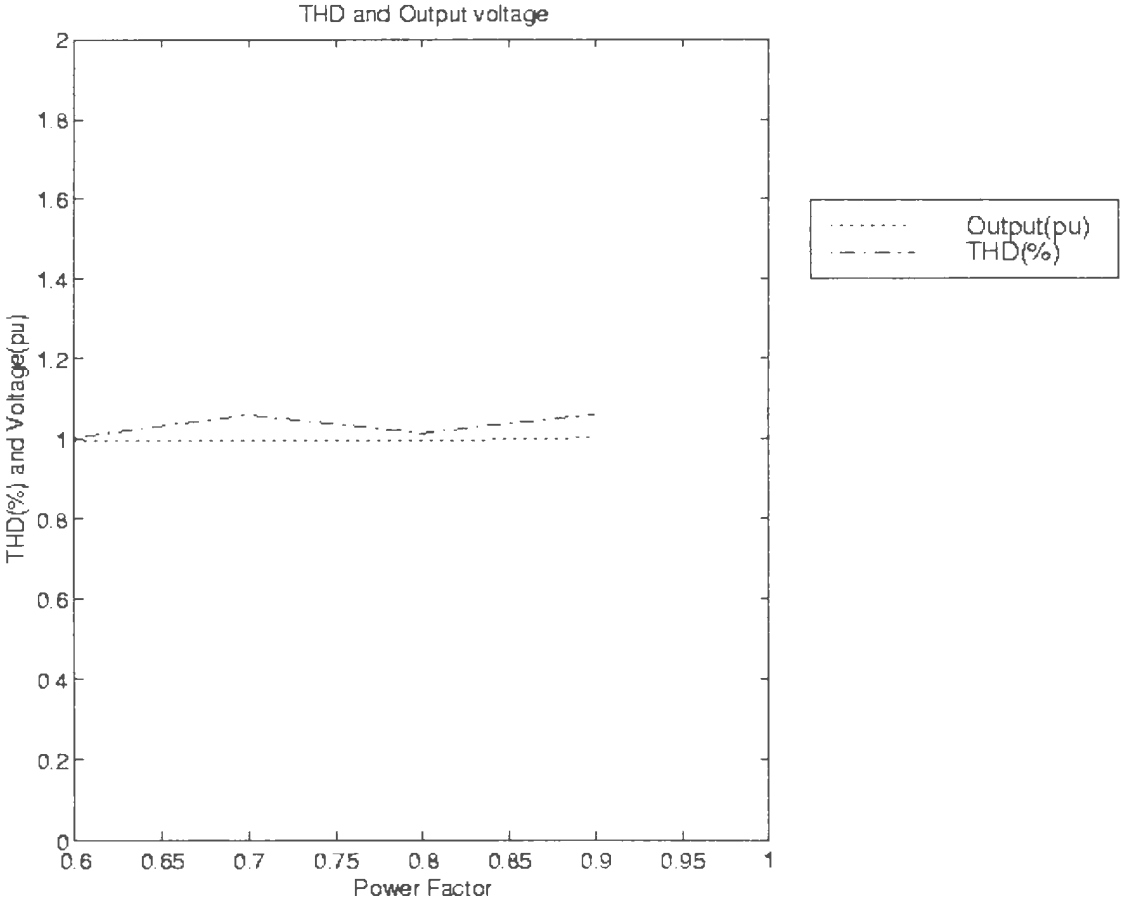

Figure 5.20: THD and peak value of output voltage as a function of power factor frequency at f=60Hz
(Three-loop control scheme)
(V_{dc}=100V, f_s=4.2kHz, L_f=3.8mH, C_f=83.3μF, Z_l=20Ω)

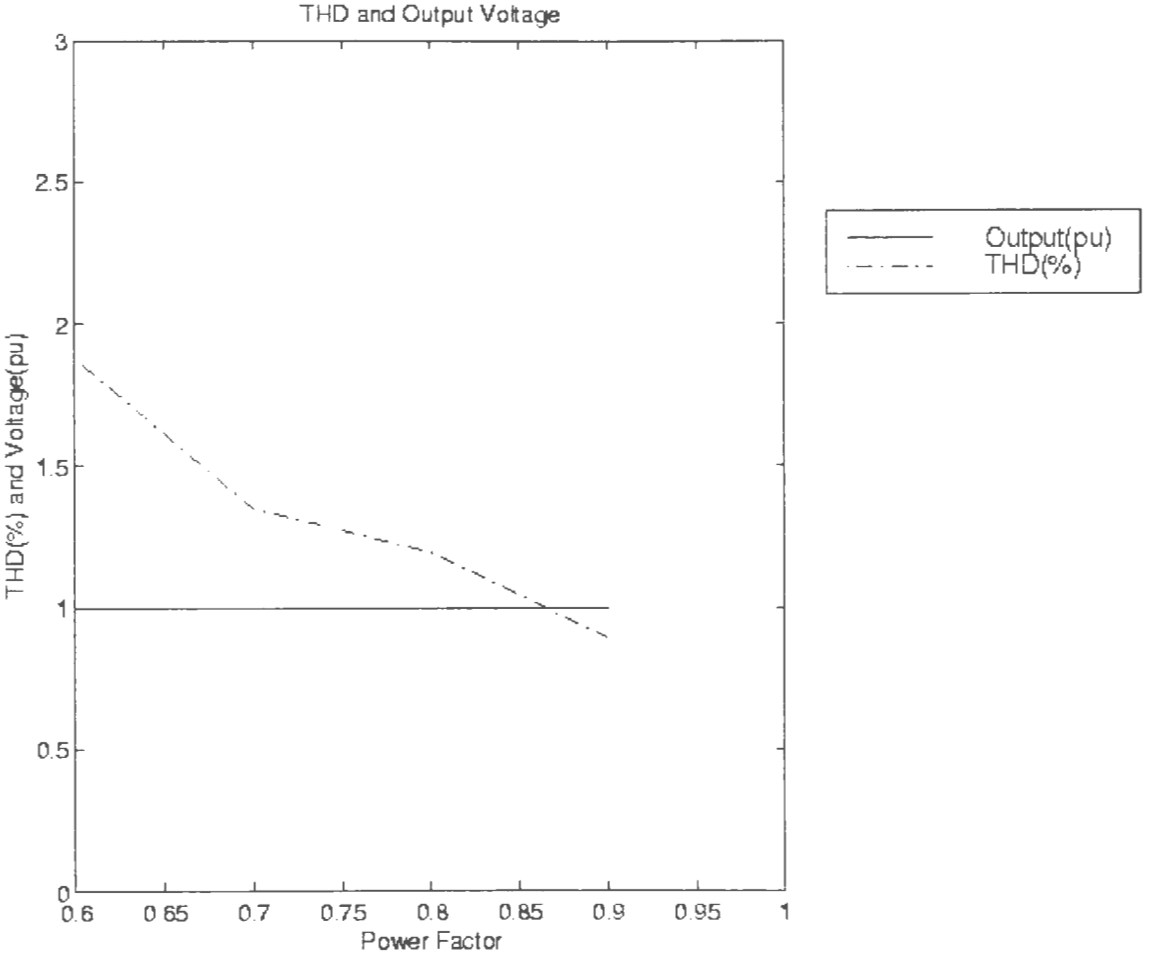

Figure 5.21: THD and peak value of output voltage as a function of power factor frequency at f=400Hz
(Three-loop control scheme)
(V_{dc}=100V, f_s=4.2kHz, L_f=3.8mH, C_f=83.3μF, Z_l=20Ω)

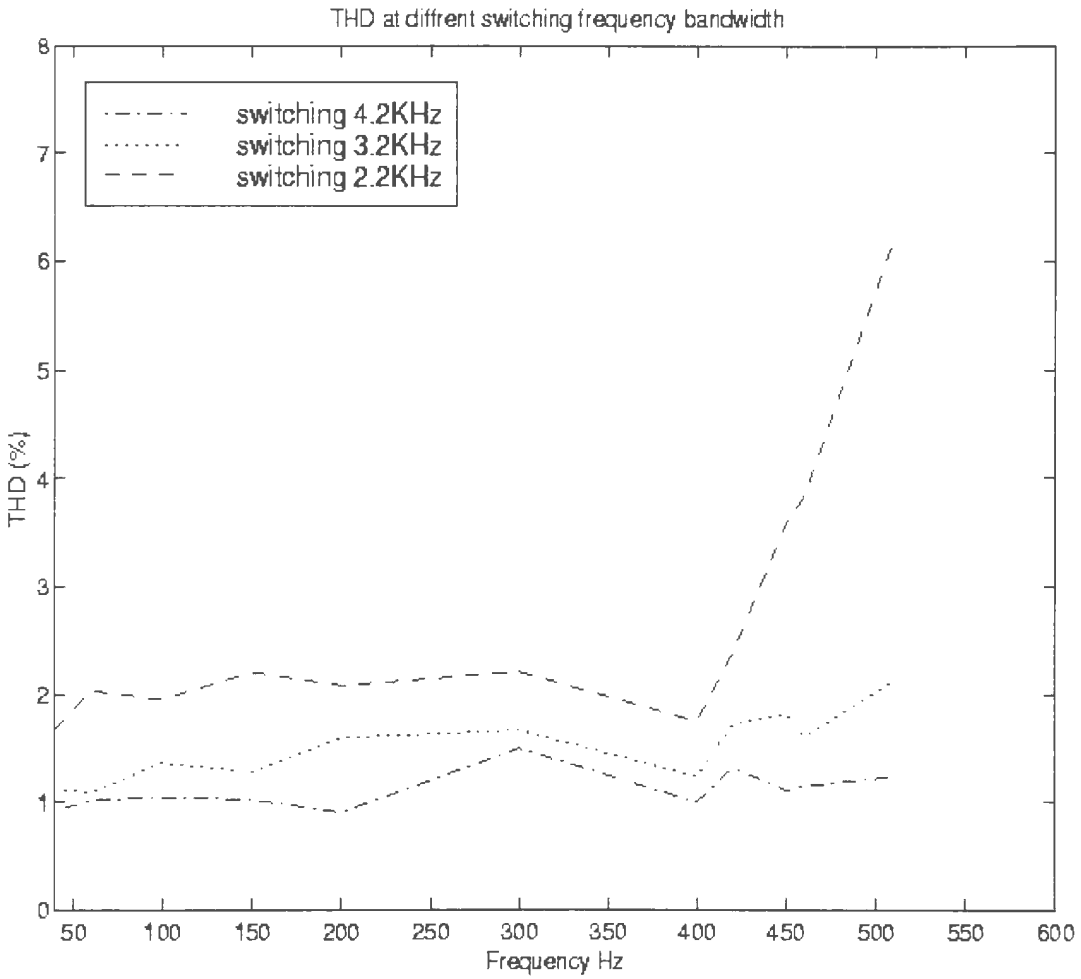

Figure 5.22: THD value for comparison at different switching frequency (Three-loop control scheme)
(V_{dc}=100V, f_s=4.2kHz, L_f=3.8mH, C_f=83.3μF, Z_l=20Ω)

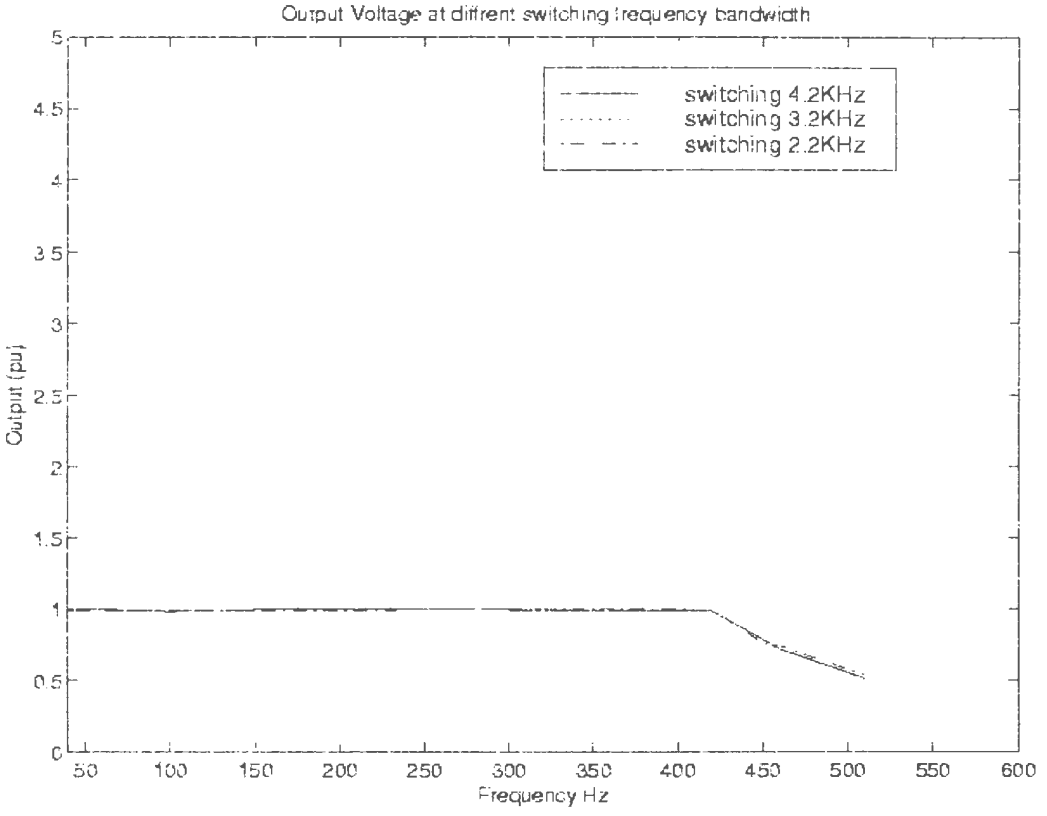

Figure 5.23: Peak output voltage for comparison at different switching frequency
(Three-loop control scheme)
(V_{dc}=100V, f_s=4.2kHz, L_f=3.8mH, C_f=83.3μF, Z_l=20Ω)

5.6 Summary

In this chapter, the characteristics of the basic and modified two-loop and three-loop control strategies are presented. The steady-state and dynamic performances of the two control strategies are investigated through simulation performance measures, such as steady state output voltage, capacitor current and inductor current waveforms, THD, voltage utilization and dynamic response. It is shown that the control strategies can deliver and maintain the desired output.

The results of the simulation indicate that the proposed three-loop control strategy provides improved performance in terms of high quality of the output voltage waveform, higher voltage utilization and faster dynamic response.

Chapter 6

Conclusions and Further Studies

Computer simulations of multiple feedback control schemes for an UPS system using SIMULINK are performed and the results are presented in the thesis to describe the performance of the various strategies.

In order to investigate the steady-state and dynamic behavior of the UPS system, models and transfer functions of the feedback variables, the inverter, the filter and load were developed. Using Fourier analysis and through PWM, the initial discrete model (representing the switching function) was converted into a continuous model where only the low-frequency components were considered. In the dynamic model, the feedback variables were chosen and expressed in the state-space equation.

Normally, there are two types of controllers that are used in power electronic systems: proportional controller and PI controllers. Proportional controllers are easy to build and implement. However, in most applications, the chosen gain is not large enough to boost the dynamic response. In addition, the gain of the proportional controller is fixed to a certain frequency. It is shown from the results obtained from the control system with proportional controllers (the basic control strategy) that it is difficult to achieve a stable and high quality output voltage over a wide frequency range. Compared to the

proportional controller, the PI controller is more desirable because it has the potential for achieving stable operation and minimizing the steady-state error over a wide frequency range. Therefore, PI controllers were used in the proposed control strategies.

Frequency response analysis was presented for three-possible PI controllers, as well as the steady-state error analysis. Based on the criteria of wide frequency operation and minimum steady-state error, the second-order PI controller was selected as the PI controller. A second-order type feedback controller was also selected to improve the signal to noise ratio of the feedback variables. Appropriate compensator parameters which result in stable operation and high quality output waveforms were selected after several simulation trials.

The basic two-loop control strategy consisting of an inner capacitor current loop, an output capacitor voltage loop, a PI controller in the current loop, filters in the feedback loop, and a reference current command was investigated. It was found that the control system could work well at f=400 Hz, but did not perform reliably at f=60Hz. The basic control strategy was modified to include PI controllers in both current loop and voltage loop with no reference current command. A three-loop control strategy consisting of inner capacitor current loop, an inner inductor current loop and an outer voltage loop was proposed.

The features of the proposed control strategies were investigated. It is shown that the three-loop control strategy is feasible. Moreover, based on the simulation results, the proposed strategy is capable of achieving 100% voltage utilization, high quality output

voltage with very low THD, fast transient response, negligible steady-state error, and constant output voltage at the two standard frequencies of 60Hz and 400Hz.

The major contributions and achievements of this thesis are:

1. The development of analytical models of the individual blocks for SIMULINK implementation of multiple feedback control schemes for voltage sources UPS systems.
2. The implementation of PI controllers in the forward path and filters in the feedback paths of the UPS system.
3. The successful development of high performance control strategies capable of operating at 60 Hz and 400 Hz. The control system can be controlled by an input voltage command without an external current command.
4. The presentation of simulation results which provide insight into the features of the different control strategies under steady-state and dynamic operation.

6.1 Suggestions for Future Studies

The goal of this thesis was to develop control strategies to obtain high quality output voltage and fast dynamic response at the standard frequency f=60Hz and f=400Hz. The proposed two-loop control strategy and three-loop control strategy have been demonstrated to be feasible and to meet the objectives. Further work is suggested to be carried in the following three areas.

- A single-phase UPS system was considered in this study. Further work is required for three-phase systems.

- An experimental implementation of the UPS system is required to validate the proposed control strategies.
- A fuzzy-logic based system is expected to improve the performance of the UPS system. Further work is required to implement a fuzzy-logic based model of the UPS system.

Reference:

[1] C.A.Ayres, "A Family of Converters for UPS Production Burn-In Energy Recovery," IEEE Trans., Power Electron., vol.12, no. 4, July 1997, pp. 615 -622.

[2] D.Dorr, "UPS Response to Power Disturbances:A Proposed Method for Determination of UPS Response to Power Disturbances," IEEE Applied Power Electronics Conference (APEC), Orlando, USA, 1994, pp. 675-682

[3] Wong Da Feng, "Improved GTR's Quasi-Resonant DC Link Inverter," APEC'91, Texas, 1991, pp. 506-510.

[4] L.Rossetto, "Quai-Resonant Multi-Output DC/DC Converter with Push-Pull Topology," Orlando, 1994, pp. 971-977.

[5] D. Balocco, "The Half-Wave Quasi-Resonant ZCS Flycack Converter as an Automatic Power Facotr Preregulator: An Evaluation," IEEE Applied Power Electronics Conference and Expositon (APEC'96), California, USA, 1996, pp.138-144.

[6] S.C. Yeh, "Adaptive Repetitive Control of a PWM Inverter for AC Voltage Regulation with low Harmonic Distortion," IEEE Power Electronics Specialists Conference (PESC), Atlanta, USA, 1995, pp. 157-163.

[7] K.J.Talbot, "Speed Sensorless Field Oriented Control of a CSI-fed Induction Motor by a Transputer Based Digital Controller," PESC'95, Atlanda, USA, 1995, pp. 785-791.

[8] D.Patterson, "The Design and Development of a High Power Factor Current Source Controller for Small Appliance Brushless DC Motors," Applied Power Electronics Conference (APEC'96), California, USA, 1996, pp. 778-781.

[9] S.Jung, "DSP-Based Digital Control of a PWM Inverter for Since Wave Tracking by Optimal State Feedback Technique," IEEE Power Electronics Specialists Conference (PESC), Taipei, Taiwan, 1994, pp. 546-551.

[10] J.Xu, "Generalized State Space Averaging Approach and Its Application to the Analysis of Quasi-Resonant Converters," PESC'94, Taipei, Taiwan, 1994, pp. 1046-1052.

[11] S.L. Jung, "Discrete Sliding-Mode Control of a PWM inverter for Sinusoidal

Output Synthesis with Optimal Sliding Curve," IEEE Trans. Power Electron. vol. 11, no. 4, July 1996, pp.567-577.

[12] A.Kislovski, "Current-Mode Control: A Unified Model for Open-loop Instability," APEC'91, Texas, 1991, pp. 459-465.

[13] J.W. Choi, "New Current Concept-Minimum Time Current Control in 3-Phase PWM Converter," PESC'94, Taipei, Taiwan, 1994, pp. 623-629.

[14] Q.Chen, "Small-Signal Modeling and Analysis of Current-Mode Control for Multiple-Output Forward Converters," PESC'94, Taipei, Taiwan,1994, pp.1026-1033.

[15] Akira Nabae, "A Novel Control Strategy of the Inverter with Sinusoidal Voltage and Current Outputs," PESC's 94 Taipei, Taiwan, 1994, pp.154-159

[16] N.Abdel-Rahim and J.E. Quaicoe, "Analysis and Design of a Multiple Feedback Loop Control Strategy for Single-Phase Voltage-Source UPS Inverters," IEEE Trans., Power Electron., vol. 11, no. 4, July 1996, pp. 532-540.

[17] M.C. Chandorkar, "Control of Distributed UPS Systems," IEEE Power Electronics Specialists Conference," Taipei, Taiwan, 1994, pp. 197-204.

[18] N. Mohan, Undeland and Robbins, Power Electronics, New York: John Wiley & Sons, 1995.

[19] Yoichi Hayashi, "A Novel Control of a Current-Source Active Filter for ac Power System Harmonic Compensation," IEEE Trans. Ind. Appl. vol. 27, no. 2, March 1991, pp.380-385.

[20] Q.Chen, "Small-Signal Modeling and Analysis of Current-Mode Control for Multiple-Output Forward Converters," PESC'94, Taipei, Taiwan,1994, pp.1026-1033.

[21] J. Sun, S. Beineke, "Optimal PWM Based on Real-Time Solution of Harmonic Elimination Equations," IEEE Trans. Power Electron., vol. 11, no. 4, July 1996, pp.612-621.

[22] Carlos Augusto Ayres, "A Family of Converters for UPS Production Burn-in Energy Recovery," IEEE Trans. Power Electron. vol. 12, no. 4, July/1997, pp. 615-622.

[23] Francis H. Raven, Automatic Control Engineering, New York: McGraw-Hill, 1995

[24] W. Leonhard, Control of Electrical Drives, Berlin: Springer-Verlag, 1985

[25] Guy Se'guier , Power Electronic Converters, Berlin: Springer-Verlag, 1993.

[26] N.Abdel-Rahim and J. E. Quaicoe, "A Single-Phase Delta Modulated Inverter for UPS Application," IEEE Trans. Ind. Electron. , vol. 40, no. 4, June, 1993, pp. 347-354.

[27] Burece W. Char, First Leaves: A tutorial Introduction to Maple V, Springer-Verlag, 1992.

[28] Rusong Wu, "Analysis of an ac-to-dc Voltage Source Converter Using PWM with Phase and Amplitude Control," IEEE Trans. Ind. Appl. vol. 27, no. 2, 1991, pp. 355-363.

[29] Gyugyi L., Pelly B.R., Static Power Frequency Changers, New York: J. Wiley-Interscience Publication, 1981.

[30] Simon S. Ang , Power- Switching Converters, New York: Marcel Dekker, Inc. 1995.

[31] David C. Griffith, Uninterruptible Power Supplies, New York: Marcel Dekker Inc. 1989.

[32] Gene F. Franklin, Feedback Control of Dynamic Systems, New York : Addison-Wesley,1991.

[33] The MathWorks, Inc, SIMULINK: Dynamic System Simulation for Matlab, Version 2, Massachusetts,1996.

[34] Ludger Szklaraki, Electric Drive Systems Dynamics, New York : Polish Scientific Publishers-Warszawa, 1990.

[35] The MathWorks, Inc. Control System Toolbox, User's Guide, Massachusetts, 1996.

[36] The MathWorks, Inc. Matlab Reference Guide, Massachusetts,1994.

[37] Naser. Abdel-Rahim, "A Current-Regulated Voltage-Controlled Scheme for DC AC Voltage-Source Static Power Supplies", Ph.D thesis, Memorial University of Newfoundland, Jan. 13, 1996.

[38] N.Abdel-Rahim and J.E. Quaicoe, "Analysis and Design of a Multiple Feedback Loop Control Strategy for Single-Phase Voltage-Source UPS Inverters," IEEE Trans., Power Electron., Vol.11, no. 4, July 1996, pp. 532-540.

Appendix A
SIMULINK Models of the Control Strategies

The detailed SIMULINK models of the various control strategies are presented in this Appendix.

A.1 The two-loop control strategy

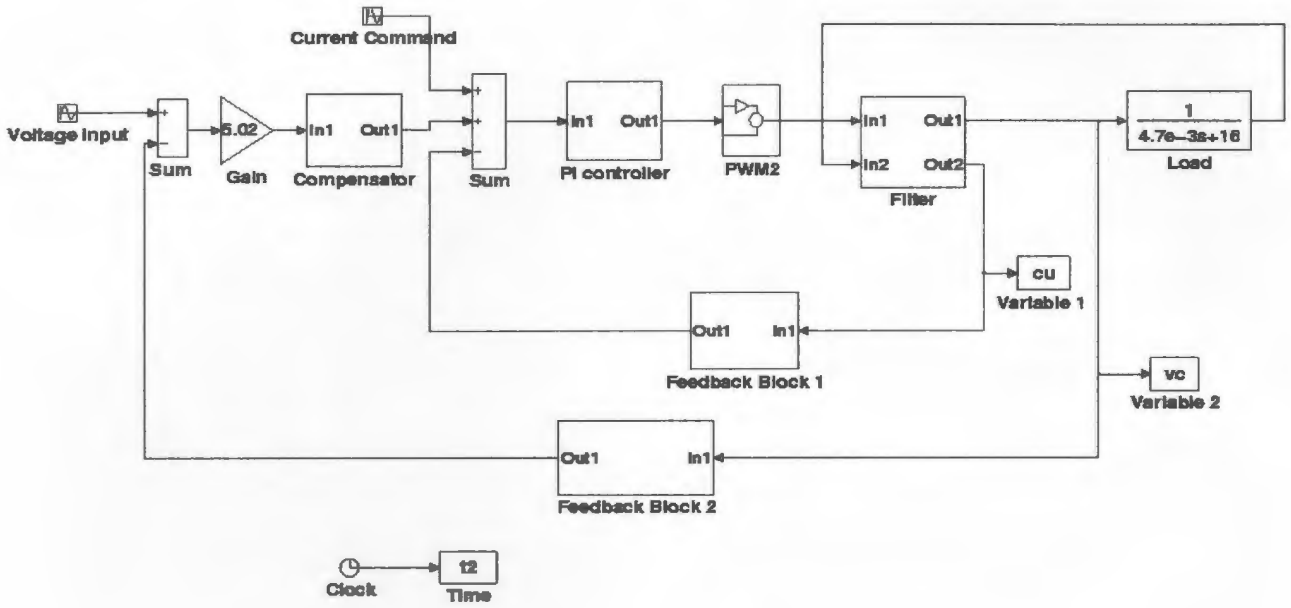

Figure A.1: The structure of basic two-loop control strategy

The transfer functions and parameters of the individual blocks are as follows:

$$Compensator = \frac{2.2\times10^{-6}s+4.22}{6.6\times10^{-12}s^2+4.43\times10^{-7}s+1} \times \frac{3.58\times10^{-6}s+1}{4.15\times10^{-11}s^2+2.74\times10^{-7}s+1}$$

PI controller:

$$PI_c = \frac{2.626\times10^{-3}s+1}{9.162\times10^{-4}s}$$

Feedback Block1:

$$f_1 = \frac{4.99\times10^{-5}s+1}{6.72\times10^{-10}s^2+7.69\times10^{-5}s+1}$$

Feedback Block2:

$$f_2 = \frac{4.99\times10^{-5}s+1}{8.4\times10^{-11}s^2+9.6\times10^{-6}s+0.125}$$

A.2 The modified two-loop control strategy

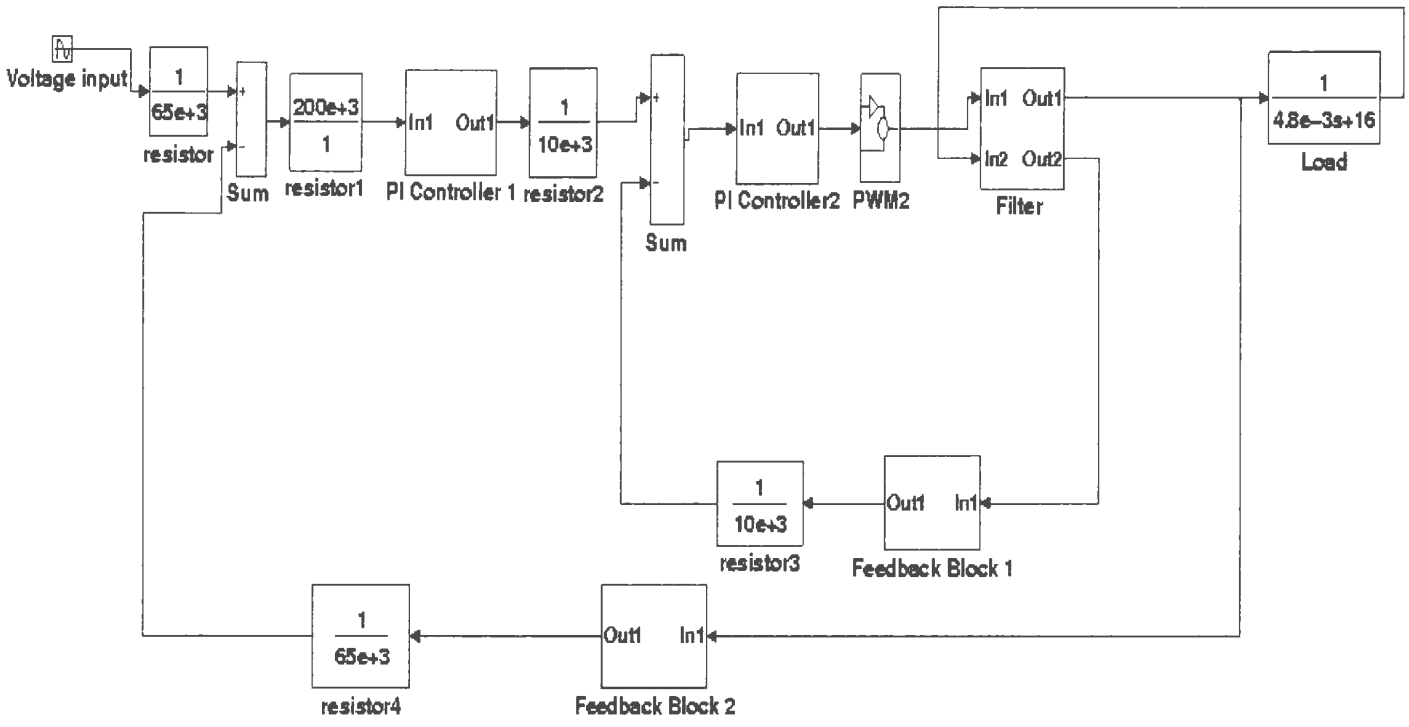

Figure A.2: The structure of modified two-loop control strategy

The transfer functions and parameters of the individual blocks are as follow :

PI Controller 1:

$$PI_v = \frac{1.6575s + 107.5}{6.6\times10^{-5}s^2 + 4.4015\times10^{-1}s + 1}$$

PI Controller 2:

$$PI_c = \frac{3.952\times10^{7}s + 3.6499\times10^{5}}{5.93\times10^{-5}s^2 + 0.7974s + 1}$$

Feedback Block 1:

$$f_1 = \frac{4.99\times10^{-5}s + 1}{6.72\times10^{-10}s^2 + 7.69\times10^{-5}s + 1}$$

Feedback Block 2:

$$f_2 = \frac{4.99\times10^{-5}s + 1}{8.4\times10^{-11}s^2 + 9.6\times10^{-6}s + 0.125}$$

The resistor blocks are used to scale the various signals in the control system.

A.3 The three-loop control strategy

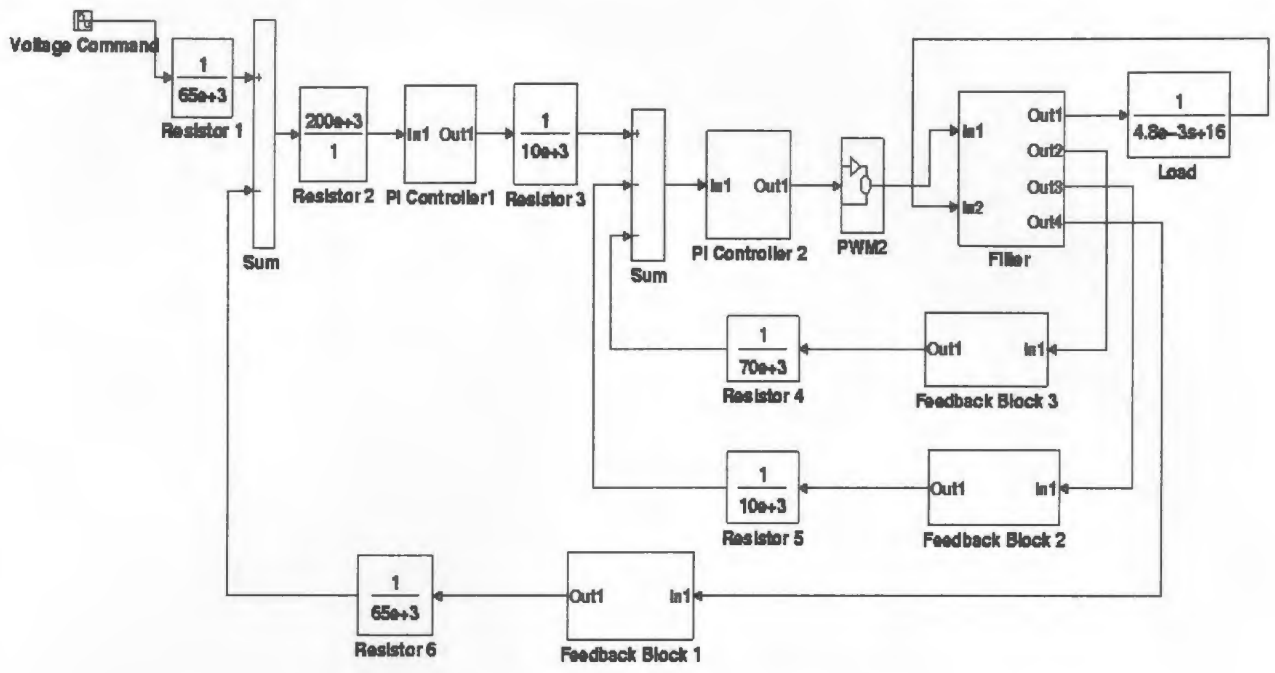

Figure A.3: The structure of three-loop control strategy

The transfer functions and parameters of the individual blocks are as follow :

PI Controller 1:

$$PI_v = \frac{1.6575s + 107.5}{6.6\times 10^{-5}s^2 + 4.4015\times 10^{-1}s + 1}$$

PI Controller 2:

$$PI_c = \frac{3.952\times 10^{7}s + 3.6499\times 10^{5}}{5.93\times 10^{-5}s^2 + 0.7974s + 1}$$

Feedback Block 1:

$$f_1 = \frac{4.99\times 10^{-5}s + 1}{6.72\times 10^{-10}s^2 + 7.69\times 10^{-5}s + 1}$$

Feedback Block 2:

$$f_2 = \frac{4.99\times 10^{-5}s + 1}{8.4\times 10^{-11}s^2 + 9.6\times 10^{-6}s + 0.125}$$

Feedback Block 3:

$$f_3 = \frac{4.99\times 10^{-5}s + 1}{6.72\times 10^{-10}s^2 + 7.69\times 10^{-5}s + 1} \times \frac{4.99\times 10^{-5}s}{6.72\times 10^{-10}s^2 + 7.69\times 10^{-5}s + 1}$$

The resistor blocks are used to scale the various signals in the control system.

These parameters applied in a two-loop system can provide normal output of 60Hz. However, it can not provide 400 Hz output. To satisfy the requirement of this approach, these parameters were changed in the modified two-loop system presented in Chapter 5. As a result of this change, the bandwidth of the whole system is expanded and hence a high frequency of 400 Hz is provided. In comparison with the modified two-loop system, the three-loop system developed in Chapter 5 produces less voltage loss and higher quality of output waveform. This improvement was achieved by adding an inductor current loop which would decrease the influence of harmonics and current stress.

Appendix B

Additional Waveforms for the Three-Loop Control Strategy

The waveforms for different load parameters are shown in figure B.1 to B.4 at standard frequencies of f=60Hz and f=400Hz with Z_l=15Ω and Z_l=25Ω. Based on these figures, it is shown that the three-loop control system is insensitive to load parameters change.

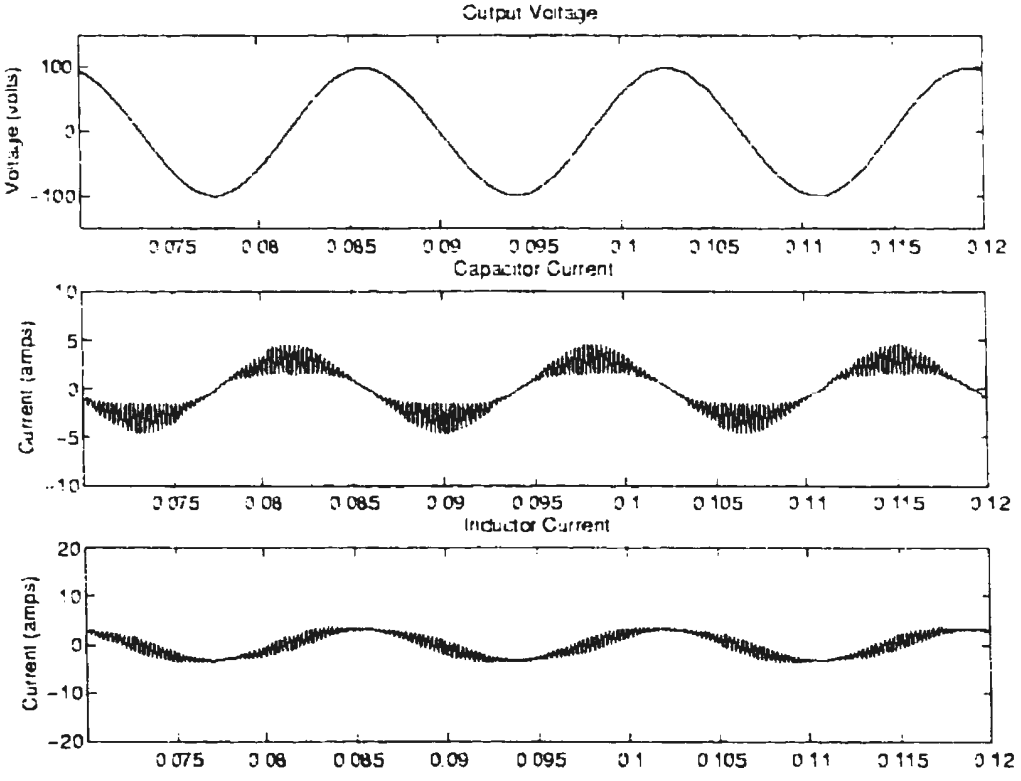

B.1: Output voltage, capacitor current and inductor current waveforms at 60Hz
(Three-loop control)
(R_l=12Ω, L_l=23.87mH, L_f=3.8mH, C_f=83.3μF, V_{dc}=100V, f_s=4.2kHz)

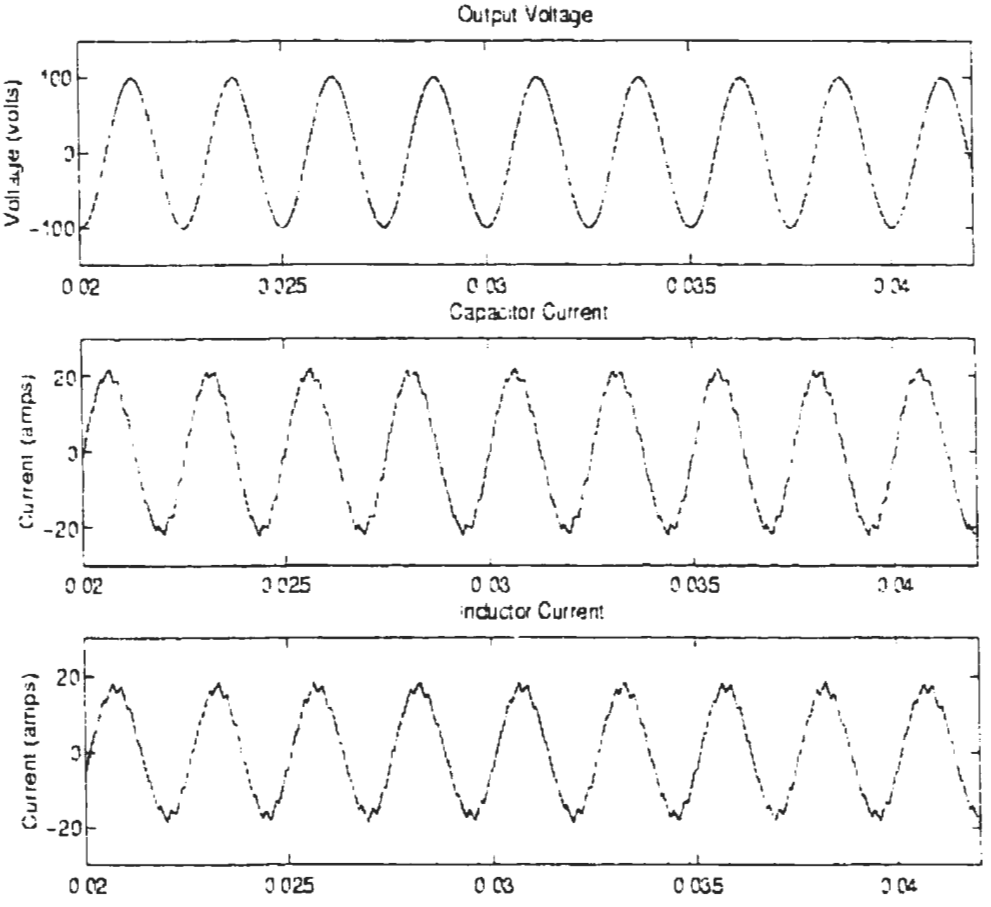

B.2: Output voltage, capacitor current and inductor current waveforms at 400Hz
(Three-loop control)
(R_l=12Ω, L_l=3.58mH, L_f=3.8mH, C_f=83.3μF, V_{dc}=100V, f_s=4.2kHz)

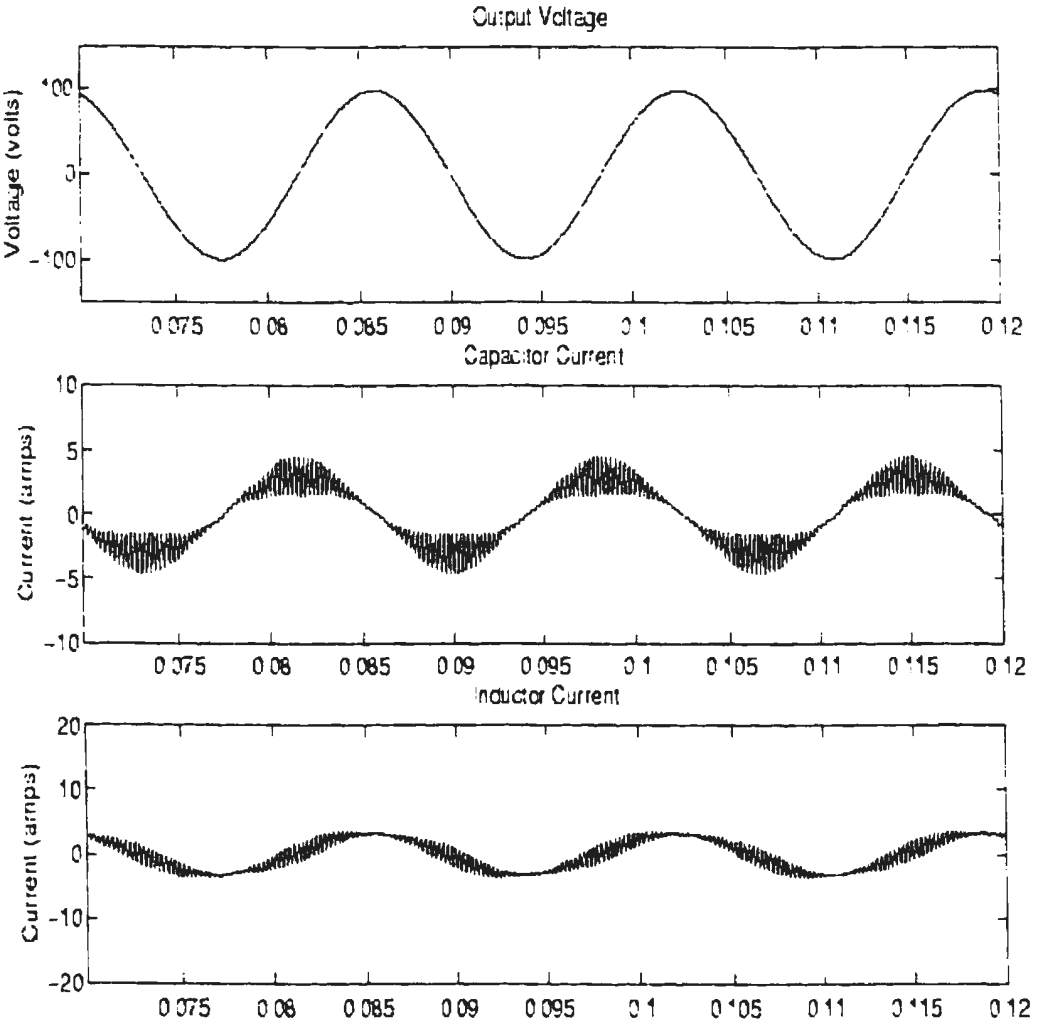

B.3: Output voltage, capacitor current and inductor current waveforms at 60Hz
(Three-loop control)
(R_l=20Ω, L_l=39.7mH, L_l=3.8mH, C_f=83.3μF, V_{dc}=100V, f_s=4.2kHz)

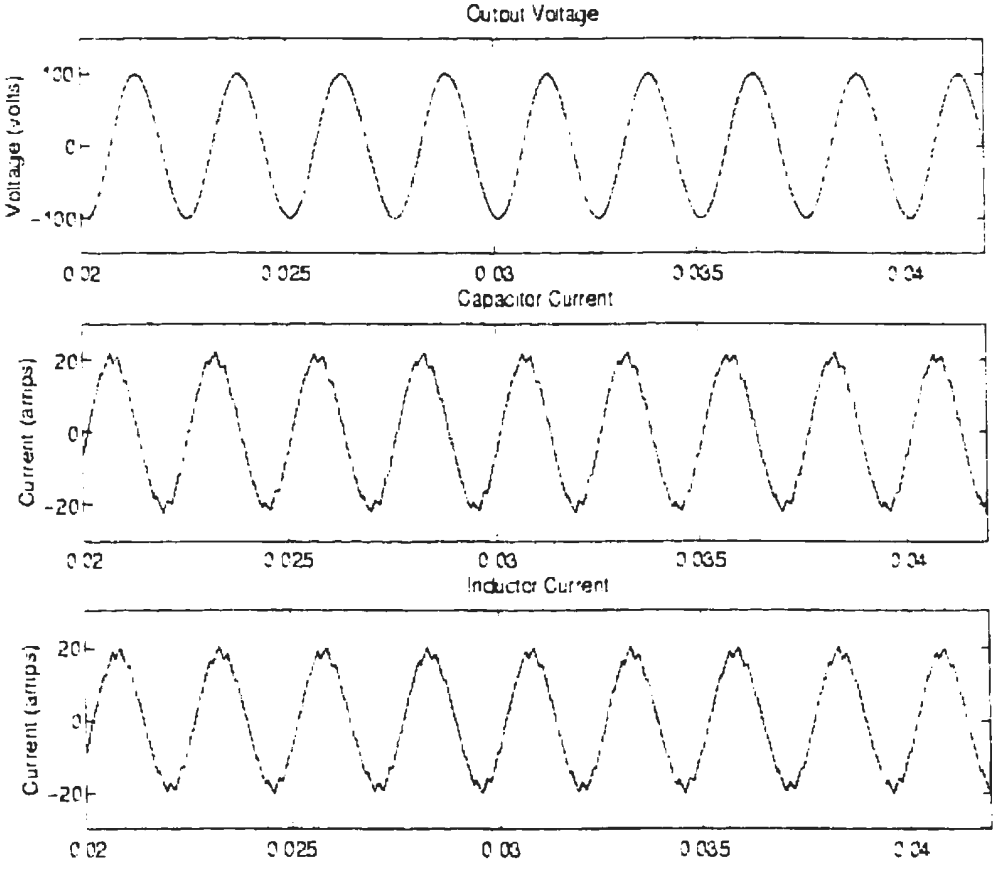

B.4: Output voltage, capacitor current and inductor current waveforms at 400Hz
(Three-loop control)
(R_l=20Ω, L_l=5.97mH, L_f=3.8mH, C_f=83.3μF, V_{dc}=100V, f_s=4.2kHz)

Appendix C
Simulation Procedure

In this appendix, a structured window application, supported by MATLAB [38] and m-files, is introduced to show the simulation procedure graphically. It starts with a central window, Figures C.1 and C.2, which includes all components of the design. A user can directly input control command from the input window and get the output from the running window. Other components of the design such as the system blocks, simulation, adaptive system, dynamic response and frequency response can be viewed by clicking the corresponding icon. The most useful window is the overview window, which links a general window to various windows for the display of the system waveforms and features, as shown in Fig.C.3-C.5.

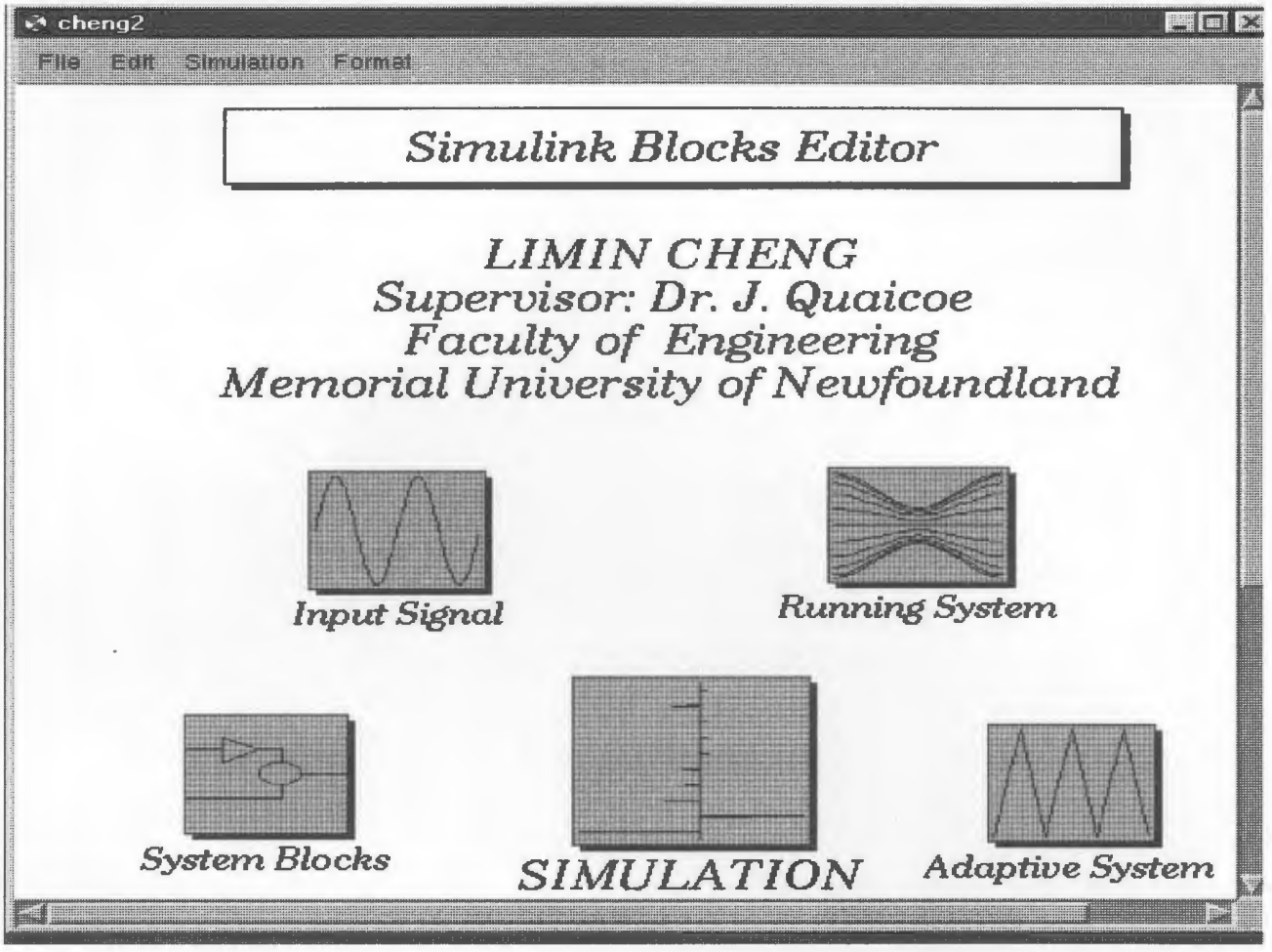

Figure C.1: Part of center window

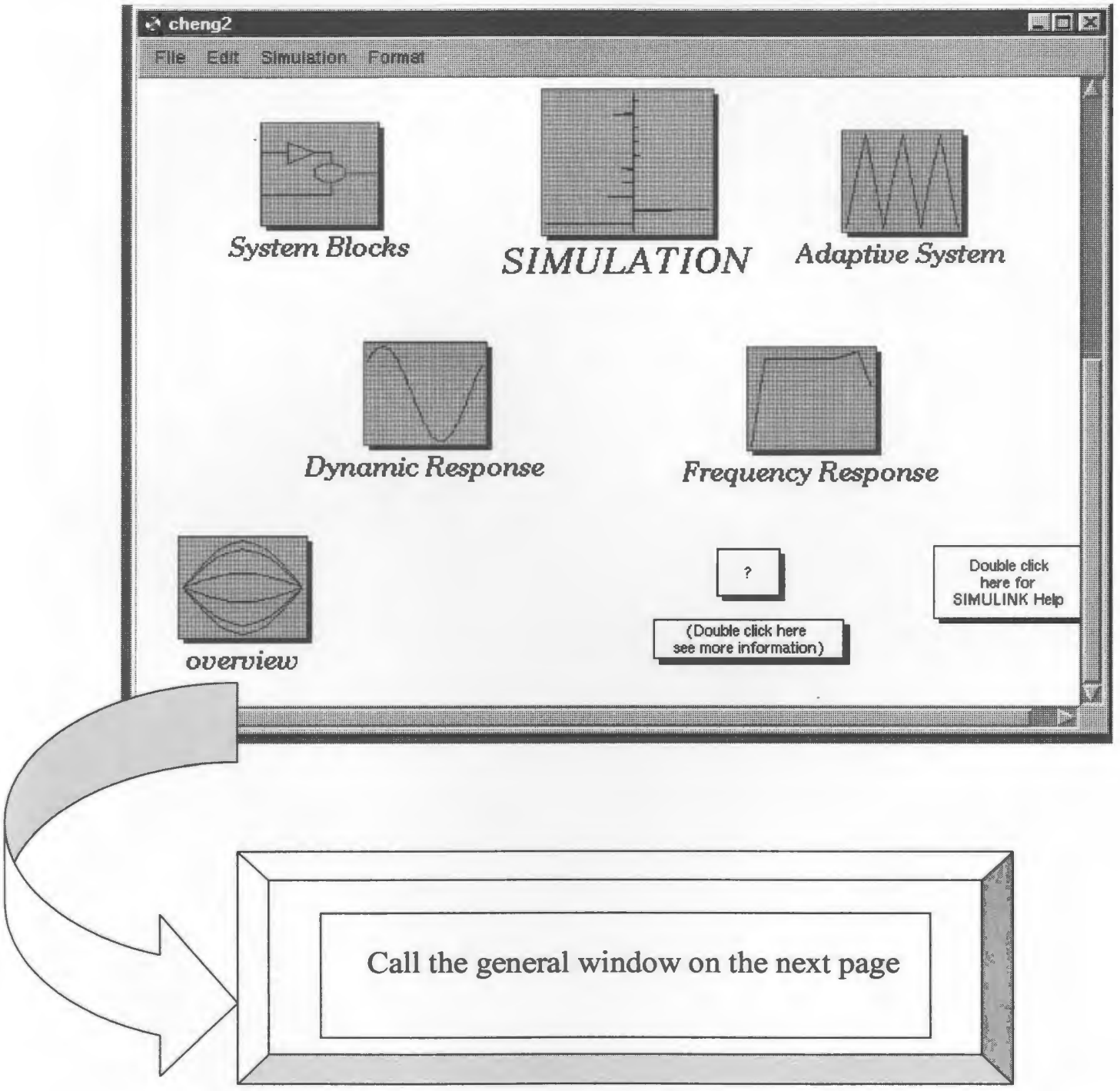

Figure C.2: The main window (Cont.)

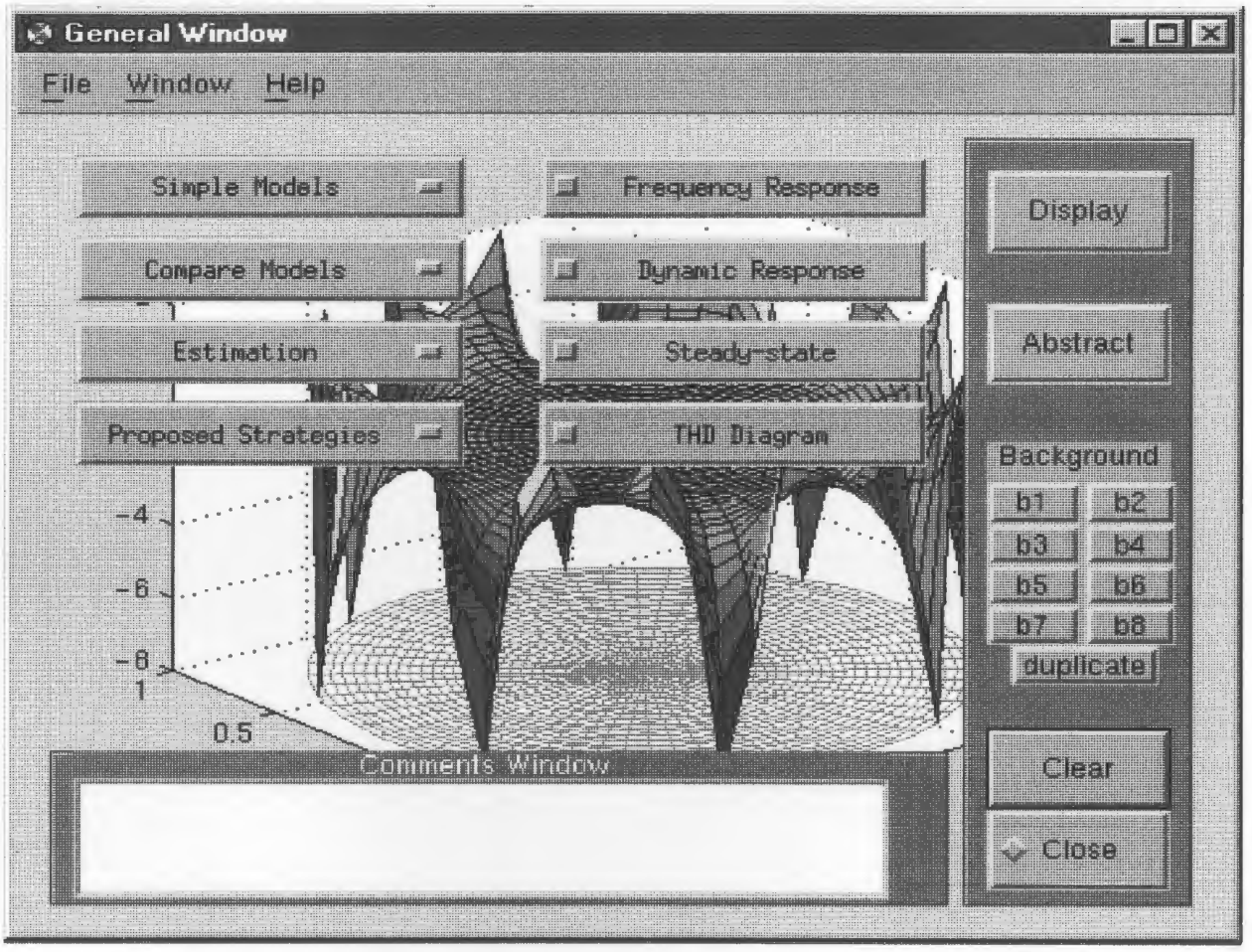

Figure C.3: The general window

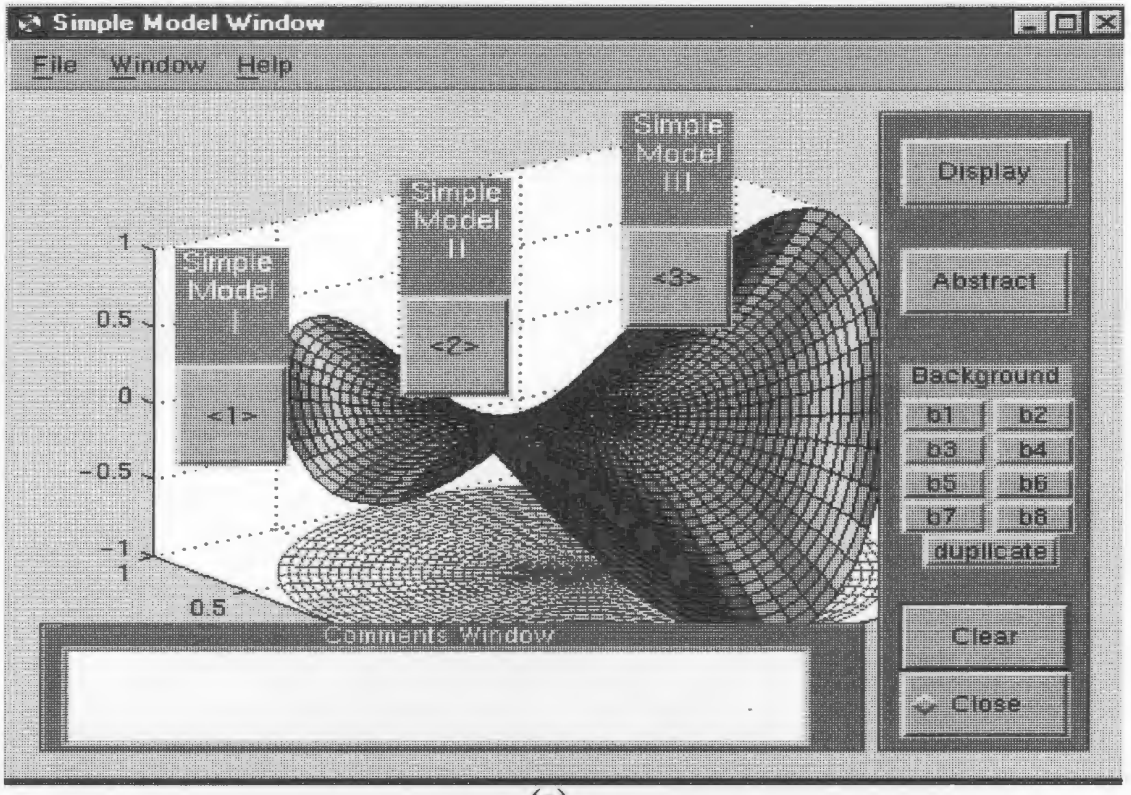

(a)

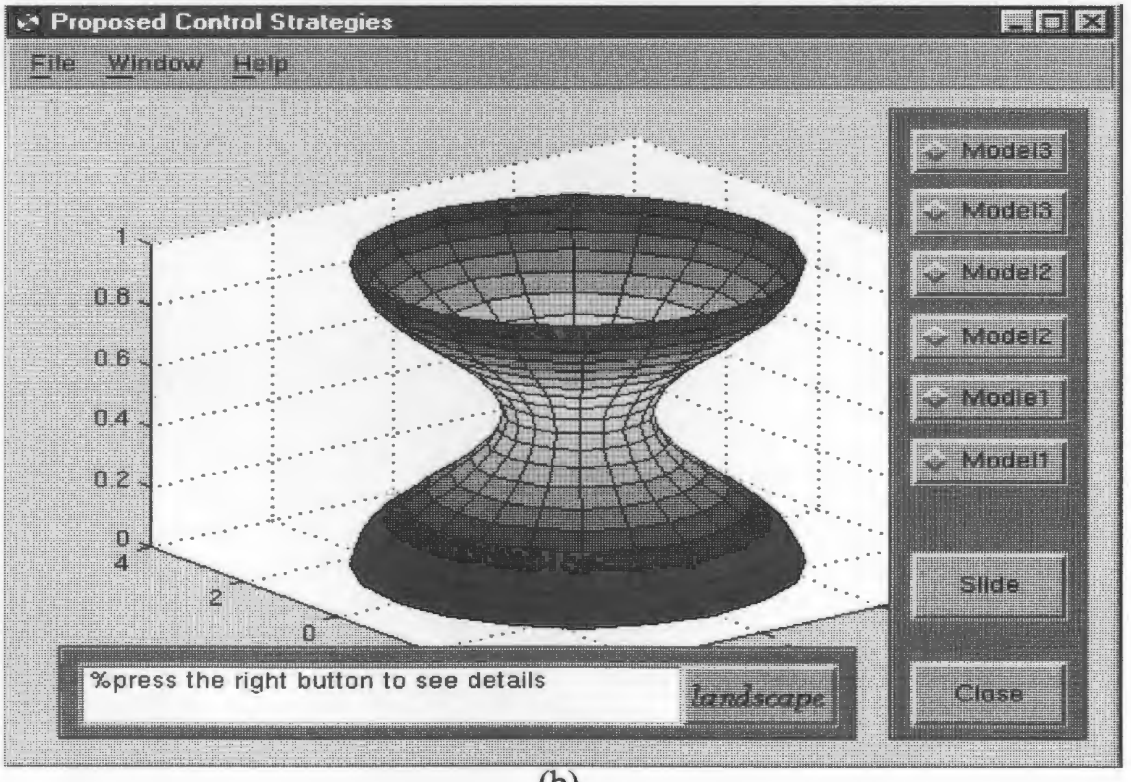

(b)

Figure C.4 (a) Simple models window (b) Proposed control strategies with Models

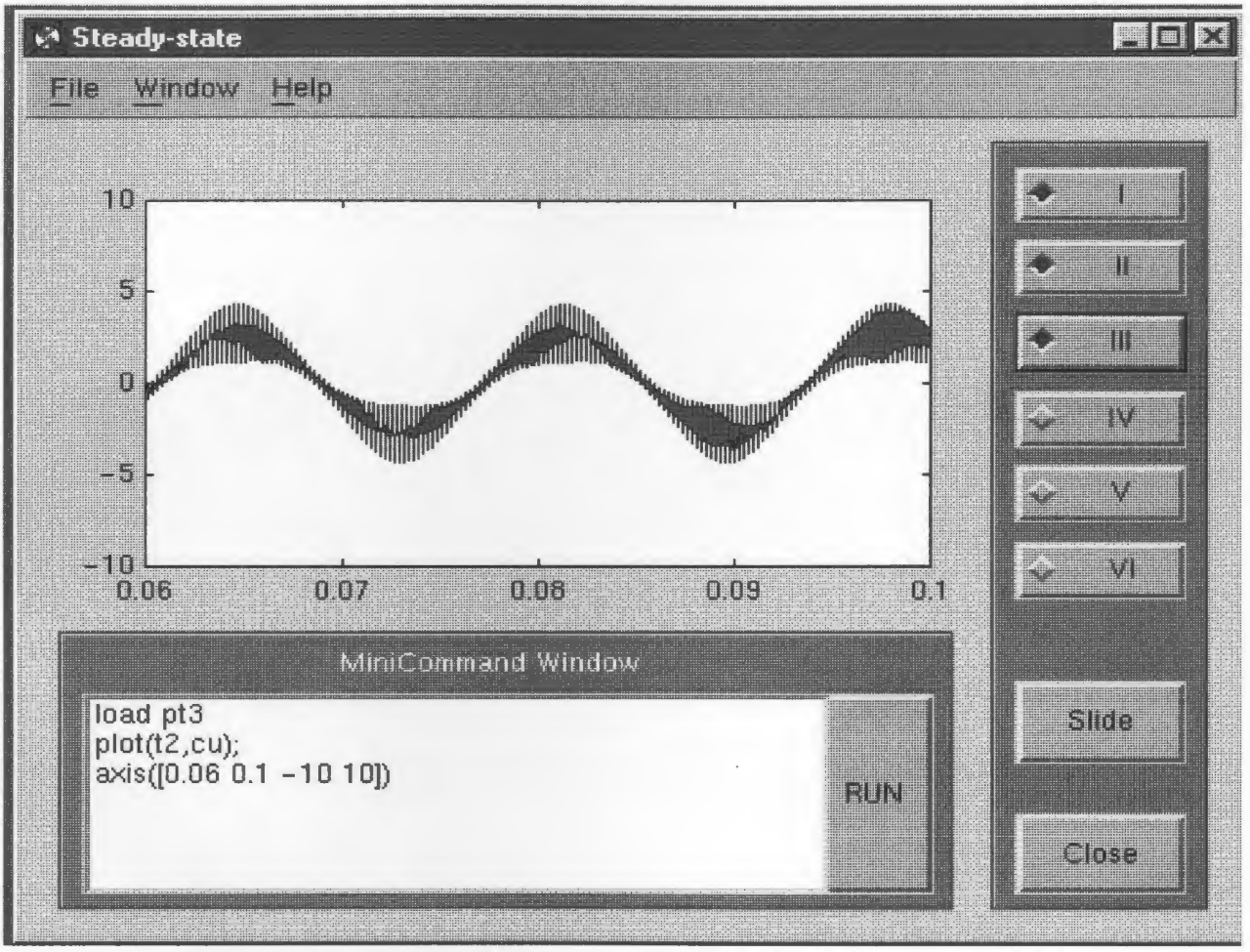

Figure C.5: Output voltage and capacitor current waveforms at 60Hz (Modified two-loop control)
(R_l=16Ω, L_l=31.85mH, L_f=3.8mH, C_f=83.3μF, V_{dc}=100V, f_s=4.2kHz)

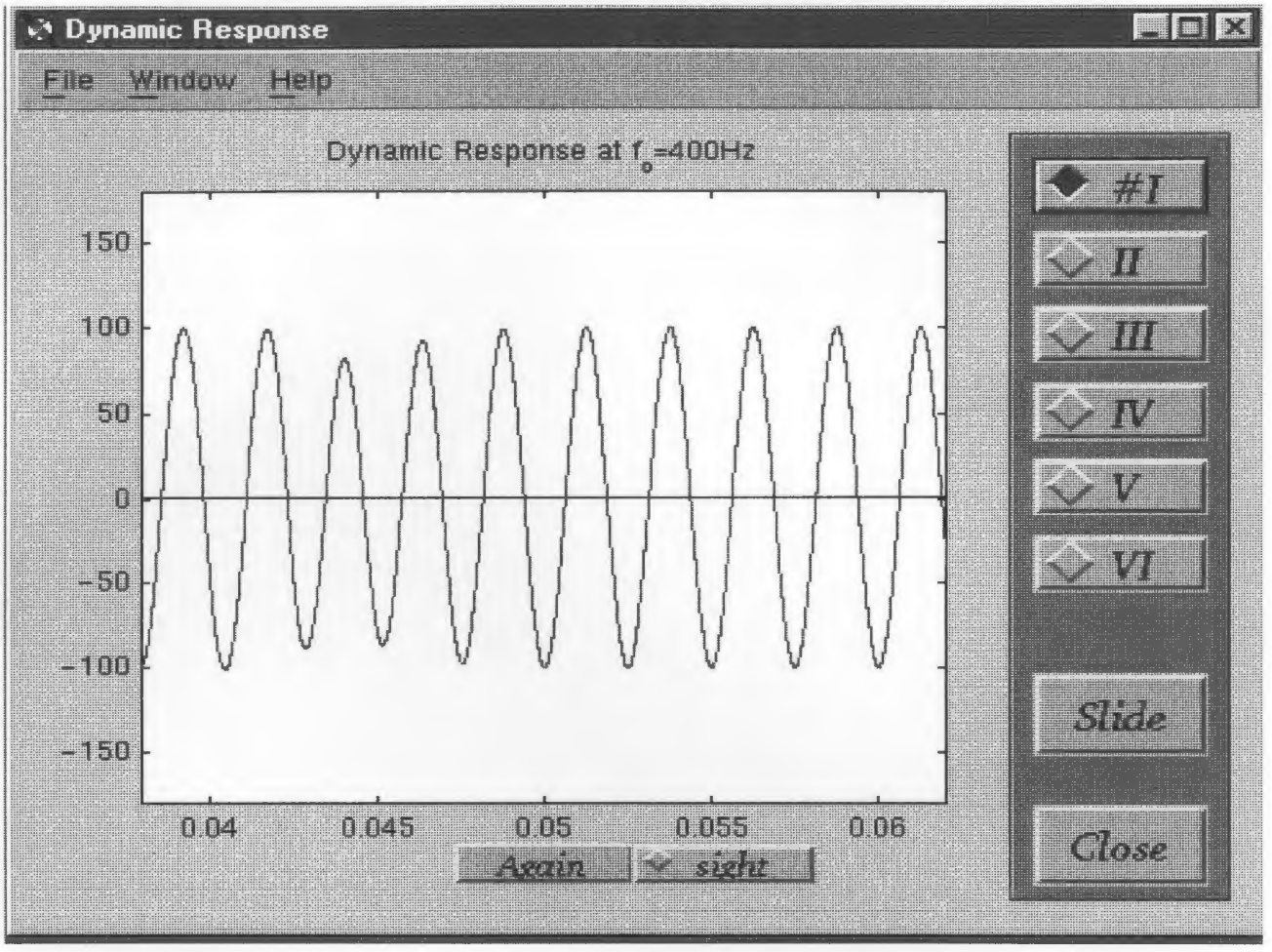

Figure C.6: Dynamic response (full load to no load) at 400Hz
(Three-loop control)
(R_l=16Ω, L_l=4.8mH, L_f=3.8mH, C_f=83.3μF, V_{dc}=100V,
f_s=4.2kHz)